6 31

RHC LIBRARY
BF
Ren
614,563
Oct. 84

GEOMETRIC ABERRATIONS IN CYLINDRICALLY SYMMETRIC ELECTROSTATIC LENSES

A Thesis Prepared for the Degree of Doctor of Philosophy for the University of London.

Anthony Renau March 1984

RHC 614563 6

a30214 006145636b

ProQuest Number: 10107337

All rights reserved

INFORMATION TO ALL USERS
The quality of this reproduction is dependent upon the quality of the copy submitted.

In the unlikely event that the author did not send a complete manuscript
and there are missing pages, these will be noted. Also, if material had to be removed
a note will indicate the deletion.

ProQuest 10107337

Published by ProQuest LLC(2016). Copyright of the Dissertation is held by the Author.

All rights reserved.
This work is protected against unauthorized copying under Title 17, United States Code
Microform Edition © ProQuest LLC.

ProQuest LLC
789 East Eisenhower Parkway
P.O. Box 1346
Ann Arbor, MI 48106-1346

ABSTRACT

Using a computer model of a two cylinder electrostatic lens, some novel relationships have been found to exist between the input and output parameters of meridional rays. These relationships have been developed and used to show that, for a wide range of practical lens geometries, it is possible to represent all the third and fifth order aberrations in terms of just two of the normal parameters. Formulae have been derived to describe some of the quantities associated with this type of lens defect and the problems of minimising the aberrations are discussed.

I.C.
LIBRARY

CONTENTS

1.0	INTRODUCTION	7
1.1	Gaussian optics	8
1.2	Aberrations in ion lenses	16
1.3	Geometric aberration	19
1.4	Classification of geometric aberrations	22
1.5	Further relationships	22
1.5.1	Ray reversal	23
1.5.2	The Lagrange invariant	25
2.0	THE COMPUTER MODEL	31
2.1	Potential and field distribution	31
2.2	Variational method for calculating potential distribution	32
2.2.1	Evaluation of Bessel functions	37
2.2.2	Accuracy and speed of calculations	38
2.3	Trajectory calculation	40
2.3.1	Variation of the integration step length	42
2.4	Testing the computer model	44
2.4.1	Paraxial rays	44
2.4.2	Aberrated rays	46
3.0	RESULTS	49
3.1	Relationships between image and object space	51
3.2	Parallel input and output	63
3.3	Relationships between aberration coefficients	75
3.4	Calculating the aberration coefficients	77

3.5 Ray reversal 82

4.0 FURTHER TREATMENT OF RESULTS 83

4.1 Range of application 83

4.2 Other lens geometries 88

4.3 Further simplification of aberration coefficients 97

4.4 Spherical aberration 104

4.4.1 Relationship to total aberration 104

4.4.2 Magnitude of the aberration 108

4.4.3 Retarding lenses 109

4.5 Disc of least confusion 112

4.6 Curvature of the principal surfaces 115

4.7 Application to lens design 117

4.7.1 Optimum magnification 117

4.7.2 Best lens for finite magnification 119

4.7.3 Best lens for zero magnification 123

4.7.4 Figures of merit for retarding lenses 125

4.7.5 Choice of lens geometry 127

4.8 Current density profiles 131

5.0 CONCLUSION 137

5.1 Summary 137

5.2 Future work 139

APPENDIX: Lenses of planar geometry 141

REFERENCES 145

ACKNOWLEDGEMENTS 147

LIST OF TABLES

1	Axial potential of a two cylinder lens	39
2	Angular magnification and image distance of paraxial rays	45
3	Third order aberration coefficients of parallel rays	48
4	The coefficient σ for a two cylinder lens	79
5	Aberration coefficients in the expansion of r_2'	80
6	Aberration coefficients in the expansion of r_2	81
7	Focal lengths of a two cylinder lens	87
8-9	Spherical aberration coefficients of double cylinder lenses	90-91
10-11	Spherical aberration coefficients of a triple cylinder lens	92-93
12	Spherical aberration coefficients of double aperture lenses	94
13-14	Spherical aberration coefficients of a triple aperture lens	95-96
15-18	Image ray parameters for a two cylinder lens	100-103
19	The figure of merit of double element lenses	128
20	Spherical aberration coefficients of planar lenses	144

LIST OF FIGURES

1	Symmetric double element lenses	9
2	Asymmetric double element lenses	10
3	Triple element lenses	11
4	Definition of the cardinal points	15
5	Definition of the ray parameters	20
6	Derivation of the Lagrange invariant	26
7	The two cylinder lens modelled by the computer	34
8	Aberration of a point axial object	50
9-16	Variation of r_1'/r_2' with Q at different magnifications and voltage ratios	52-59
17-21	Variation of Q with r_1/r_2' for parallel input rays	64-68
22-26	Variation of Q with r_1^2 for parallel input rays	70-74
27	Abberation of an off axis object	106
28	Spherical aberration as a function of magnification	110
29	Disc of least confusion	113
30	The principal surfaces	116
31	Derivation of the figure of merit for finite magnification	120
32	Derivation of the figure of merit for zero magnification	124
33	Figure of merit for a three cylinder lens	129
34	Figure of merit for a three aperture lens	130
35	Derivation of current density profiles	132
36	Image current density profiles in a two cylinder lens	135
37	Planar lens geometries	143

SECTION ONE

INTRODUCTION

In the fifty or sixty years since the first electron lenses were produced by Busch (1926) and by Davisson and Calbick (1931), ion optics has become one of the most ubiquitous branches of physics. In addition to the well established cathode ray tube technology, ion lenses are essential in the fields of electron microscopy and spectroscopy, ion accelerators and the rapidly growing areas of electron beam lithography and ion implantation. Despite these many applications, the theory that describes the influence of a lens on an ion beam has remained particularly cumbersome.
The properties of a lens are usually described by two sets of parameters. The first will pertain to the ideal lens, where we can define ideal focussing as occuring when all rays from a point in object space converge to a single point in image space and, moreover, the geometric relationship between object points is reproduced in image space. A second set may then be needed to account for the particular defects of the system. These aberrations will depend not only on the type of lens used but also on the operating conditions.
This thesis is concerned with the imaging properties of cylindrically symmetric electrostatic lenses. We shall show how it is possible to simplify the treatment of one the most common aberrations of this type of lens. The discussion is in five parts. In the remainder of this section we will review

the focussing properties of electrostatic lenses and establish some important relationships that will be used elsewhere in the report. Section two deals with the production and testing of an efficient computer model of a two cylinder lens. The observations that have been made on this model are discussed in section three and a series of novel relationships are deduced and investigated. Section four examines the application of these results to lens design and the equations governing the geometric aberrations are shown to be reducable to very simple expressions. In the concluding section the most important results are summarised and discussed further.

1.1) GAUSSIAN OPTICS

The branch of electron optics that is confined to ideal imaging is commonly called Gaussian optics. It is essentially the optics of paraxial rays. In this section, as indeed in the rest of the thesis, discussion will pertain only to systems of rotational symmetry about the optic axis. These will usually be composed of simple tubes or apertures as are shown, for example, in Figures 1, 2 and 3.

For all electrostatic systems the potential distribution in space is entirely defined by the geometry and potential of the electrodes. In the absence of space charge this will satisfy Laplace's equation:-

$$\nabla^2 \phi(r,z) = 0 \qquad (1)$$

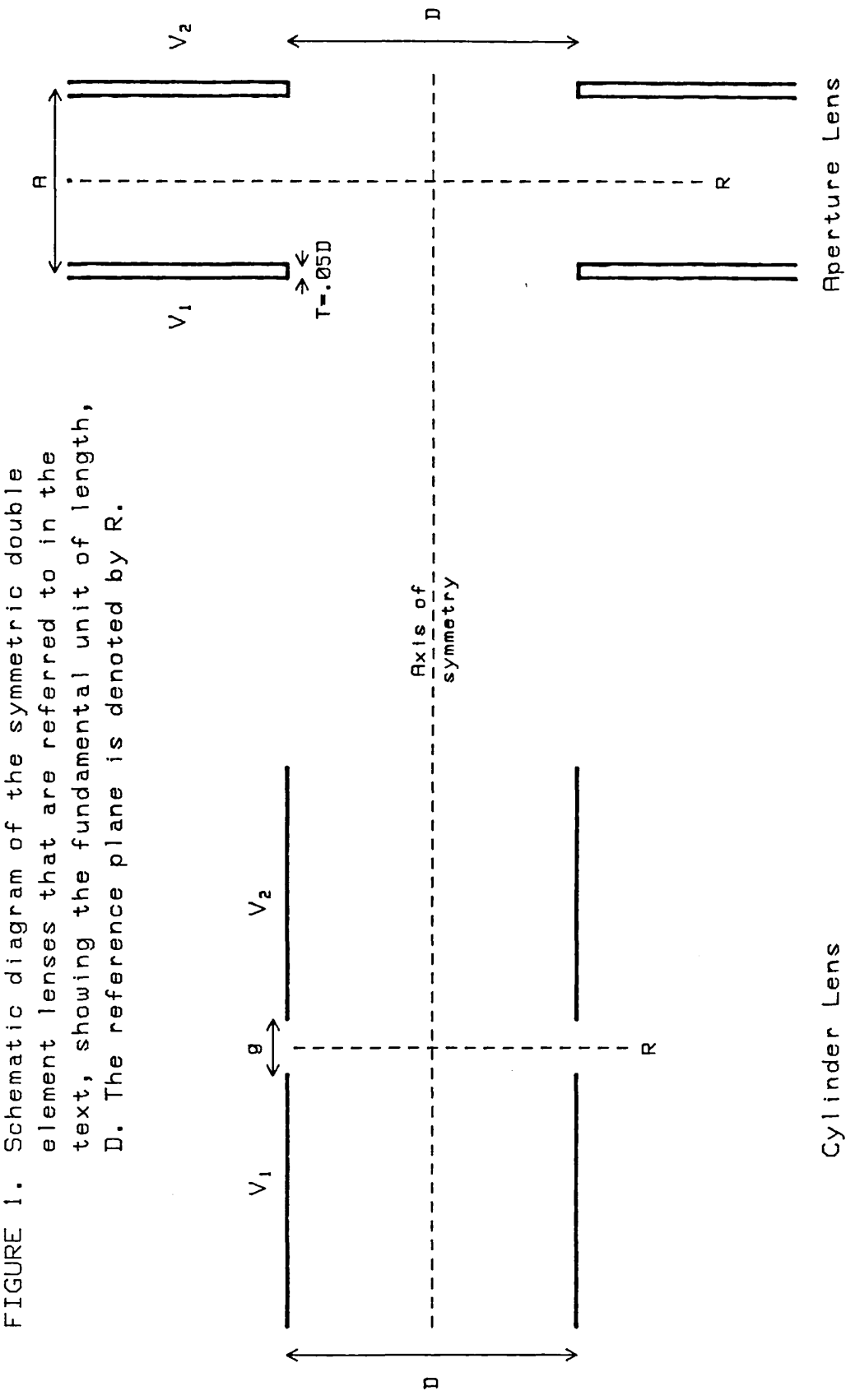

FIGURE 1. Schematic diagram of the symmetric double element lenses that are referred to in the text, showing the fundamental unit of length, D. The reference plane is denoted by R.

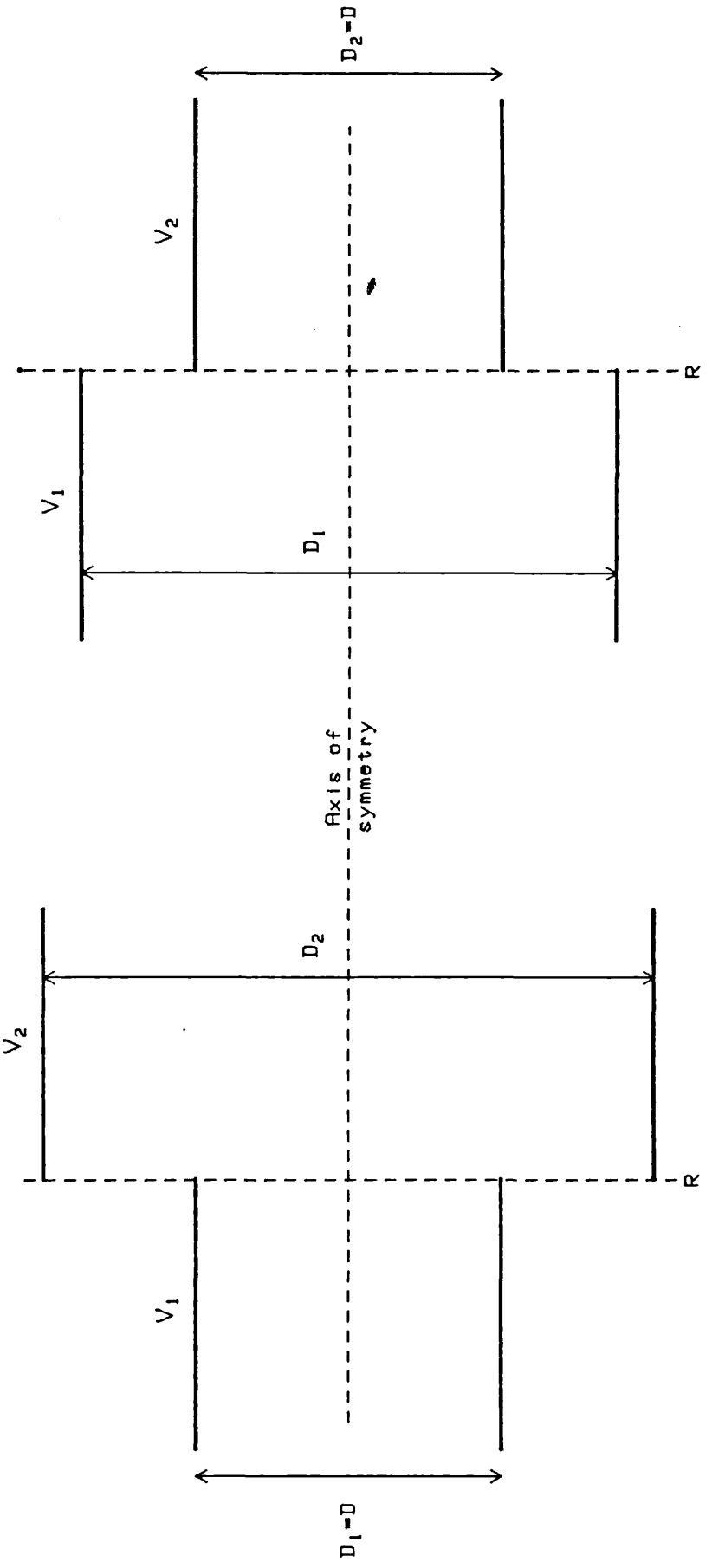

FIGURE 2. Schematic diagram of the asymmetric double element lenses that are referred to in the text. D is the lesser of the cylinder diameters.

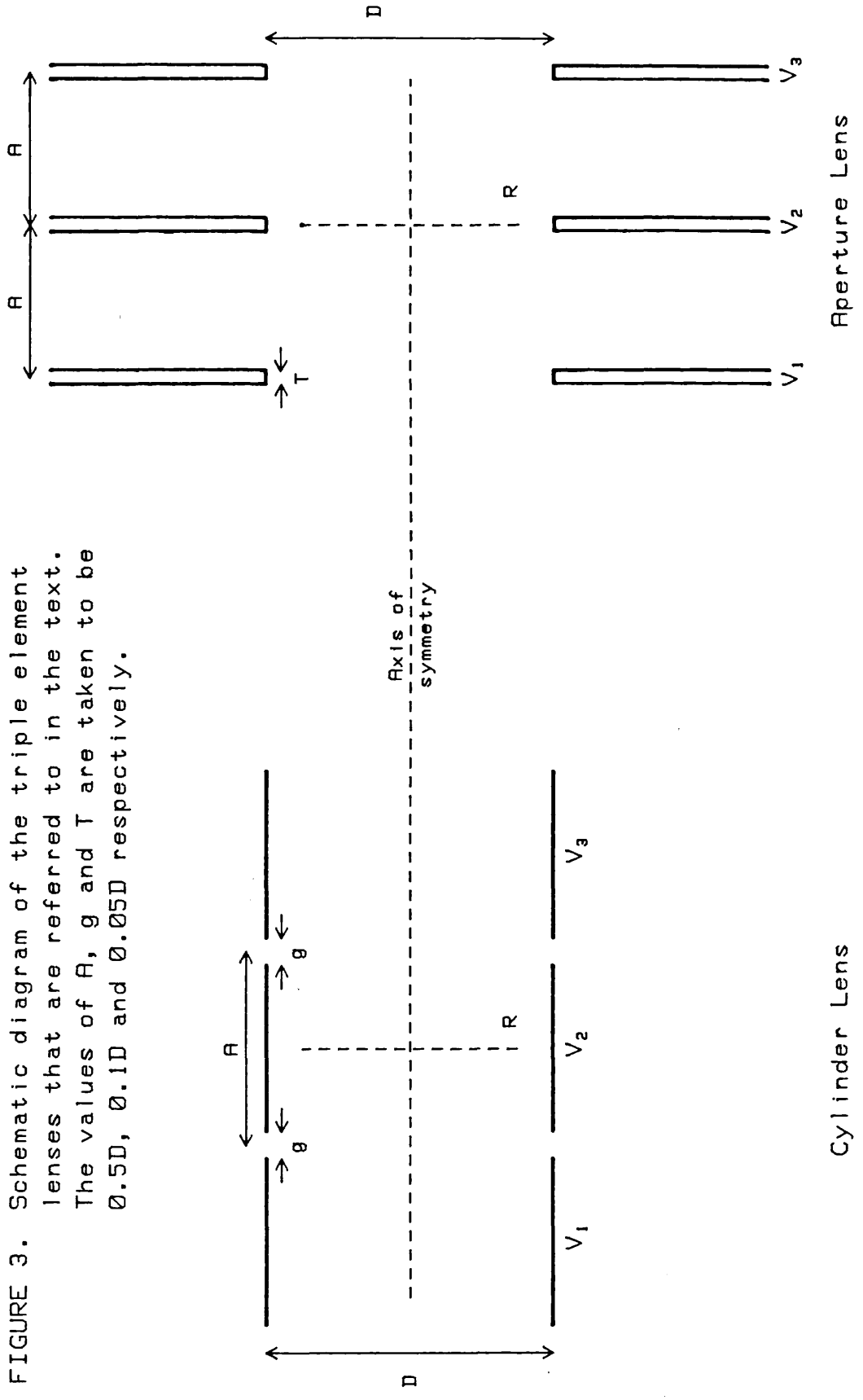

FIGURE 3. Schematic diagram of the triple element lenses that are referred to in the text. The values of A, g and T are taken to be 0.5D, 0.1D and 0.05D respectively.

Apart from the most trivial of electrode structures, it is impossible to derive the potential distribution by analytical integration of this equation. However when a lens has an axis of symmetry, Laplace's equation can be used to show that the distribution of potential along this axis, $\phi_o(z)$, uniquely determines the potential in all space. (See, for example, Klemperer, 1971):-

$$\phi(r,z) = \phi_o(z) - \frac{r^2}{2^2}\frac{d^2\phi_o(z)}{dz^2} + \frac{r^4}{2^2 4^2}\frac{d^4\phi_o(z)}{dz^4} - \ldots\ldots \qquad (2)$$

It can be seen that for small values of r, the potential is similar to that on axis. It is this insensitivity to radial displacement that enables the focal lengths of paraxial rays to be calculated readily. We shall briefly outline the derivation of an equation of motion for such rays and show how this leads to the usual characterisation of a lens by 2 focal and 2 mid-focal lengths.

For non-relativistic systems the motion of an electron will be governed by the Newtonian equations:-

$$\frac{d^2z}{dt^2} = \eta\frac{\partial\phi(r,z)}{\partial z} \qquad (3)$$

$$\frac{d^2r}{dt^2} = \eta\frac{\partial\phi(r,z)}{\partial r} \qquad (4)$$

Where η is the electronic charge to mass ratio.

If we confine our discussion to paraxial rays, then we can neglect the potential and field terms of higher than first

order in r. Hence we can rewrite (3) and (4) as:-

$$\frac{d^2 z}{dt^2} = \frac{e}{m}\frac{d\phi_o(z)}{dz} \tag{5}$$

$$\frac{d^2 r}{dt^2} = -\frac{e}{m}\frac{r}{2}\frac{d^2\phi_o(z)}{dz^2} \tag{6}$$

Furthermore, since $(dr/dz)^2 \ll 1$ we can write, in the absence of thermal velocity:-

$$(dz/dt)^2 = 2\frac{e}{m}\phi_o(z) \tag{7}$$

A differential equation for the electron trajectory can be derived by noting that:-

$$\frac{d^2 r}{dt^2} = \frac{d}{dt}\left(\frac{dr}{dz}\cdot\frac{dz}{dt}\right) \tag{8}$$

$$= \frac{dr}{dz}\frac{d^2 z}{dt^2} + \frac{d^2 r}{dz^2}\left(\frac{dz}{dt}\right)^2 \tag{9}$$

Substituting (5), (6) and (7) into (9):-

$$-\frac{r}{2}\frac{d^2\phi_o(z)}{dz^2} = \frac{dr}{dz}\frac{d\phi_o(z)}{dz} + 2\frac{d^2 r}{dz^2}\cdot\phi_o(z) \tag{10}$$

Therefore:-

$$\frac{d^2 r}{dz^2} + \frac{d\phi_o(z)}{dz}\frac{dr}{dz}\frac{1}{2\phi_o(z)} + \frac{d^2\phi_o(z)}{dz^2}\frac{r}{4\phi_o(z)} = 0 \tag{11}$$

A more usual form of the ray equation (Picht, 1939) can be derived from (11) by making the substitution:-

$$R(z) = r\left(\phi_0(z)\right)^{1/4} \tag{12}$$

Hence:-

$$\frac{d^2R(z)}{dz^2} + \frac{3}{16}\left(\frac{d\phi_0(z)}{dz}\cdot\frac{1}{\phi_0(z)}\right)^2 \cdot R(z) = 0 \tag{13}$$

It can be seen that the equation of motion contains neither the charge nor the mass of the particle. It and all the data and relationships that are given here may be applied not only to electrons but to any non-relativistic charged particle. In the case of positive ions the signs of the applied voltages need to be reversed.

Since (11) is a linear second order differential equation its general solution can be obtained by a linear combination of two particular solutions. Typically two rays, parallel to the optic axis in image and object space respectively, are numerically integrated using equation (13).

By integration of the Picht equation or otherwise, the four cardinal points of the lens can be found and thus the focal and mid focal lengths.

It can be seen from Figure 4 that for conjugate points P and Q_0 in object and image space repectively:-

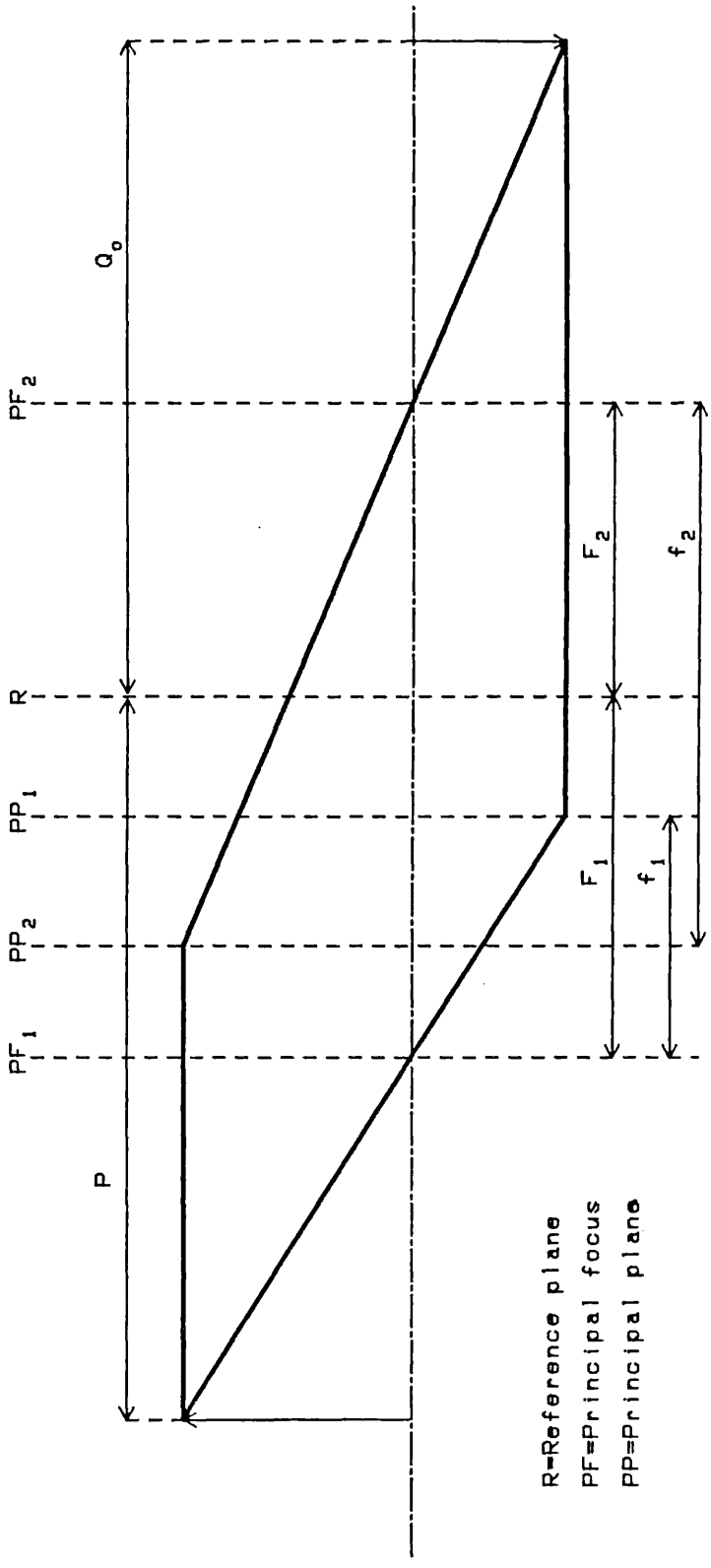

FIGURE 4. Schematic representation of the cardinal points and focal lengths of a thick lens. The full lines represent the asymptotes of two rays through the lens. The cardinal points are defined by the intersections of these Gaussian rays with one another and with the axis of symmetry.

$$(P-F_1)(Q_0-F_2) = f_1 \cdot f_2 \qquad (14)$$

and the linear magnification of the system is given by:-

$$M = -f_1/(P-F_1) = -(Q_0-F_2)/f_2 \qquad (15)$$

It follows that the asymptotic angular magnification of a paraxial ray is given by:-

$$M_\alpha = -(P-F_1)/f_2 = -f_1/(Q_0-F_2) \qquad (16)$$

1.2) ABERRATIONS IN ION LENSES

The assumptions made in the last section may be valid for many lens systems. However, when image quality is of particular importance and the particle interactions cannot be so simply defined, the Gaussian approximation can serve only as a guideline to the image properties.

The aberrations of ion lenses may be loosely classified into those which result from the interaction of the ray with other than the lens' field, and into those which are geometric aberrations. This work is concerned with the latter type only, so we shall merely identify the most common non-geometric aberrations. A more detailed review can be found, for example,

in the texts of Zworykin et al (1945) or Grivet (1972).

i) Chromatic aberrations will result from a spread in incident energies. In addition, aberrations which could be considered chromatic will result from fluctuations in the applied electrode potentials.
The longitudinal chromatic aberration for paraxial rays is given by:-

$$\Delta l_c = C_c (\delta V_1 / V_1) \qquad (17)$$

Where C_c is the principal chromatic aberration coefficient and the incident particles have energy $q(V_1 + \delta V_1)$. The potential of the first electrode is V_1. (See, for example, Berger, 1982).

ii) Ion-ion interactions could have a significant effect on the image definition and intensity in higher current systems. A useful measure of the magnitude of the space charge effects within the beam is the perveance ($=I/V^{3/2}$ for electrons). For example, the role of space charge in an electron beam of perveance less than $10^{-8}\ AV^{3/2}$ would be negligible, whereas a perveance greater than $10^{-7}\ AV^{3/2}$ could impose fundamental limitations on the design of the system.
Since the perveance is greatest when the beam energy is low, the most dramatic effect of space charge is generally in the extraction region of a system (for example near to the cathode of an electron gun). Indeed the normal operating condition for

most practical systems is with space charge limited emission current (see, for example, Dahl, 1973). In the lens region these effects are usually much less important, although the Coulombic interactions will give rise to additional transverse and longtitudinal forces. The former will diminish image quality by causing the beam to spread, whilst the latter will give rise to chromatic aberration.

iii) Diffraction effects will result if the system has apertures which are comparable to the De Broglie wavelength of the ions. For non-relativistic electrons this is given by:-

$$\lambda \simeq 1.23\phi^{-1/2} \text{ (nM)} \qquad (18)$$

Where ϕ is the potential in Volts.
In practice, diffraction errors are important only in the field of high magnification electron microscopy, where the structure of the object gives rise to these tiny apertures.
iv) Very high voltage lenses will not normally suffer from additional aberrations, however, relativistic transformations will be needed to calculate their 1st order properties. The relativistically corrected form of the Picht equation is given by:-

$$\frac{d^2R^*(z)}{dz^2} + \frac{3}{16}G(z)\left(\frac{d\phi_o(z)}{dz}\cdot\frac{1}{\phi_o(z)}\right)^2 . R^*(z) = 0 \qquad (19)$$

(See, for example, Klemperer, 1971)

Where:-

$$R^{*}(z) = r(\phi_0^{*}(z))^{1/4} \tag{20}$$

$$G(z) = \left(\frac{\phi_0(z)}{\phi_0^{*}(z)}\right)^2 \cdot \left(1 + \frac{2\mathcal{J}\phi_0^{*}(z)}{3c^2}\right) \tag{21}$$

$\phi_0^{*}(z)$ being the relativistically corrected axial potential, which is given by:-

$$\phi_0^{*}(z) = \phi_0(z)(1 + \mathcal{J}\phi_0(z)/2c^2) \tag{22}$$

Any of the effects (i)-(iii) could detract from the image quality of certain systems. However, even when they are negligible, Gaussian theory should be applied only to paraxial rays, because of the presence of geometric aberration.

1.3) GEOMETRIC ABERRATION

The Gaussian approximation may be regarded as a first order theory, since in its formulation terms of higher than first order in r were neglected. For a meridional ray (that is one which is contained in a plane which includes the optic axis) a trajectory through the system can be defined uniquely by its slope and radial displacement at two, non-coincident planes normal to the optic axis. If we take these planes as those which pass through the principal foci of the lens (see Figure 5) and, furthermore, we define r_1, r_1', r_2 and r_2' as the

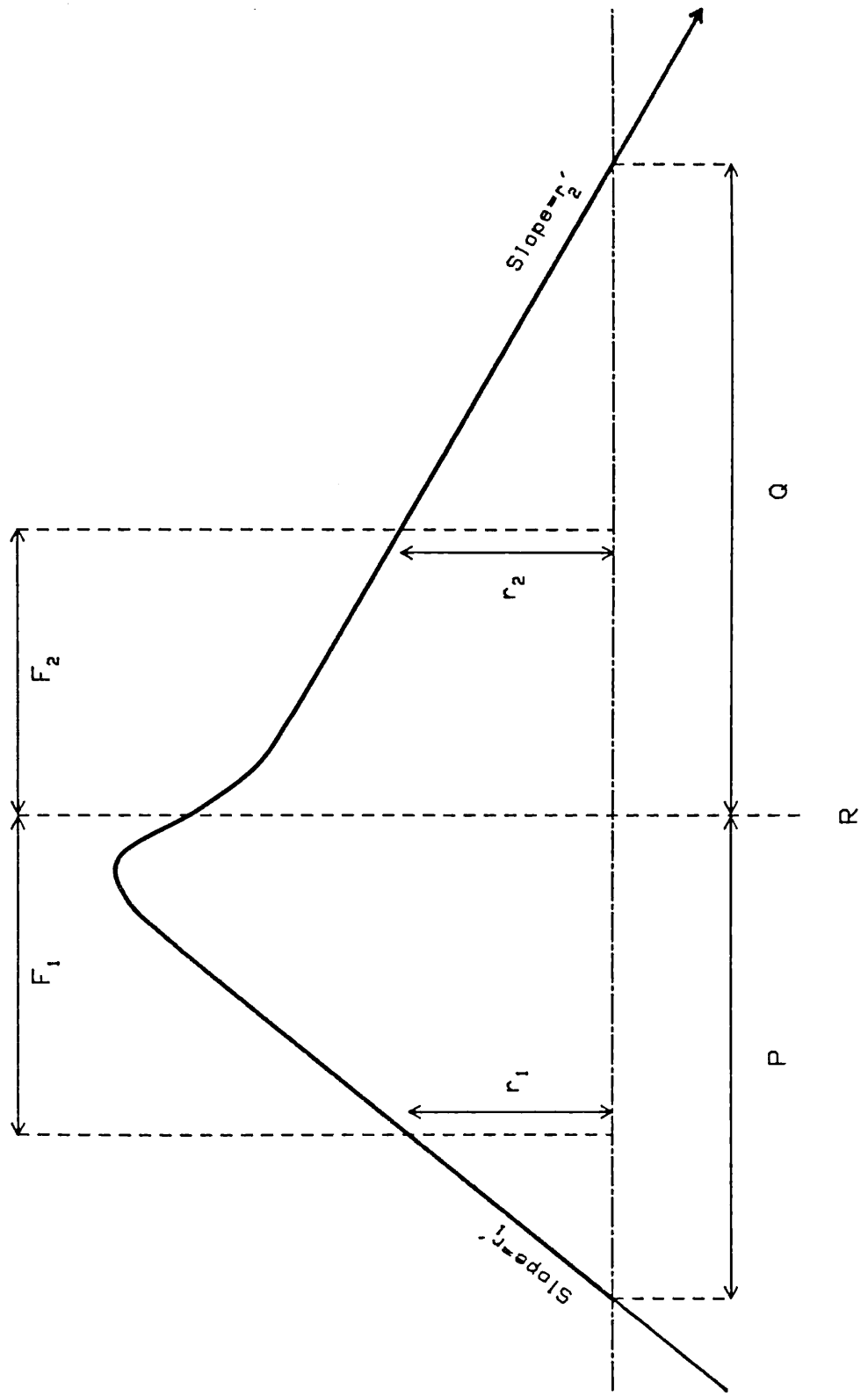

FIGURE 5. Definition of the ray parameters. R is the reference plane of the lens.

asymptotic radial displacement and slope of a ray at these two planes, then it follows that we could express r_2 and r_2' as a power series of r_1 and r_1'. Moreover, because of the cylindrical symmetry of the system, the coefficients of all the even powered terms must be null.

Hence:-

$$r_2' = -r_1/f_2 + m_{13}r_1'^3 + m_{14}r_1'^2 r_1/f_2 + m_{15}r_1'r_1^2/f_2^2 + m_{16}r_1^3/f_2^3 + q_{11}r_1'^5 + q_{12}r_1'^4 r_1/f_2 + q_{13}r_1'^3 r_1^2/f_2^2 + q_{14}r_1'^2 r_1^3/f_2^3 + q_{15}r_1'r_1^4/f_2^4 + q_{16}r_1^5/f_2^5 + \ldots\ldots \quad (23)$$

$$r_2/f_1 = r_1' + m_{23}r_1'^3 + m_{24}r_1'^2 r_1/f_2 + m_{25}r_1'r_1^2/f_2^2 + m_{26}r_1^3/f_2^3 + q_{21}r_1'^5 + q_{22}r_1'^4 r_1/f_2 + q_{23}r_1'^3 r_1^2/f_2^2 + q_{24}r_1'^2 r_1^3/f_2^3 + q_{25}r_1'r_1^4/f_2^4 + q_{26}r_1^5/f_2^5 + \ldots\ldots \quad (24)$$

Where the coefficients of the first order terms follow directly from the paraxial approximation.

The m_{ij} and q_{ij} coefficients give rise to third and fifth order geometric aberrations respectively. These coefficients are system constants and depend on electrode potential and geometry alone. It can be seen that there are 8 third order and 12 fifth order coefficients. It will be shown later that the isotropic properties of the electrostatic field enable these to be reduced to 5 and 7 distinct coefficients respectively.

It must be emphasised that r' is defined by:-

$$r' = dr/dz \tag{25}$$

and it is the slope and not the angular inclination of the ray with respect to the optic axis. For paraxial rays these will be similar.

1.4) CLASSIFICATION OF GEOMETRIC ABERRATIONS

The multiplicity of coefficients in (23) and (24) give rise to a number of characteristic imaging defects. Verster (1963) has shown that it is possible to associate each of the third order errors with particular coefficients. Whilst it is felt that no useful purpose would be served here by extending this treatment to the fifth order, it should be realised that since (23) and (24) are general relationships between incident and emergent meridional rays, they could be used not only to quantify spherical aberration, but also the other geometric errors such as isotropic coma, field curvature, astigmatism and isotropic distortion.

1.5) FURTHER RELATIONSHIPS

We shall now establish some further relationships between incident and emergent rays that, along with (23) and (24) will enable us to investigate the meridional aberrations in ion

lenses.

1.5.1) Ray Reversal

Equations (23) and (24) enable us to express the output parameters of a ray in terms of its slope and displacement at a point in object space. We shall now establish the converse relationship.

A ray traversing the system given in Figure 5 from right to left will perceive a lens with focal lengths $\tilde{F}_1$, $\tilde{F}_2$, $\tilde{f}_1$ and $\tilde{f}_2$ such that:-

$$\tilde{f}_1 = f_2 , \tilde{f}_2 = f_1 , \tilde{F}_1 = F_2 , \tilde{F}_2 = F_1 \qquad (26)$$

where F_1 , F_2 , f_1 and f_2 are the focal lengths for a ray travelling from left to right.

If we denote the ray parameters by $\tilde{r}_1$, $\tilde{r}_1'$, $\tilde{r}_2$ and $\tilde{r}_2'$ (the "1" suffix denotes object space, which is now on the right hand side) then it follows that:-

$$\tilde{r}_2' = -\tilde{r}_1/\tilde{f}_2 + \tilde{m}_{13}\tilde{r}_1'^3 + \tilde{m}_{14}\tilde{r}_1'^2\tilde{r}_1/\tilde{f}_2 + \tilde{m}_{15}\tilde{r}_1'\tilde{r}_1^2/\tilde{f}_2^2 + \tilde{m}_{16}\tilde{r}_1^3/\tilde{f}_2^3 + \tilde{q}_{11}\tilde{r}_1'^5 + \ldots\ldots\ldots + \tilde{q}_{16}\tilde{r}_1^5/\tilde{f}_2^5 \qquad (27)$$

$$\tilde{r}_2/\tilde{f}_1 = \tilde{r}_1' + \tilde{m}_{23}\tilde{r}_1'^3 + \tilde{m}_{24}\tilde{r}_1'^2\tilde{r}_1/\tilde{f}_2 + \tilde{m}_{25}\tilde{r}_1'\tilde{r}_1^2/\tilde{f}_2^2 + \tilde{m}_{26}\tilde{r}_1^3/\tilde{f}_2^3 + \tilde{q}_{21}\tilde{r}_1'^5 + \ldots\ldots\ldots + \tilde{q}_{22}\tilde{r}_1^5/\tilde{f}_2^5 \qquad (28)$$

We can now consider a second ray travelling in the opposite direction whose trajectory, although reversed, coincides with the first. The input and output parameters of this ray are related by equations (23) and (24). Since the rays are coincident it follows that:-

$$\tilde{r}_1 = r_2 \,,\ \tilde{r}_2 = r_1 \,,\ \tilde{r}_1' = -r_2' \,,\ \tilde{r}_2' = -r_1' \tag{29}$$

Equations (26), (27), (28) and (29) may be substituted into equations (23) and (24), enabling us to inter-relate the m, q and $\tilde{m}$, $\tilde{q}$ coefficients. Hence it can be shown that:-

$$\tilde{m}_{13} = m_{26} \,,\ \tilde{m}_{14} = m_{25} \,,\ \tilde{m}_{15} = m_{24} \,,\ \tilde{m}_{16} = m_{23} \tag{30}$$

$$\tilde{m}_{23} = m_{16} \,,\ \tilde{m}_{24} = m_{15} \,,\ \tilde{m}_{25} = m_{14} \,,\ \tilde{m}_{26} = m_{13} \tag{31}$$

$$\tilde{q}_{11} = q_{26} + 3m_{26}m_{16} - m_{25}m_{26} \,, \quad \tilde{q}_{16} = q_{21} + m_{13}m_{24} - 3m_{23}^2 \tag{32}$$

$$\tilde{q}_{21} = q_{16} + 3m_{16}^2 - m_{15}m_{26} \,, \quad \tilde{q}_{26} = q_{11} + m_{15}m_{14} - 3m_{23}m_{13} \tag{33}$$

Using these identities in equations (27) and (28) enables us to express the ray parameters in object space as a function of those in image space:-

$$\begin{aligned} r_1' = {} & r_2/f_1 + m_{26}r_2'^3 - m_{25}r_2'^2 r_2/f_1 + m_{24}r_2' r_2^2/f_1^2 - m_{23}r_2^3/f_1^3 \\ & + (q_{26} + 3m_{26}m_{16} - m_{25}m_{26})r_2'^5 - \ldots - (q_{21} + m_{13}m_{24} - 3m_{23}^2)r_2^5/f_1^5 \end{aligned} \tag{34}$$

$$r_1/f_2 = -r_2' - m_{16}r_2'^3 + m_{15}r_2'^2 r_2/f_1 - m_{14}r_2' r_2^2/f_1^2 + m_{13}r_2^3/f_1^3 - (q_{16} + 3m_{16} - m_{15}m_{26})r_2'^5 + \ldots + (q_{11} + m_{13}m_{14} - 3m_{23}m_{13})r_2^5/f_1^5 \quad (35)$$

1.5.2) The Lagrange Invariant

Consider a ray through a lens with arbitary terminal points in image and object space (Figure 6). The ray can be described by position and momentum vectors $\underline{x}$ and $\underline{p}$.
Suppose that this ray suffers separately or simultaneously two perturbations. If we denote the generalised coordinates of the unperturbed ray by V, then the two resultant rays will have coordinates (V+dV) and (V+δV) respectively. It has been shown (see, for example, Sturrock, 1955) that the perturbations of the terminal points can be inter-related:-

$$\delta\underline{p}_1 . d\underline{x}_1 - d\underline{p}_1 . \delta\underline{x}_1 = \delta\underline{p}_2 . d\underline{x}_2 - d\underline{p}_2 . \delta\underline{x}_2 \quad (36)$$

Equation (36) represents the Lagrange Invariant. It is a general equation that is valid for all electron optic sytems (see Verster, 1963). We shall now proceed to express (36) in terms of our coordinate system.

Since we are considering meridional rays only and furthermore, we could, without loss of generality, restrict ourselves to initial perturbations in the r direction, we can write:-

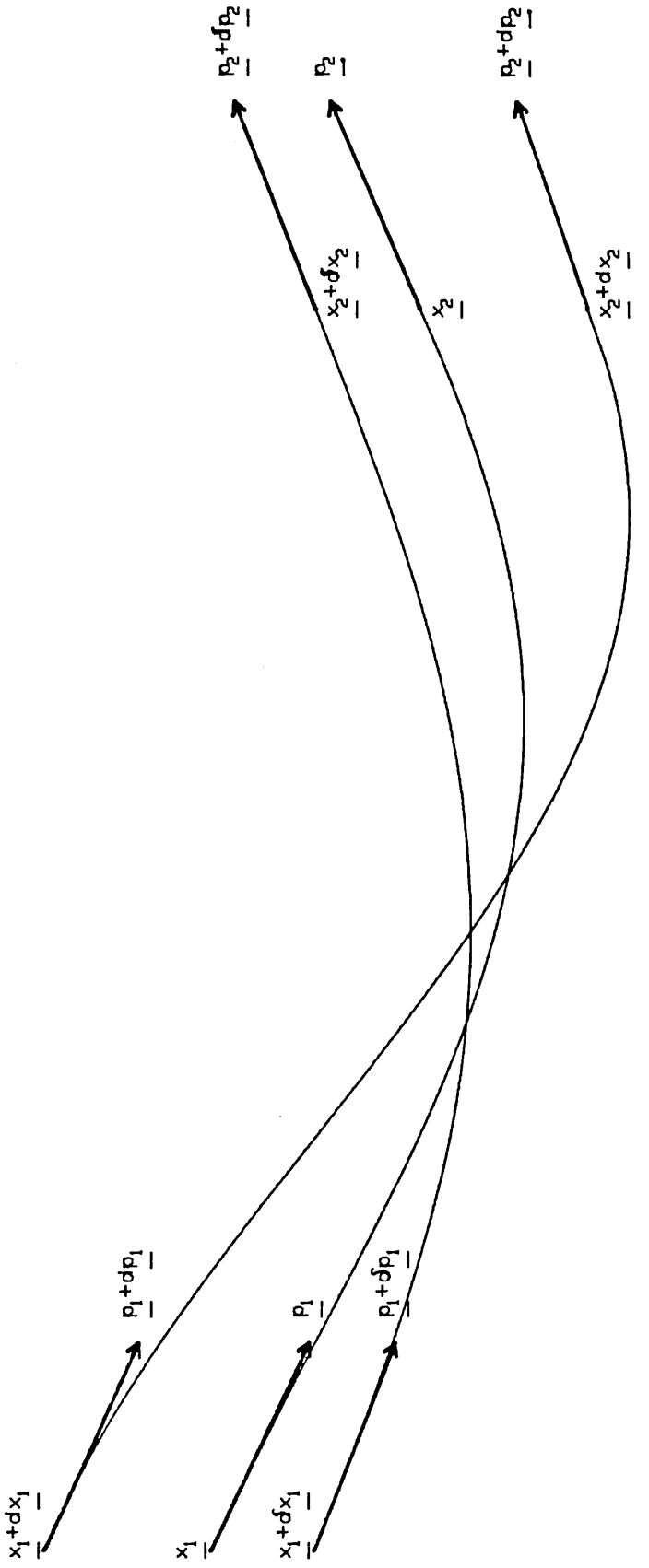

FIGURE 6. The increments which make up the Lagrange invariant. d and δ represent separate perturbations of the position and momentum vectors $\underline{x}$ and $\underline{p}$. The suffixes 1 and 2 denote object and image space respectively.

$$d\underline{x} = \underline{i}_r dr \tag{37}$$

$$\delta\underline{x} = \underline{i}_r \delta r \tag{38}$$

where $\underline{i}_r$ is a unit vector parallel to the r axis.

If $\underline{s}$ is a unit vector tangental to the ray:-

$$\underline{p} = p\,\underline{s} \tag{39}$$

Where the magnitude of the position vector, $\underline{p}$, is given by:-

$$p = (2em\phi + e^2\phi^2/c^2)^{1/2} \tag{40}$$

Hence, if we express $\underline{s}$ in terms of its radial and axial components and we assume that the terminal points of all three rays are in field free space, then:-

$$d\underline{p} = p\,(\underline{i}_r ds_r + \underline{i}_z ds_z) \tag{41}$$

$$\delta\underline{p} = p\,(\underline{i}_r \delta s_r + \underline{i}_z \delta s_z) \tag{42}$$

From (37), (38), (41) and (42):-

$$\delta\underline{p}.d\underline{x} - d\underline{p}.\delta\underline{x} = p\,(\delta s_r dr - ds_r \delta r) \tag{43}$$

We may eliminate s_r from (43) by realising that since r' is the gradient of the ray:-

$$s_r = r'(1 + r'^2)^{-1/2} \tag{44}$$

Therefore:-

$$\delta s_r = \delta r' \ (1 + r'^2)^{-3/2} \tag{45}$$

$$ds_r = dr' \ (1 + r'^2)^{-3/2} \tag{46}$$

Using (45) and (46) in (43):-

$$\delta \underline{p}.d\underline{x} - d\underline{p}.\delta \underline{x} = p \ (1 + r'^2)^{-3/2}.(\delta r'dr - dr'\delta r) \tag{47}$$

Substituting (47) into (36):-

$$p_1 (1+r_1'^2)^{-3/2}.(\delta r_1'dr_1 - dr_1'\delta r_1) = p_2 (1+r_2'^2)^{-3/2}.(\delta r_2'dr_2 - dr_2'\delta r_2) \tag{48}$$

If we note that:-

$$dr_2 = (\partial r_2/\partial r_1)dr_1 + (\partial r_2/\partial r_1')dr_1' \tag{49}$$

$$dr_2' = (\partial r_2'/\partial r_1)dr_1 + (\partial r_2'/\partial r_1')dr_1' \tag{50}$$

$$\delta r_2 = (\partial r_2/\partial r_1)\delta r_1 + (\partial r_2/\partial r_1')\delta r_1' \tag{51}$$

$$\delta r_2' = (\partial r_2'/\partial r_1)\delta r_1 + (\partial r_2'/\partial r_1')\delta r_1' \tag{52}$$

Then we can write:-

$$\delta r_2' dr_2 - dr_2'\delta r_2 = \left(\frac{\partial r_2'}{\partial r_1'}\frac{\partial r_2}{\partial r_1} - \frac{\partial r_2}{\partial r_1'}\frac{\partial r_2'}{\partial r_1}\right).(\delta r_1' dr_1 - dr_1'\delta r_1) \tag{53}$$

Furthermore, since the ratio of the focal lengths and the ratio of the refractive indices in object and image space are equivalent, it follows that (See Born and Wolf, 1959):-

$$f_1/f_2 = p_1/p_2 \tag{54}$$

(cf. non-relativistic limit: $f_1/f_2 = (V_1/V_2)^{1/2}$).

Using (53) and (54) in (48):-

$$f_1(1 + r_2'^2)^{3/2} = f_2(1 + r_1'^2)^{3/2}.\left(\frac{\partial r_2'}{\partial r_1'}\frac{\partial r_2}{\partial r_1} - \frac{\partial r_2'}{\partial r_1}\frac{\partial r_2}{\partial r_1'}\right) \tag{55}$$

This differential equation represents the Lagrange Invariant for the system that we are considering. It will be used later to simplify the relationship between incident and emergent rays. It is important to note that its use is restricted by the assumptions made in its derivation. In particular, it is applicable only to meridional rays in a lens whose focal

planes are in field free space.

SECTION TWO

THE COMPUTER MODEL

In this section we shall deal with the method used for simulating an electrostatic lens and calculating electron trajectories through it.

2.1) POTENTIAL AND FIELD DISTRIBUTION

There are a number of methods which can be used for calculating the potential distribution of an electrostatic lens in the absence of space charge. They are all based on the solution of Laplace's equation:-

$$\nabla^2\Psi(r,z) = 0 \qquad (56)$$

i) Probably the most readily implemented method involves approximating the continuous distribution by calculating the potential at discrete points on a mesh. (See, for example, Carre and Wreathall, 1964). Unfortunately the lack of continuity in the derived potential distribution could impose limitations on the accuracy to which first and second order derivatives can be calculated. The method was judged to be unsuitable for very accurate trajectory calculations.

ii) Since it is the charge on the electrodes that is ultimately responsible for the potential distribution, it is possible to deduce the latter by firstly calculating the distribution of surface charge (Read et al, 1971.) The method enables the accurate calculation of the potential and its derivatives and can be used to evaluate direct raypaths (Renau et al, 1982).

iii) In examining aberrations it will be necessary to calculate a large number of trajectories through a lens using a direct ray tracing technique. If fifth order effects are to be observed then each ray will have to be numerically integrated using a very large number of steps (this was found to be in the order of 10^6). So for practical reasons the method used had to be not only accurate but fast. The method used, therefore, was based on that described by Cook and Heddle (1976) which we shall now outline.

2.2) VARIATIONAL METHOD FOR CALCULATING POTENTIAL DISTRIBUTION

Given an approximate solution:-

$$\phi(r,z) = \sum_{i=1}^{n} \alpha_i \phi_i \qquad (57)$$

to Laplace's equation in a volume, Ω, we can define the function:-

$$W(\phi) = 0.5 \int_{\Omega} (\nabla\phi)^2 \, d\Omega \tag{58}$$

Where the Variational principle would suggest:-

$$W(\Psi) \leq W(\phi) \tag{59}$$

The two cylinder lens system that we are considering is shown in Figure 7. The volume of the lens can be treated as three regions as shown. Denoting the potential in the ith region by $\phi_i(r,z)$ it follows that:-

$$\phi_1(D/2,z) = V_1 \tag{60}$$

$$\phi_3(D/2,z) = V_2 \tag{61}$$

Where V_1 and V_2 are the electrode potentials. If the electrode gap, g, is small in comparison to the diameter, D, then we can write:-

$$\phi_2(D/2,z) = (z + g/2)(V_2 - V_1)/g + V_1 \tag{62}$$

Where we have assumed that the boundary potential for region 2 varies linearly with z. Cook has shown that for small gaps the discrepancy in axial potentials thus found and those calculated by a relaxation method (Natali et al, 1972) are negligible. This has been verified by Bonjour (1979) whose

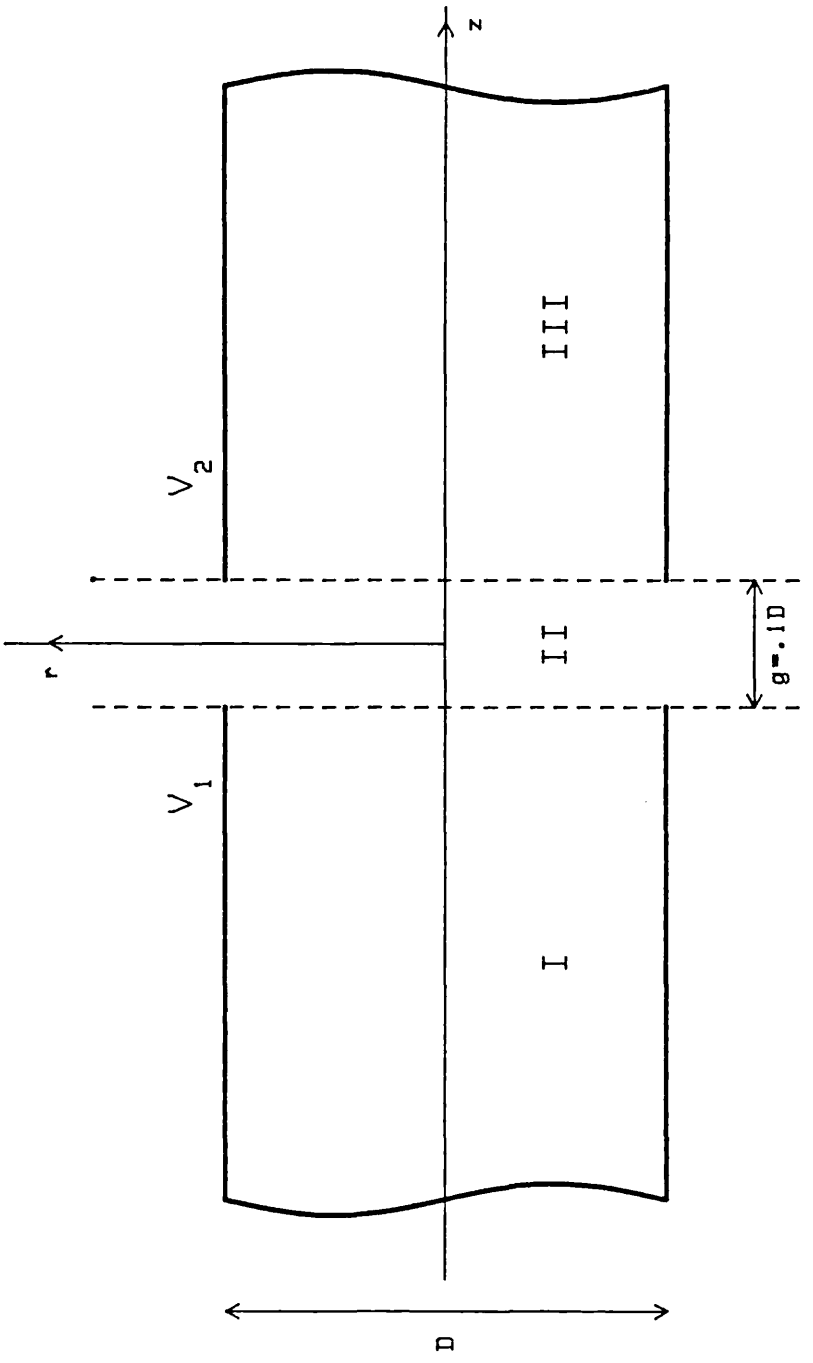

FIGURE 7. Schematic diagram of the two cylinder lens that was modelled by the computer, showing the three regions in which the various potential and field expressions apply.

variational method used a third order approximation for the central boundary potential. Moreover, for thick walled lens sytems the linear hypothesis is directly justified. We therefore feel that a useful analysis of aberrations can be founded on this potential model. This is validated by the good agreement of our measuments of third and fifth order aberration coefficients with those produced by other authors.

Using the boundary conditions of equations (60), (61) and (62), the coefficients, α_i, of (57) can be detemined by minimising the potential energy, $W(\phi)$, of the system. Hence, it can be shown that the potential in each of the three regions is given by:-

$$\phi_1(R,Z) = V_1 + \frac{(V_2 - V_1)}{G} \sum_{n=1}^{\infty} Q_n J_0(k_n R)(A_n - B_n) \tag{63}$$

$$\phi_2(R,Z) = \frac{(V_1 + V_2)}{2} + \frac{(V_2 - V_1)Z}{G} + \frac{(V_2 - V_1)}{G} \sum_{n=1}^{\infty} Q_n J_0(k_n R)(A_n^{-1} - B_n) \tag{64}$$

$$\phi_3(R,Z) = V_2 - \frac{(V_2 - V_1)}{G} \sum_{n=1}^{\infty} Q_n J_0(k_n R)(B_n^{-1} - A_n^{-1}) \tag{65}$$

Where:-

$$A_n(z) = \exp\left(k_n(2z+G)\right), \quad B_n(z) = \exp\left(k_n(2z-G)\right) \tag{66}$$

And:-

$$G = g/D, \quad Z = z/D, \quad R = 2r/D \tag{67}$$

$J_0(x)$ is the Bessel function of order zero and k_n is the nth root of $J_0(x)$. Finally:-

$$Q_n = \left(2k_n^2 . J_1(k_n)\right)^{-1} \tag{68}$$

The derivatives of the potential can be calculated readily from these equations. For example, in the central region:-

$$\frac{\partial \phi_2}{\partial z} = \frac{(V_2 - V_1)}{GD} - \frac{2(V_2 - V_1)}{GD} \sum_{n=1}^{\infty} Q_n k_n J_0(k_n R)(A_n^{-1} + B_n) \tag{69}$$

$$\frac{\partial \phi_2}{\partial r} = -\frac{2(V_2 - V_1)}{GD} \sum_{n=1}^{\infty} Q_n k_n J_1(k_n R)(A_n^{-1} - B_n) \tag{70}$$

$$\frac{\partial^2 \phi_2}{\partial z^2} = \frac{4(V_2 - V_1)}{GD^2} \sum_{n=1}^{\infty} Q_n k_n^2 J_0(k_n R)(A_n^{-1} - B_n) \tag{71}$$

$$\frac{\partial^2 \phi_2}{\partial r^2} = \frac{-2}{DR} \frac{\partial \phi_2}{\partial r} - \frac{\partial^2 \phi_2}{\partial z^2} \tag{72}$$

$$\frac{\partial^2 \phi_2}{\partial z \partial r} = \frac{4(V_2 - V_1)}{GD^2} \sum_{n=1}^{\infty} Q_n k_n^2 J_1(k_n R)(A_n^{-1} - B_n) \tag{73}$$

The values of k_n and $J_1(k_n)$ to 10 decimal places were taken from the British Association Mathematical Tables, 1958. The similarity between the expressions for the potential and each of its derivatives enables the equations to be evaluated simultaneously, term by term. This expedient is extremely beneficial to the overall time required to determine a raypath.

2.2.1) Evaluation of Bessel Functions

The first and zeroth order Bessel functions ($J_1(x)$ and $J_0(x)$ respectively) were evaluated by a method that depended on the magnitude of their argument.

For $x<20$ the general solution of Bessel's equation was used (see, for example, Stephenson,1973):-

$$J_n(x) = \sum_{r=0}^{\infty} \frac{(-1)^r}{r!(n+r)!} \left(\frac{x}{2}\right)^{(n+2r)} \tag{74}$$

For $x\geq 20$ an asymptotic series solution was employed:-

$$J_0(x) = A_0(x)\sin(x) + B_0(x)\cos(x) \tag{75}$$

$$J_1(x) = B_1(x)\sin(x) - A_1(x)\cos(x) \tag{76}$$

Where:-

$$A_{0,1}(x) = \left(P_{0,1}(x) - Q_{0,1}(x)\right) / (\pi x)^{1/2} \tag{77}$$

$$B_{0,1}(x) = \left(P_{0,1}(x) + Q_{0,1}(x)\right) / (\pi x)^{1/2} \tag{78}$$

and:-

$$P_0(x) = 1 - \frac{1^2.3^2}{2!(8x)^2} + \frac{1^2.3^2.5^2.7^2}{4!(8x)^4} - \frac{1^2.3^2.5^2.7^2.9^2.11^2}{6!(8x)^6} + \ldots\ldots \tag{79}$$

$$Q_0(x) = -\frac{1^2}{1!8x} + \frac{1^2.3^2.5^2}{3!(8x)^3} - \frac{1^2.3^2.5^2.7^2.9^2}{5!(8x)^5} + \ldots\ldots \quad (80)$$

$$P_1(x) = 1 + \frac{1^2.3.5}{2!(8x)^2} - \frac{1^2.3^2.5^2.7.9}{4!(8x)^4} + \frac{1^2.3^2.5^2.7^2.9^2.11.13}{6!(8x)^6} - \ldots\ldots \quad (81)$$

$$Q_1(x) = \frac{1.3}{1!8x} - \frac{1^2.3^2.5.7}{3!(8x)^3} + \frac{1^2.3^2.5^2.7^2.9.11}{5!(8x)^5} - \ldots\ldots \quad (82)$$

In both regions summation stopped when a precision of 10 decimal places had been achieved or with the 80th term if $x<20$ or the 20th term if $x \geq 20$. Convergence was generally much faster than these limits.

The accuracy of the Bessel function was tested by comparison with published data. The quoted precisions were derived by extending its accuracy until raypaths through the system were found to be insensitive to the inclusion of additional terms.

2.2.2) Accuracy and Speed of Calculations

The accuracy and speed with which the potential and its derivatives could be found depended upon the number of terms that were used in equations (63)-(65) and (69)-(73). Generally these were found to be highly convergent. Each was evaluated to a precision of 6 decimal places, except when this did not occur by the 150th term (as is the case, for example, when z=+- g/2). In these cases the mean of the sums of the first 149 and 150 terms was used.

Table 1 shows the variation of axial potential for a lens with

$V_1 = 0$ and $V_2 = 1$. The number of terms (n) used for the summations are also shown. It can be seen that the results agree well with the results of other authors.

TABLE 1. AXIAL POTENTIAL FOR A TWO CYLINDER LENS.

(g/D = 0.1, V_2 = 1, V_1 = 0)

z/D	$\phi_0(z)$ Present	n	$\phi_0(z)$ Cook,1976	$\phi_0(z)$ Natali,1972
0.000	0.500000	1	0.500000	0.500000
0.025	0.467103	43	0.467101	0.467115
0.050	0.434504	150	0.434504	0.434532
0.075	0.402496	43	0.402494	0.402538
0.100	0.371344	25	0.371343	0.371399
0.125	0.341282	18	0.341283	0.341351
0.150	0.312514	14	0.312515	0.312592
0.175	0.285195	12	0.285196	0.285279
0.200	0.259440	10	0.259440	0.259528
0.225	0.235324	9	0.235323	0.235413
0.250	0.212879	8	0.212880	0.212969
0.300	0.172994	7	0.172994	0.173079
0.350	0.139489	6	0.139489	0.139566
0.400	0.111785	5	0.111785	0.111851
0.450	0.089157	5	0.089157	0.089212
0.500	0.070851	4	0.070851	0.070897
0.600	0.044407	4	0.044407	0.044436
0.700	0.027658	3	0.027658	0.027676
0.800	0.017168	3	0.017168	0.017178
0.900	0.010636	3	0.010636	0.010642
1.000	0.006583	3	0.006583	0.006586
1.100	0.004072	2	0.004072	0.004074
1.200	0.002518	2	0.002518	0.002519
1.300	0.001557	2	0.001557	0.001557
1.400	0.000962	2	0.000962	0.000962
1.500	0.000595	2	0.000595	0.000595

2.3) TRAJECTORY CALCULATION

Electron trajectories were calculated by numerically integrating the Newtonian equations of motion (see equations (3) and (4)).

The basis of this method lies in the power series expansion of the electron coordinates in terms of time:-

$$z(t) = z_o + \left(\frac{dz}{dt}\right)_o t + \frac{1}{2}\left(\frac{d^2z}{dt^2}\right)_o t^2 + \frac{1}{6}\left(\frac{d^3z}{dt^3}\right)_o t^3 + \ldots\ldots \quad (83)$$

$$r(t) = r_o + \left(\frac{dr}{dt}\right)_o t + \frac{1}{2}\left(\frac{d^2r}{dt^2}\right)_o t^2 + \frac{1}{6}\left(\frac{d^3r}{dt^3}\right)_o t^3 + \ldots\ldots \quad (84)$$

Where z(t) and r(t) are the coordinates of an electron, with initial coordinates denoted by suffix 0, after a short time, t.

The accuracy of this method will depend upon the number of terms in (83) and (84) which are used and, in turn, on the size of t used for integration. The accuracy of each step can be checked during integration by, for example, a predictor corrector method.

The method that was adopted initially was based on that described by Renau (1979), which used only the first three terms of (83) and (84). However, this was found to require a very small integration step length and, moreover, the raypaths were found not to converge to the Gaussian limit for paraxial rays. A much better method was found to be one which incorporated second order variations in potential and thus the

first four terms of (83) and (84).

The electron velocities at the end of a step are given by:-

$$\frac{dz}{dt}(t) = \left(\frac{dz}{dt}\right)_o + \left(\frac{d^2z}{dt^2}\right)_o t + \frac{1}{2}\left(\frac{d^3z}{dt^3}\right)_o t^2 \qquad (85)$$

$$\frac{dr}{dt}(t) = \left(\frac{dr}{dt}\right)_o + \left(\frac{d^2r}{dt^2}\right)_o t + \frac{1}{2}\left(\frac{d^3z}{dt^3}\right)_o t^2 \qquad (86)$$

Where the second differentials of z and r with respect to t are given by Newton's equations and hence:-

$$\left(\frac{d^3z}{dt^3}\right)_o = \mathcal{J}\left(\frac{\partial^2\phi}{\partial z^2}\right)_o\left(\frac{dz}{dt}\right)_o + \mathcal{J}\left(\frac{\partial^2\phi}{\partial z\partial r}\right)_o\left(\frac{dr}{dt}\right)_o \qquad (87)$$

$$\left(\frac{d^3r}{dt^3}\right)_o = \mathcal{J}\left(\frac{\partial^2\phi}{\partial r^2}\right)_o\left(\frac{dr}{dt}\right)_o + \mathcal{J}\left(\frac{\partial^2\phi}{\partial z\partial r}\right)_o\left(\frac{dz}{dt}\right)_o \qquad (88)$$

The final expressions are simpified if we use scaled time:-

$$T = (2\mathcal{J})^{1/2}t \qquad (89)$$

Bringing together these equations allows us to derive the recurrence relationships for the position and velocity of the electron:-

$$z(t) = z_o + \left(\frac{dz}{dT}\right)_o T + \frac{1}{4}\left(\frac{\partial\phi}{\partial z}\right)_o T^2 + \frac{1}{12}\left[\left(\frac{\partial^2\phi}{\partial z^2}\right)_o\left(\frac{dz}{dT}\right)_o + \left(\frac{\partial^2\phi}{\partial z\partial r}\right)_o\left(\frac{dr}{dT}\right)_o\right]T^3 \qquad (90)$$

$$r(t) = r_o + \left(\frac{dr}{dT}\right)_o T + \frac{1}{4}\left(\frac{\partial \phi}{\partial r}\right)_o T^2 + \frac{1}{12}\left[\left(\frac{\partial^2 \phi}{\partial r^2}\right)_o \left(\frac{dr}{dT}\right)_o + \left(\frac{\partial^2 \phi}{\partial z \partial r}\right)_o \left(\frac{dz}{dT}\right)_o\right] T^3 \quad (91)$$

$$\frac{dz}{dT}(t) = \left(\frac{dz}{dT}\right)_o + \frac{1}{2}\left(\frac{\partial \phi}{\partial z}\right)_o T + \frac{1}{4}\left[\left(\frac{\partial^2 \phi}{\partial z^2}\right)_o \left(\frac{dz}{dT}\right)_o + \left(\frac{\partial^2 \phi}{\partial z \partial r}\right)_o \left(\frac{dr}{dT}\right)_o\right] T^2 \quad (92)$$

$$\frac{dr}{dT}(t) = \left(\frac{dr}{dT}\right)_o + \frac{1}{2}\left(\frac{\partial \phi}{\partial r}\right)_o T + \frac{1}{4}\left[\left(\frac{\partial^2 \phi}{\partial r^2}\right)_o \left(\frac{dr}{dT}\right)_o + \left(\frac{\partial^2 \phi}{\partial z \partial r}\right)_o \left(\frac{dz}{dT}\right)_o\right] T^2 \quad (93)$$

The values of $(dz/dT)_o$ and $(dr/dT)_o$ at the beginning of a trajectory may be derived from the angle, θ, that it makes with the optic axis:-

$$(dz/dT)_o = \phi_o^{1/2} \cos(\theta_o) \quad (94)$$

$$(dr/dT)_o = \phi_o^{1/2} \sin(\theta_o) \quad (95)$$

Equations (90)-(95) therefore enable the calculation of a raypath from object to image space. The accuracy of the method is dependent on the choice of time interval, T, for the step length. This interval of normalised time is related to the trajectory step length, Δs, by:-

$$T = \Delta s / (\phi)^{1/2} \quad (96)$$

2.3.1) Variation of the Integration Step Length

Two shortcomings result from integration by fixed step

length:-

i) Computing time is wasted by using steps which need to be small enough for the regions of highest field strength and are therefore unnecessarily large in other regions.

ii) Whenever a lens with different electrode potentials is considered, new checks will have to be made to ensure optimum choice of step length.

By allowing the routine to have variable step length it becomes both more efficient and universal. In regions of low field the step would be large and vice versa. A number of methods of incorporating this modification were tried, each based on testing the field strength either directly, or indirectly by examining deviations in path direction and velocity. The simple method which was finally adopted was based on the accuracy of the potential calculation routine. Denoting initial values by suffix 0 and final values by suffix 1, the change in electron kinetic energy during a step is given by:-

$$\Delta E = m(V_1^2 - V_0^2)/2 \qquad (97)$$

The discrepancy between the apparent and calculated potential difference is therefore:-

$$\varepsilon = \left| (\phi_1 - \phi_0) - \Delta E/e \right| \qquad (98)$$

Since the potential at a point was calculated to a precision

of 10^{-6}, we could use the following criteria to govern the integration step length: If after calculating a step it was found that $\varepsilon > 10^{-6}$, then T was halved and the step recalculated; If $\varepsilon < 2*10^{-7}$, then T was doubled for the next step in the integration. Minimum and maximum values of T had to be fixed and these were 10^{-7} and 10^{-1} lens diameters respectively. The first step of a trajectory was calculated with the minimum step length.
The numeric values that have been quoted were each determined by variation until the raypath became stationary with respect to increasing precision.

2.4) TESTING THE COMPUTER MODEL

In addition to checking the accuracy of particular aspects of the model such as the potential and field distributions, it was necessary to evaluate its overall performance. We shall outline the two principal checks that have been made.

2.4.1) Paraxial Rays

When trajectories progressively fill the aperture of a lens, the resultant geometric aberrations can be considered as systematic perturbations of the paraxial focus. It is of fundamental importance to our present study that calculated trajectories should have a Gaussian limit to their paraxial

focus. A simple test of the ray tracing procedure was therefore to compare the parameters of emergent paraxial rays to those predicted by Gaussian optics.

The Picht equation (13) was numerically integrated by the Fox-Goodwin method (see, for example, Buckingham, 1962), using a short step length (10^{-3} lens diameters). The paths of rays, integrated from axis with a launch angle of 10^{-4} radians, were compared to those calculated by the model. The overall correlation was extremely good.

A typical set of results is shown in Table 2. The small discrepancy between the two results is a consequence of the finite launch angle of the rays. The presence of spherical aberration causes the non-Gaussian ray to have both slightly larger angular magnification and to be imaged nearer the lens. This conclusion was justified by examining rays with diminished launch angles. The Gaussian limit was further approached but never exceeded.

TABLE 2. ANGULAR MAGNIFICATION AND IMAGE DISTANCE OF PARAXIAL RAYS.

(Two cylinder lens. g/D=0.1 $V_2/V_1=10$)

	Picht ray		Direct ray	
P	Q	M_α	Q	M_α
1.75	15.88	-0.05428	15.86	-0.05437
1.80	11.95	-0.07408	11.94	-0.07418
1.85	9.679	-0.09389	9.622	-0.09407
1.90	8.198	-0.1137	8.189	-0.1138
1.95	7.156	-0.1335	7.145	-0.1336
2.00	6.384	-0.1533	6.378	-0.1535

2.4.2) Aberrated Rays

The final test of the accuracy of the model was to use it to calculate the aberration coefficients of equations (23), (24), (34) and (35). In a later section we will show how the model has enabled all of the third and fifth order coefficients to be evaluated but, for the present, we seek only to show how the third order aberrations of parallel rays can be calculated and to check that they are consistent with the results of other authors.

We have already seen that the behaviour of a trajectory is governed generally by eight third order coefficients. However, if we consider rays from an infinitely distant object ($r_1'=0$), it follows from (23) and (24) that:-

$$r_2' = -r_1/f_2 + m_{16}r_1^3/f_2^3 \qquad (99)$$

$$r_2/f_1 = m_{26}r_1^3/f_2^3 \qquad (100)$$

Where we have included terms up to the third order only. Conversely, if a ray emerges parallel to the optic axis, then from (34) and (35) it follows that:-

$$r_1' = r_2/f_1 - m_{25}r_2^3/f_1^3 \qquad (101)$$

$$r_1/f_2 = m_{13}r_2^3/f_1^3 \qquad (102)$$

These relationships provide us with a relatively

straightforward method of calculating four of the third order coefficients. Trajectories with $r_1'=0$ and $r_2'=0$ were used with a Least Squares fitting program to obtain m_{13}, m_{16}, m_{23} and m_{26} from equations (99)-(102). In order that fifth and higher order effects should not detract from the accuracy of the calculations, the fit was restricted to rays for which the ratio of asymptotic radial displacement at the lens centre to the radius of the lens (ie the filling factor) was less than 30%.

The results are shown in Table 3 along with the results of other authors. The results of Read have been derived from his Cs coeffients using the the data and relationships that he gives in his book (1976). Kuyatt et al (1972) quote an accuracy of 10% ("with one or two possible exceptions") for their coefficients. Verster's results were derived from an electrolytic tank model (1963).

The principal limitation to the precision of the results that we give here is the inability to decide accurately the maximum filling factor that should be considered for the third order least squares fit. Nevertheless, although we have taken this (somewhat arbitarily) to be 30%, our results are generally consistent with those of other authors. We shall return to this problem later on when we make more precise calculations of the aberration coefficients.

TABLE 3. THIRD ORDER ABERRATION COEFFICIENTS FOR PARALLEL RAYS.

(2 Cylinder Lens. g/D = 0.1)

V_2/V_1		Present	Read (1976)	Kuyatt (1972)	Verster (1963)
2	m_{13}	-305	-278	-285	
	m_{16}	-488	-467	-502	
	m_{23}	-362	-331	-364	
	m_{26}	-577	-553	-575	
5	m_{13}	-7.86	-7.02	-7.34	-7.32
	m_{16}	-22.9	-22.2	-23.6	-9.18
	m_{23}	-11.7	-10.5	-11.0	-9.21
	m_{26}	-33.7	-32.6	-34.7	-36.8
10	m_{13}	-1.72	-1.46	-1.44	-1.58
	m_{16}	-7.54	-7.34	-7.06	-1.48
	m_{23}	-3.22	-2.74	-2.71	-3.37
	m_{26}	-13.1	-12.8	-12.2	-15.7
20	m_{13}	-.570	-.470	-.460	-.480
	m_{16}	-3.66	-3.54	-3.44	-.40
	m_{23}	-1.46	-1.19	-1.16	-1.52
	m_{26}	-7.85	-7.55	-7.27	-9.68

SECTION THREE

RESULTS

The computer model was used to calculate trajectories for a large number of rays through the system shown in Figure 7. Both accelerating and decelerating lenses were considered with voltage ratios ranging from near unipotential to 40:1. Raypaths with filling factors of up to 90% and linear magnification anywhere from zero to infinity were calculated. The discussion that follows is based on the results of over 1000 trajectories.

Throughout this discussion we shall consider each ray as emerging from axis at a distance P to the left of the centre of the lens and to intercept the axis again at a distance Q to the right of the lens centre. When measurements are made in regions of finite field, P and Q correspond to the asymptotes of the ray. The same is true for the treatment of r and r' which were defined in section two. It can be seen from Figure 5 that:-

$$r_1' = r_1 / (P - F_1) \qquad (103)$$

$$-r_2' = r_2 / (Q - F_2) \qquad (104)$$

We shall use M and M_α to refer to the linear and angular magnifications of a paraxial ray from P, which recrosses the optic axis at the Gaussian image plane, a distance Q_o from the

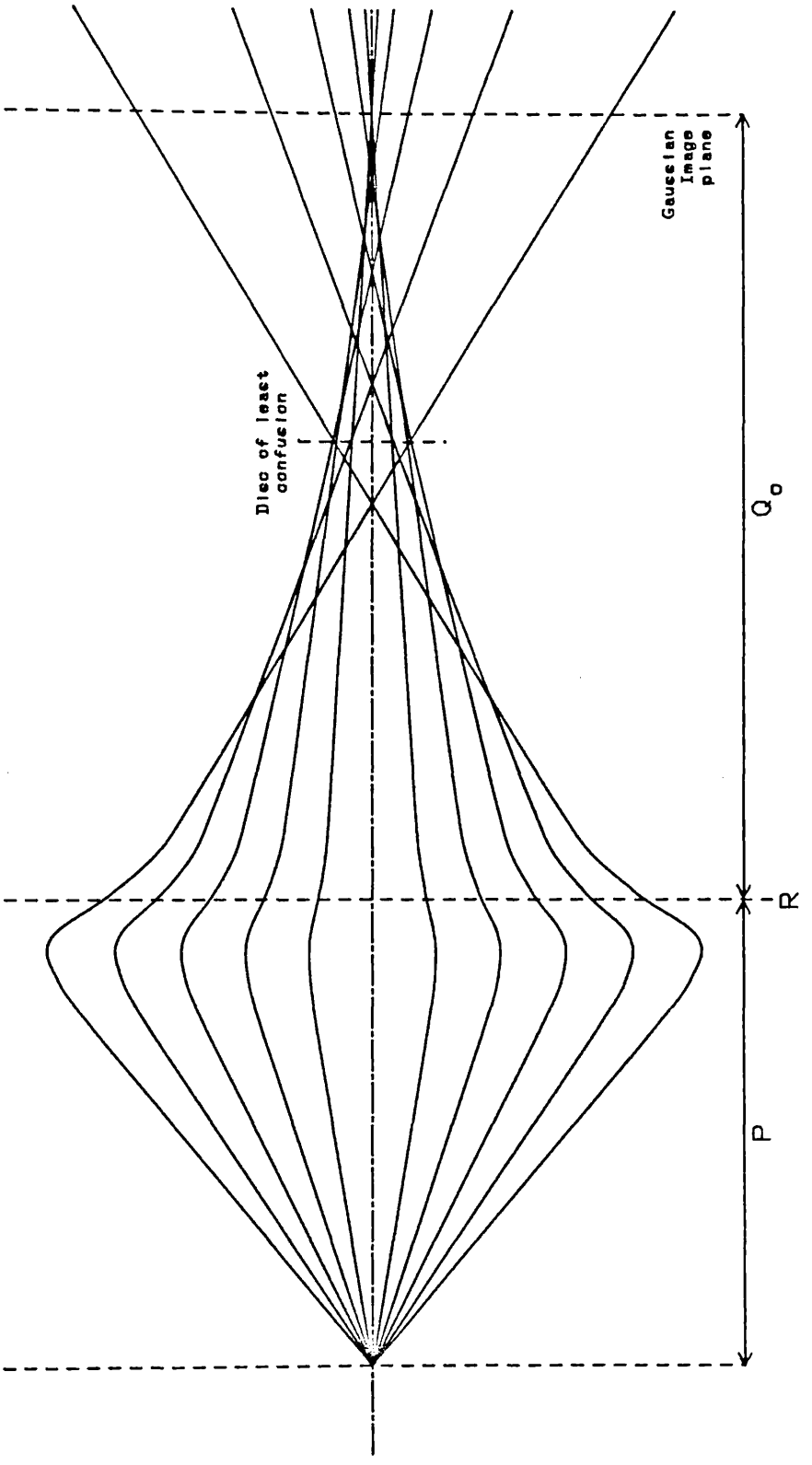

FIGURE 8. Aberration of an image of a point axial object. The disc of least confusion is defined by the minimum beam waist in image space and it occurs before the Gaussian image plane.

reference plane of the lens.
All the lenses examined exhibited positive spherical aberration ie. Q decreased with increased filling. A typical set of trajectories are shown in Figure 8.

3.1) RELATIONSHIPS BETWEEN IMAGE AND OBJECT SPACE

The evaluation of the third order aberration coefficients such as those used in equations (23) and (24) has been the subject of many papers (see, for example, Kuyatt et al, 1972 or Harting and Read, 1976). Our initial investigations are not concerned directly with the evaluation of these coefficients, but instead we shall look at alternative connections between the parameters of a ray in image and object space.
The Helmholtz-Lagrange relationship suggests that the linear and angular magnifications of a paraxial ray are simply related. By examinig this relationship for aberrated rays we have found that for rays emerging from the same axial point:-

$$r_1'/r_2' \propto Q \qquad (105)$$

This relationship is illustrated in Figures (9)-(16). Although the gradients and the intercepts of the graphs are dependent on the voltage ratio and the object distance, the relationship between the image distance and the ratio of input and output slopes of the ray proved to be linear for all tested object

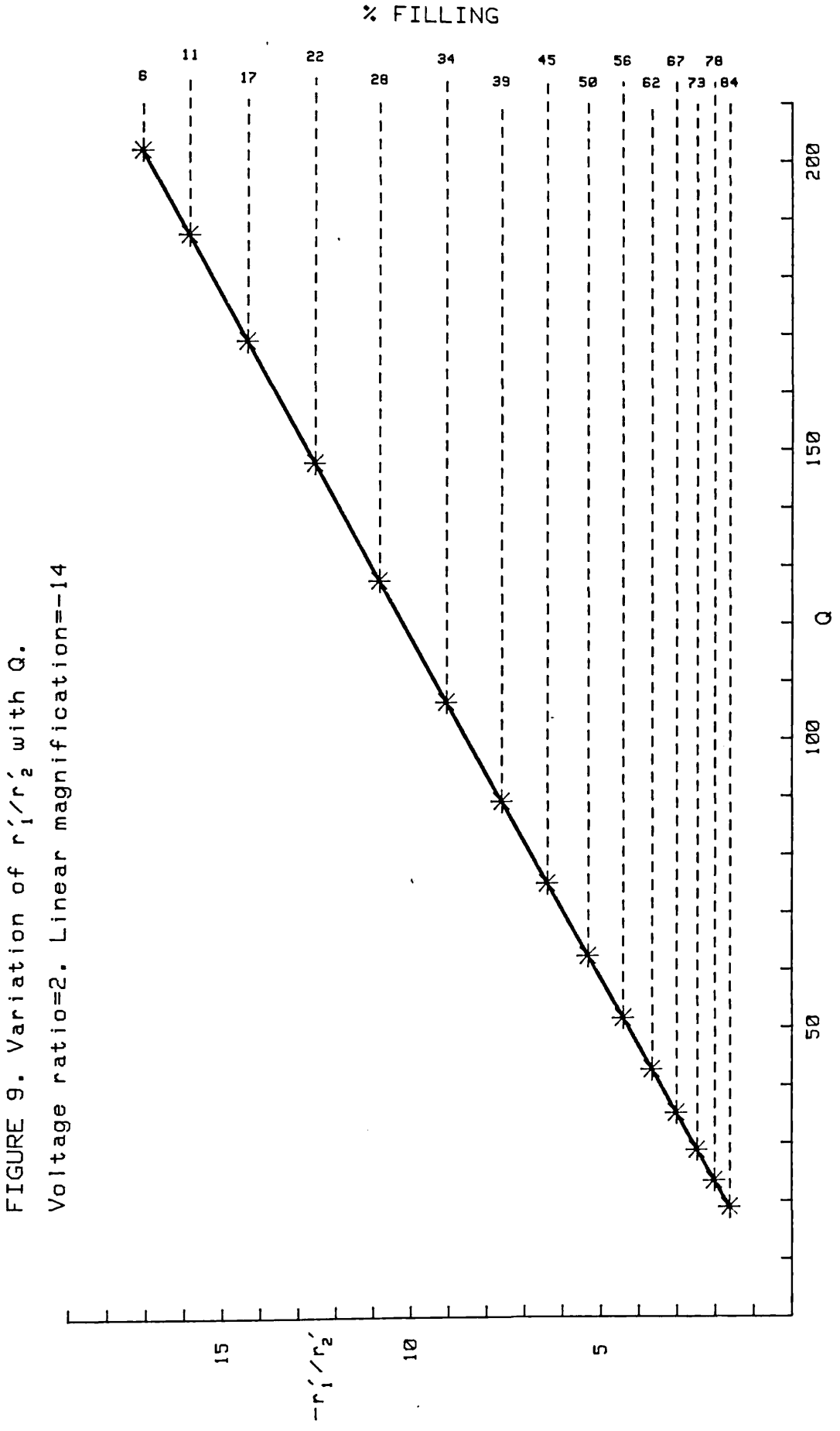

FIGURE 9. Variation of r_1'/r_2' with Q.
Voltage ratio=2. Linear magnification=-14

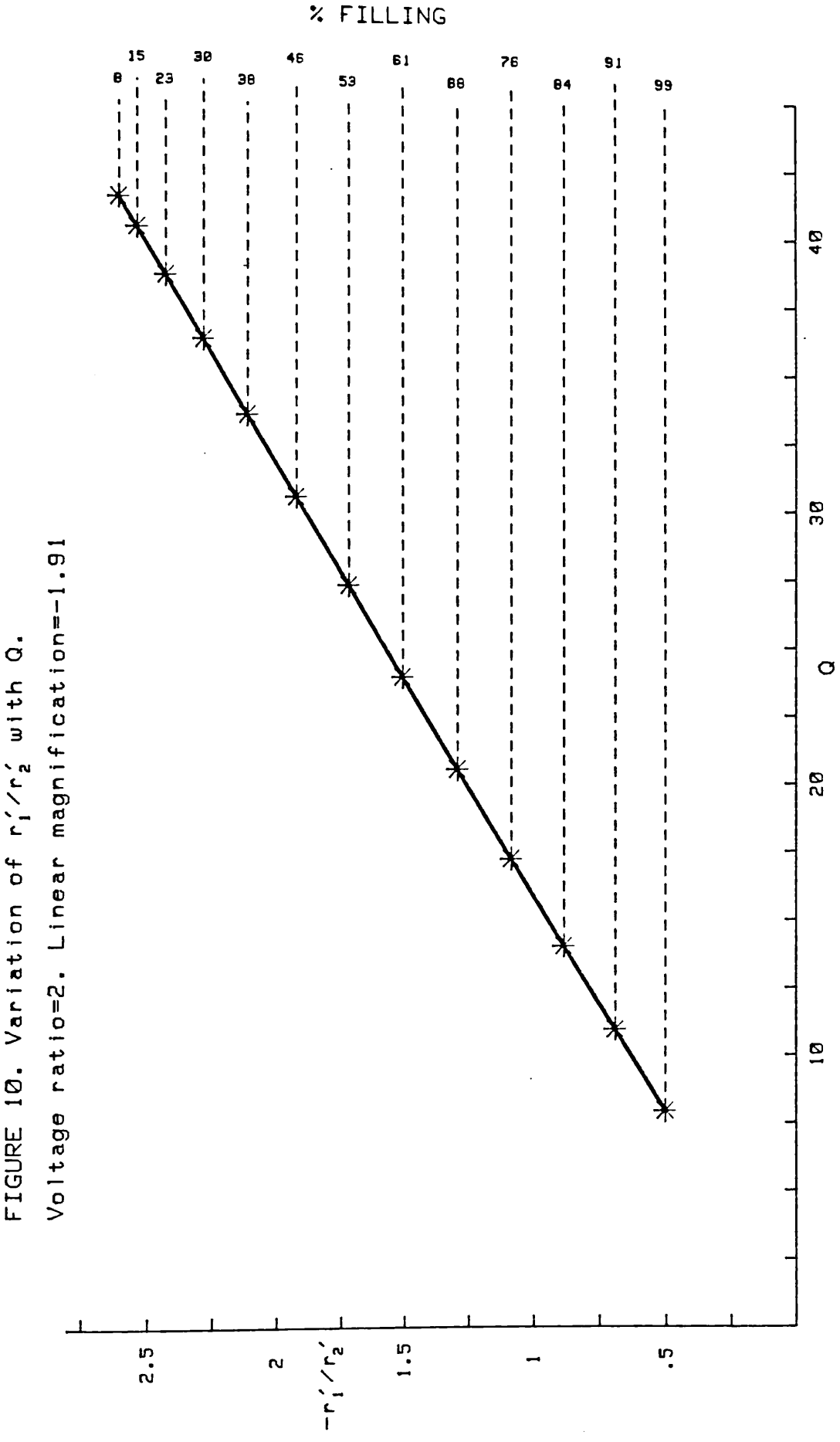

FIGURE 10. Variation of r_1'/r_2' with Q.
Voltage ratio=2. Linear magnification=-1.91

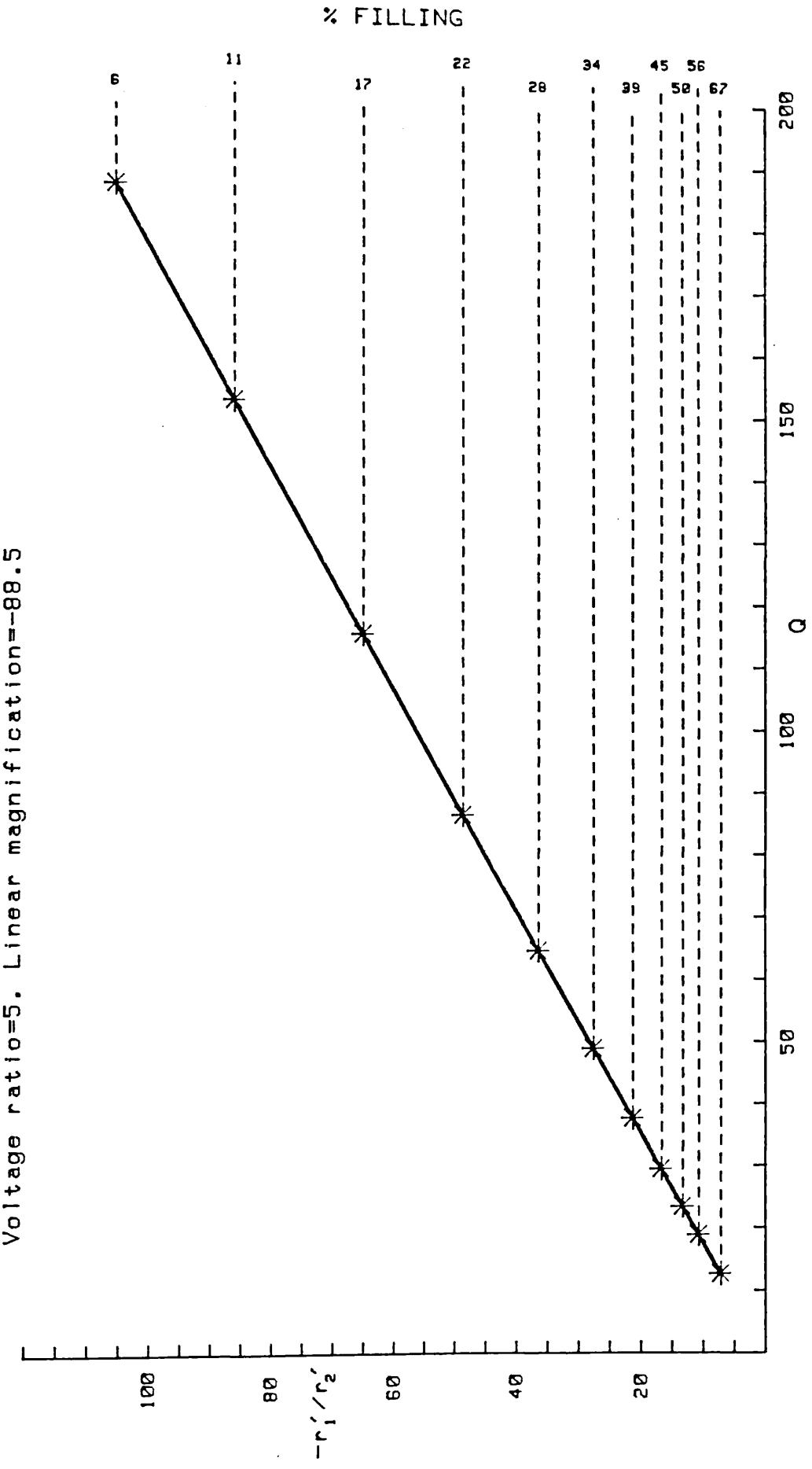

FIGURE 11. Variation of r_1'/r_2' with Q.
Voltage ratio=5. Linear magnification=-88.5

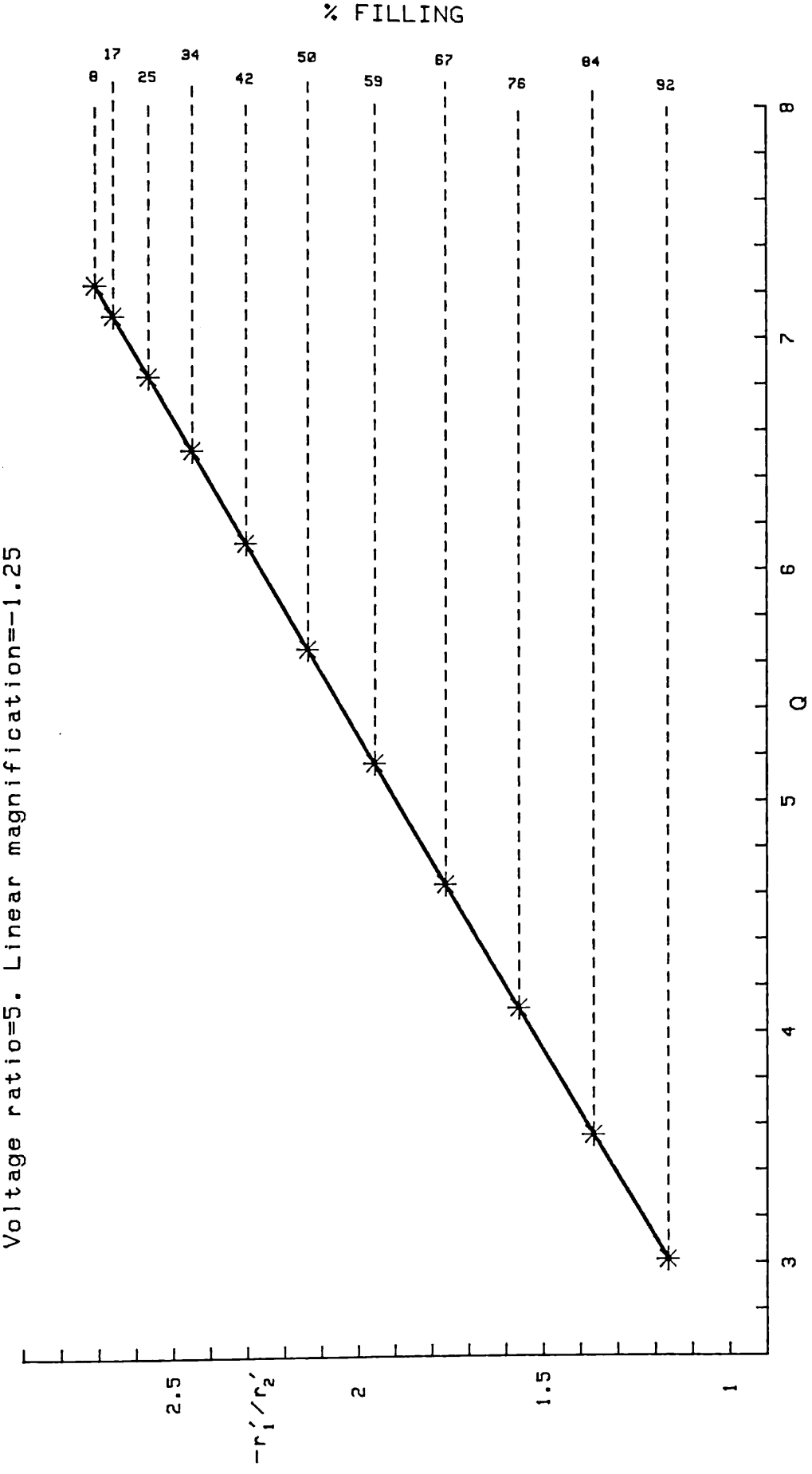

FIGURE 12. Variation of r_1'/r_2' with Q.
Voltage ratio=5. Linear magnification=-1.25

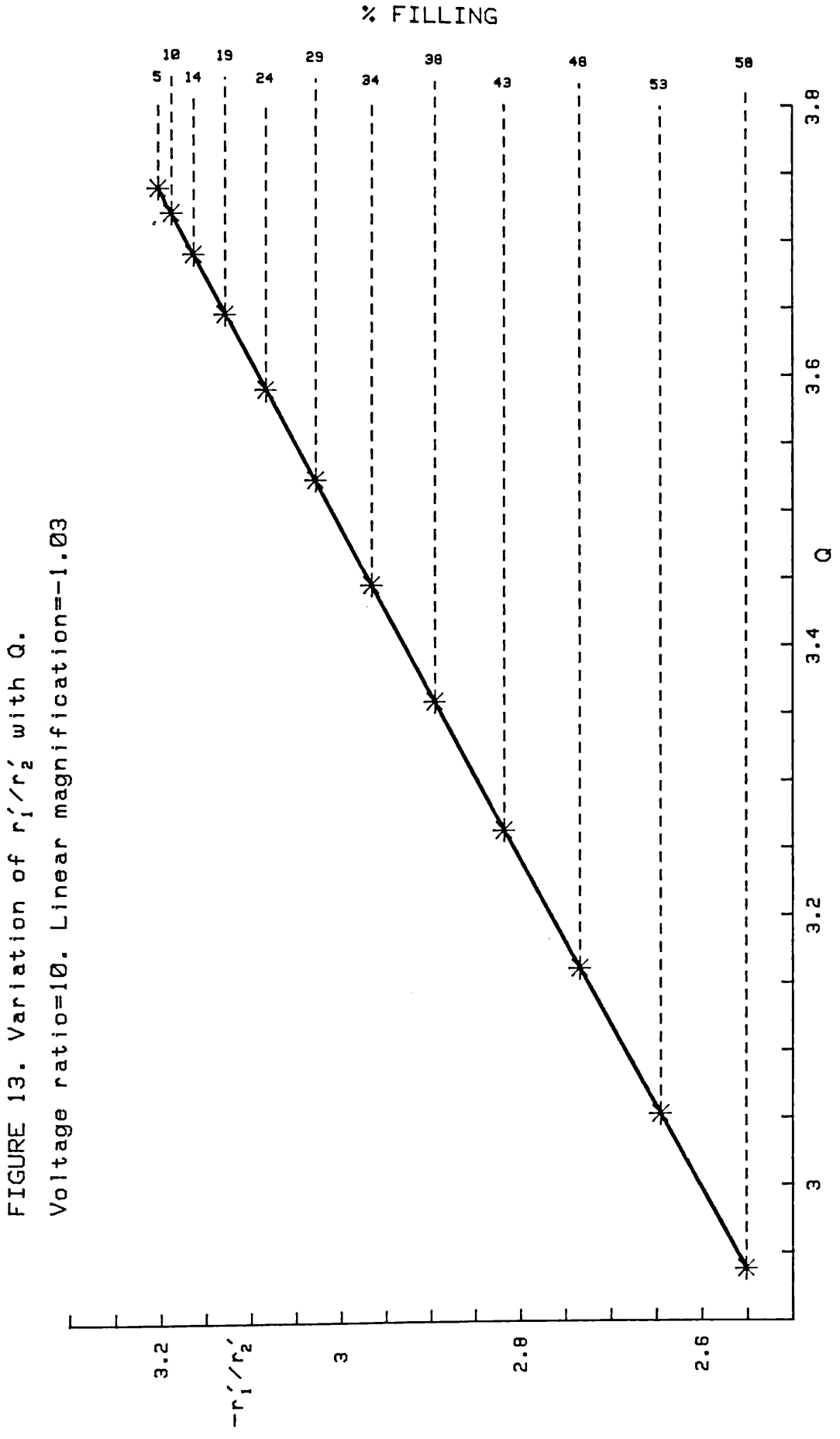

FIGURE 13. Variation of r_1'/r_2' with Q.
Voltage ratio=10. Linear magnification=-1.03

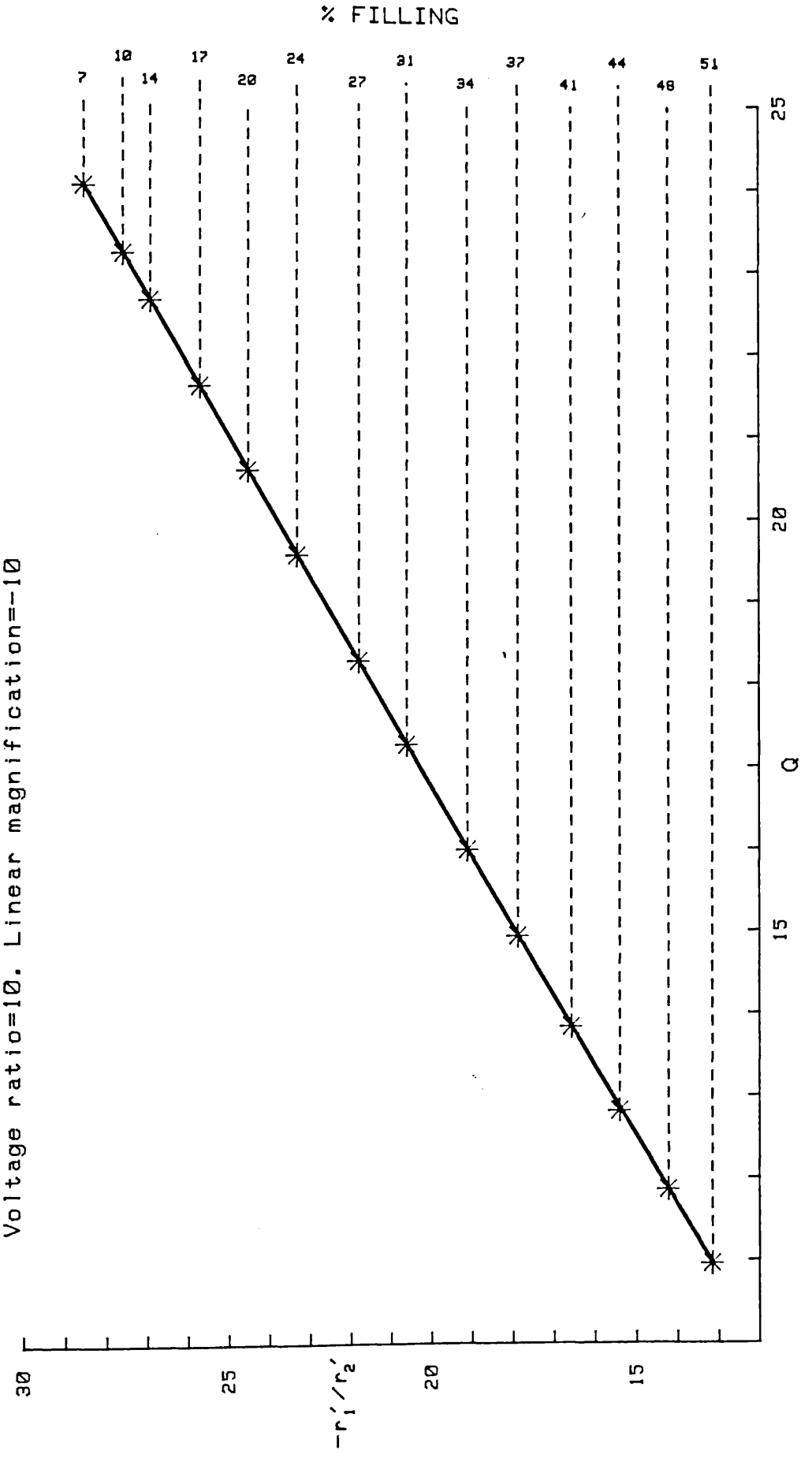

FIGURE 14. Variation of r_1'/r_2' with Q.
Voltage ratio=10. Linear magnification=-10

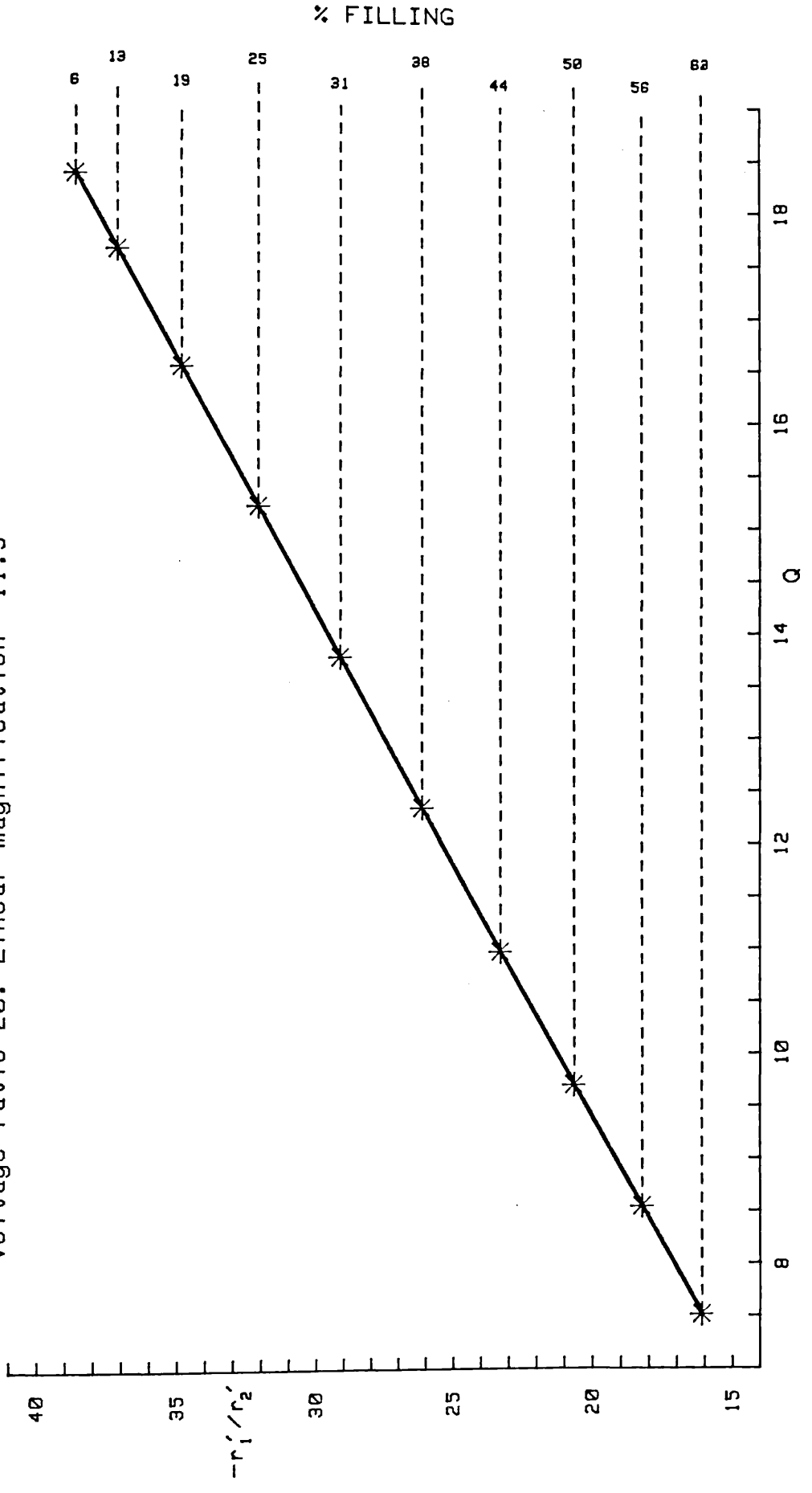

FIGURE 15. Variation of r_1'/r_2' with Q.
Voltage ratio=20. Linear magnification=-11.5

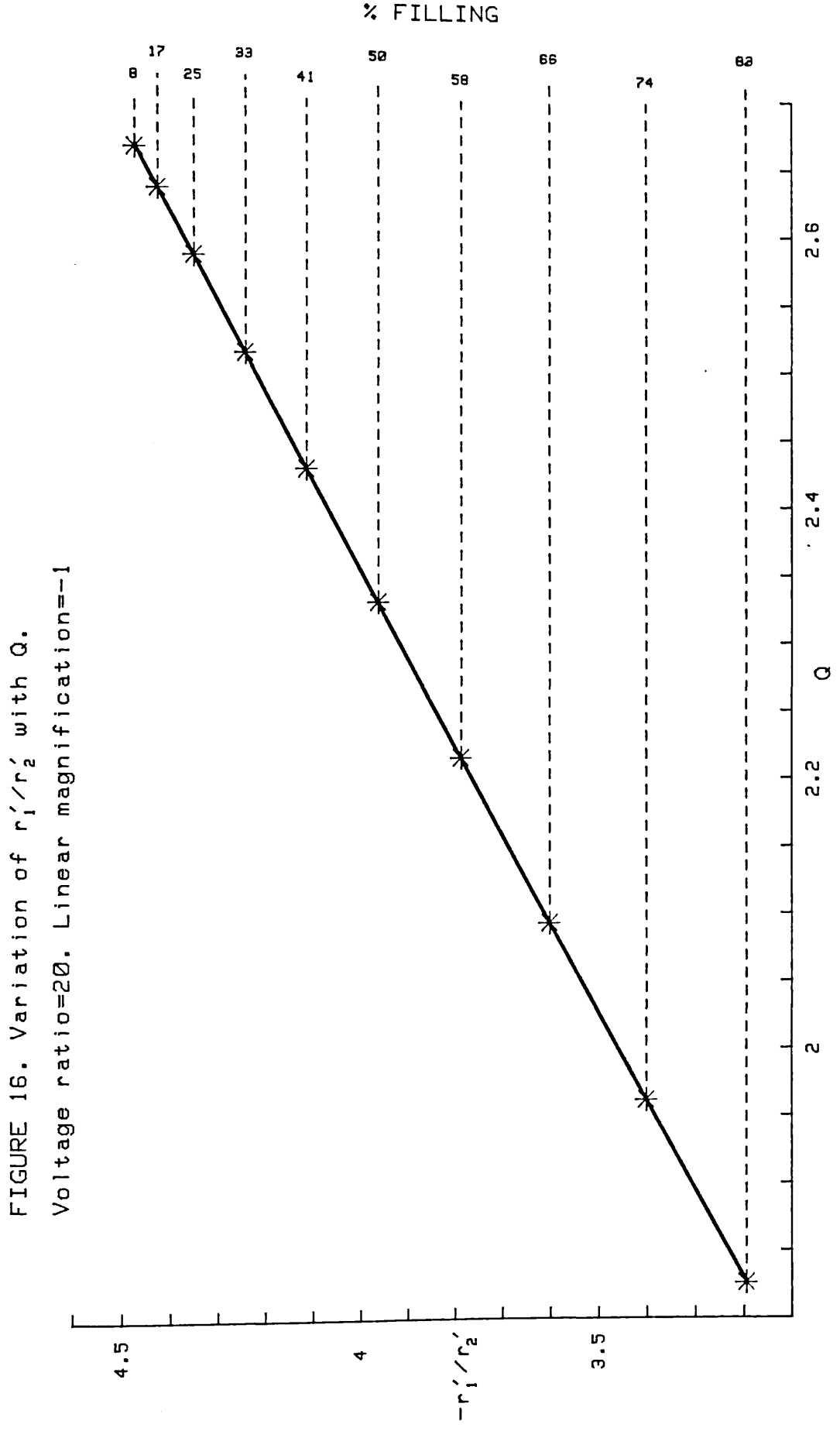

FIGURE 16. Variation of r_1'/r_2' with Q.
Voltage ratio=20. Linear magnification=-1

points and voltage ratios. In particular equation (105) was found to be independent of the degree of aberration of a ray. We shall investigate this relationship and examine its limitations and see how it affects the treatment of aberrations.

We can express (105) as:-

$$-r_1'/r_2' = b(P).Q + c(P) \qquad (106)$$

Which is easier to treat if we make the substitutions:-

$$G(P) = 1/b(P) - f_1 \qquad (107)$$

$$I(P) = c(P)/b(P) + F_2 \qquad (108)$$

So that (106) becomes:-

$$Q-F_2 = -f_1 r_1'/r_2' - G(P)r_1'/r_2' - I(P) \qquad (109)$$

It is useful to define:-

$$k = r_1/(r_1'f_2) \qquad (110)$$

It can be seen from equations (16) and (103) that k is simply $-M_\alpha$, the unaberrated angular magnification of a ray from P. Since for a given voltage ratio this is solely a function of

P, we can consider G(P) and I(P) as G(k) and I(k) respectively. Thus, if we incorporate (104), we can rewrite (109) as:-

$$r_2 = f_1 r_1' + G(k) r_1' + I(k) r_2' \tag{111}$$

We may also express (23) and (24) in terms of k:-

$$r_2' = -r_1' k + r_1'^3 M_1(k) + r_1'^5 Q_1(k) \tag{112}$$

$$r_2 / f_1 = r_1' + r_1'^3 M_2(k) + r_1'^5 Q_2(k) \tag{113}$$

where:-

$$M_1(k) = m_{13} + m_{14} k + m_{15} k^2 + m_{16} k^3 \tag{114}$$

$$M_2(k) = m_{23} + m_{24} k + m_{25} k^2 + m_{26} k^3 \tag{115}$$

$$Q_1(k) = q_{11} + q_{12} k + q_{13} k^2 + q_{14} k^3 + q_{15} k^4 + q_{16} k^5 \tag{116}$$

$$Q_2(k) = q_{21} + q_{22} k + q_{23} k^2 + q_{24} k^3 + q_{25} k^4 + q_{26} k^5 \tag{117}$$

Substituting (112) and (113) into (111) gives us a quadratic in $r_1'^2$:-

$$\left(G(k) - kI(k)\right) + r_1'^2 \left(I(k) M_1(k) - f_1 M_2(k)\right) + r_1'^4 \left(I(k) Q_1(k) - f_1 Q_2(k)\right) = 0 \tag{118}$$

Since (118) is valid for all rays from all object points:-

$$G(k) = kI(k) \tag{119}$$

$$M_2(k) = M_1(k)I(k)/f_1 \tag{120}$$

$$Q_2(k) = Q_1(k)I(k)/f_1 \tag{121}$$

It can be seen that (119)-(121) can be reconciled with equations (118) and (114)-(117) only if I is a lens constant and if:-

$$m_{2j} = \sigma m_{1j} \tag{122}$$

$$q_{2j} = \sigma q_{1j} \tag{123}$$

where:-

$$\sigma = I/f_1 \tag{124}$$

Substituting (119) and (110) into (111) gives the very simple relationship between the ray parameters in object and image space:-

$$r_2/f_1 = r_1' + \sigma r_1/f_2 + \sigma r_2' \tag{125}$$

Equations (122) and (123) effectively halve the number of

unique aberration coefficients needed to describe the behaviour of a ray. Moreover in (125) we have a linear relationship, which appears to be independent of aberration, between the input and output parameters of a trajectory through the lens. The remainder of this work will be dedicated to the investigation of the applications and limitations of these fundamental relationships.

3.2) PARALLEL INPUT AND OUTPUT

(125) has been derived from trajectories with finite magnifications. We shall now examine its application to rays which enter the lens parallel to the optic axis.
For parallel incidence (125) becomes:-

$$r_2/f_1 = \sigma r_1/f_2 + \sigma r_2' \qquad (126)$$

If we use (104) this becomes:-

$$Q = F_2 - f_1 \sigma\left(1 + \frac{r_1}{f_2 r_2'}\right) \qquad (127)$$

This relationship is compared with the results of the computer model in Figures (17)-(21). A strongly linear relationship is clearly evident for all but the 40:1 lens, where some deviation from the predicted result is apparent.

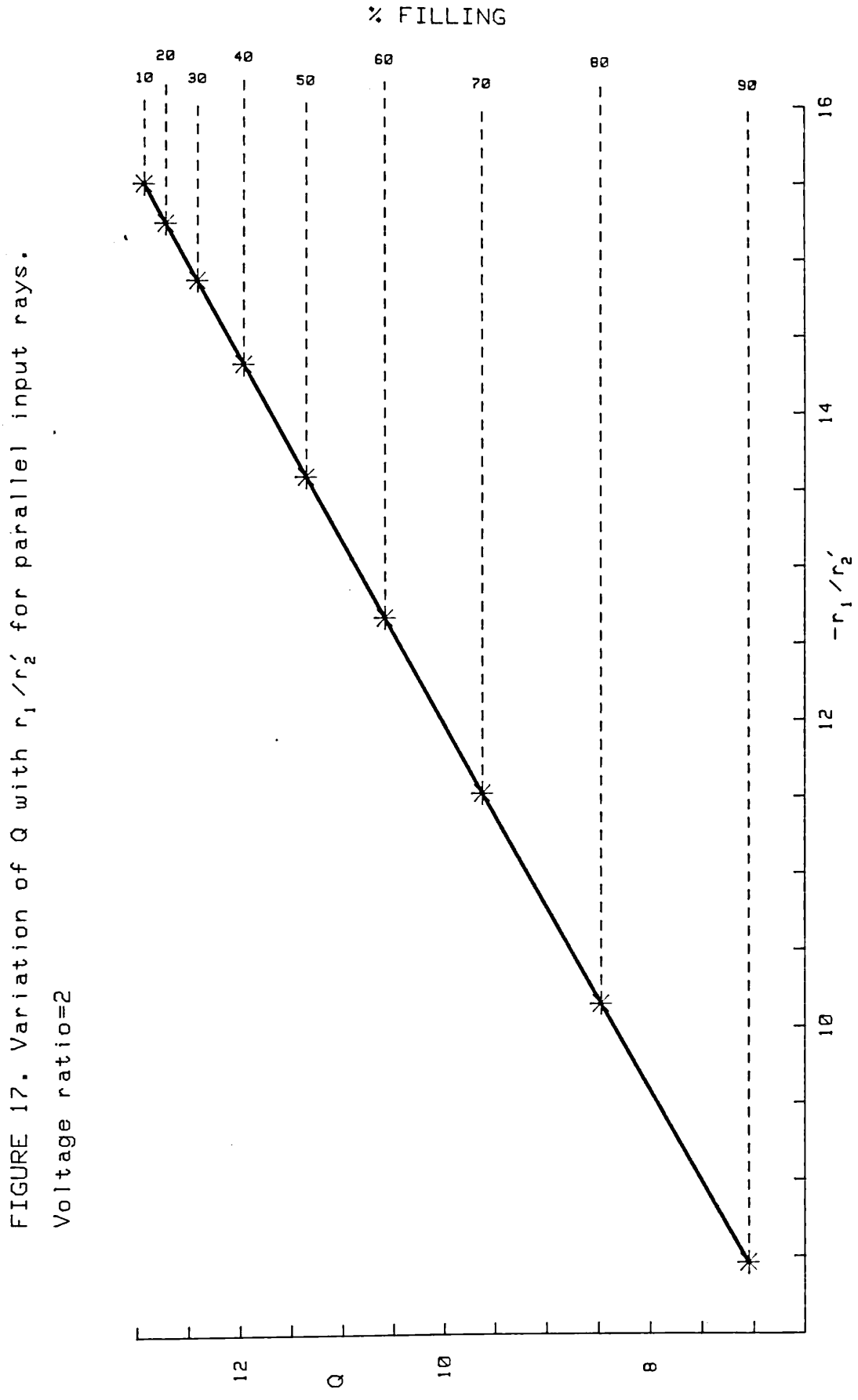

FIGURE 17. Variation of Q with r_1/r_2' for parallel input rays.
Voltage ratio=2

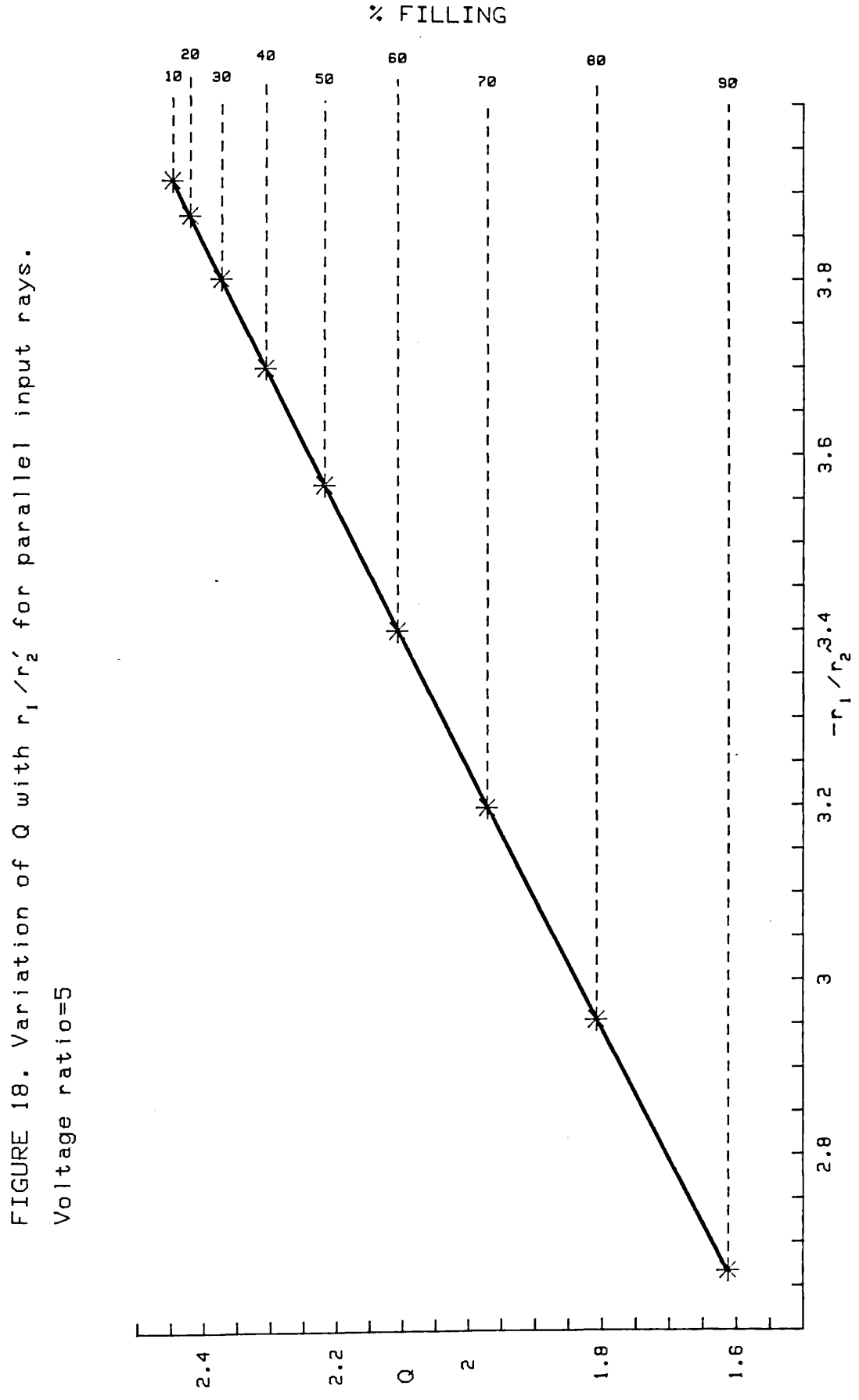

FIGURE 18. Variation of Q with r_1/r_2' for parallel input rays.

Voltage ratio=5

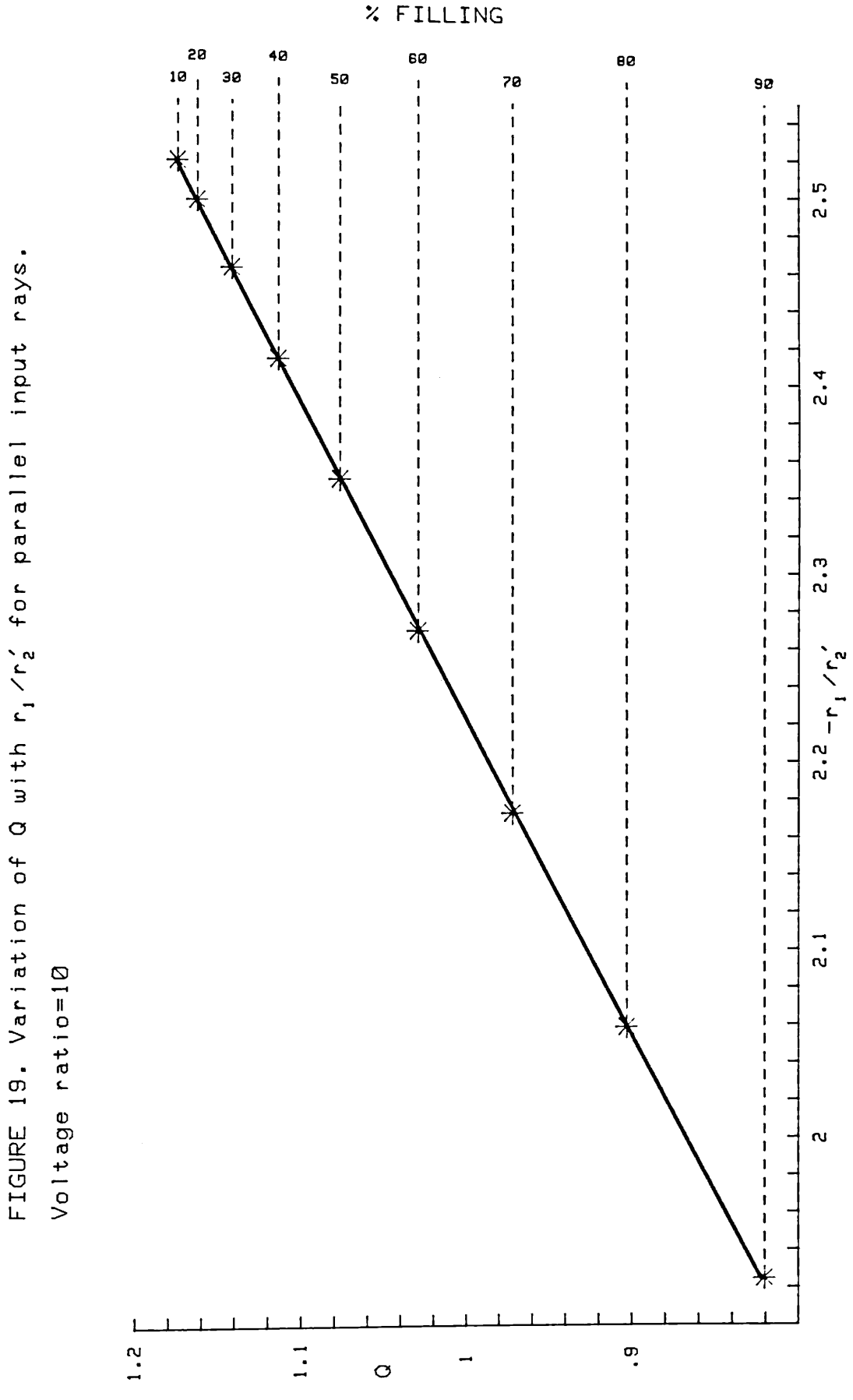

FIGURE 19. Variation of Q with r_1/r_2' for parallel input rays.
Voltage ratio=10

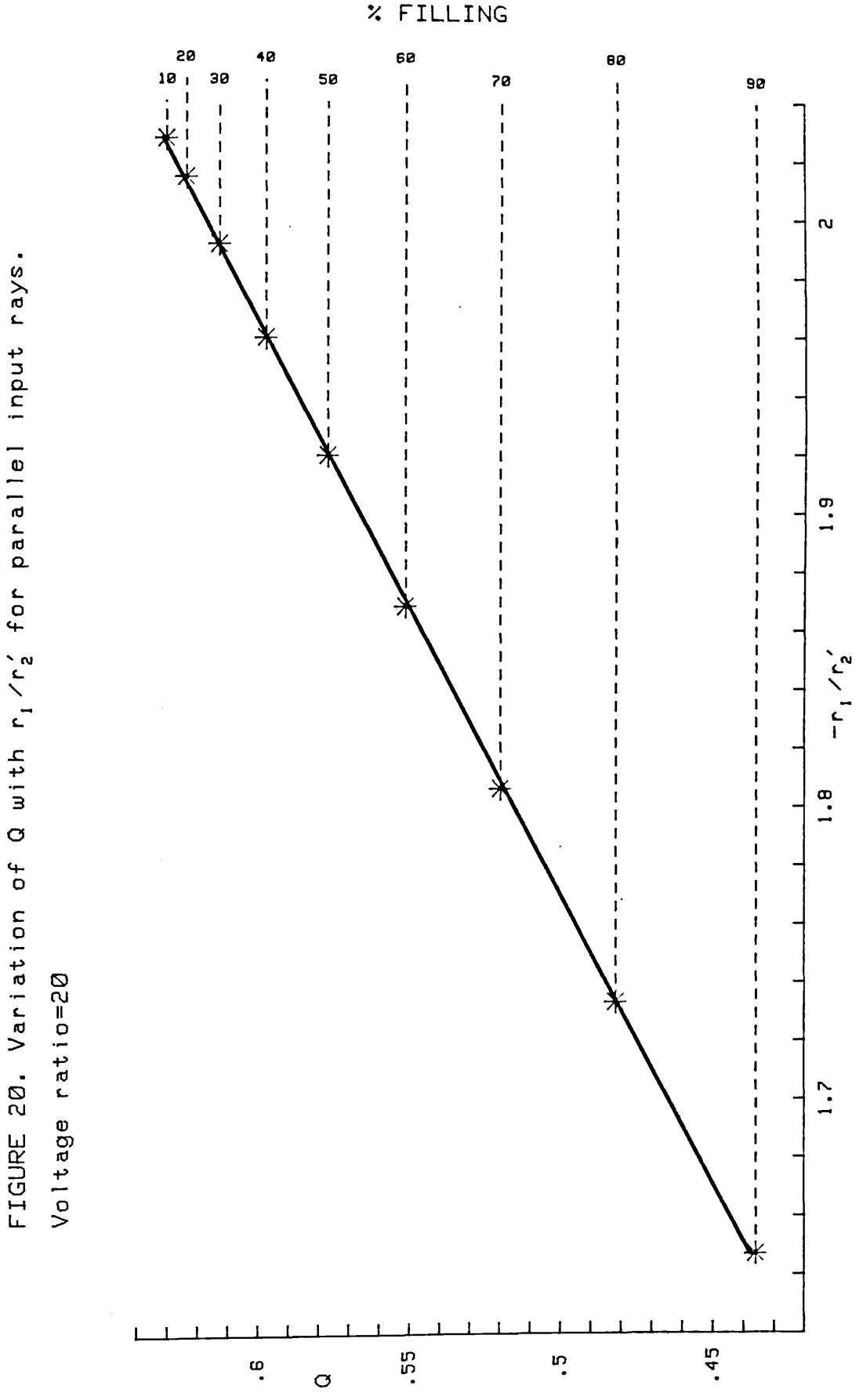

FIGURE 20. Variation of Q with r_1/r_2' for parallel input rays.

Voltage ratio=20

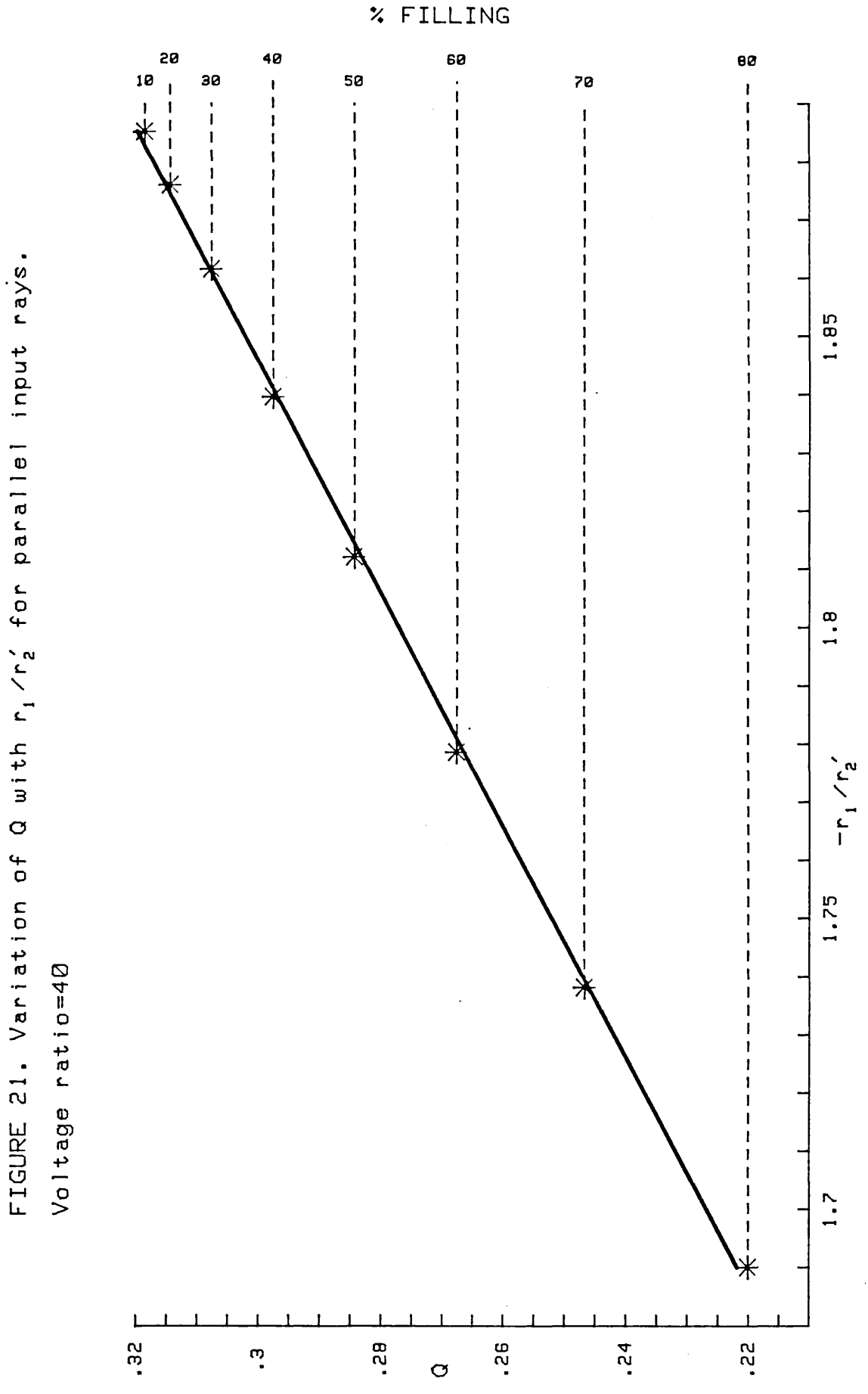

FIGURE 21. Variation of Q with r_1/r_2' for parallel input rays.

Voltage ratio=40

The longitudinal shift in focus for a spherically aberrated ray is given by:-

$$Q = F_2 - C_3 r_1^2 - C_5 r_1^4 - \ldots\ldots \qquad (128)$$

Where C_3 and C_5 represent third and fifth order aberrations respectively.

Figures (22)-(26) show the variation of Q with r_1^2 for the five voltage ratios. It can be seen that in each case fifth order effects become noticeable for rays of over about 50% filling. This was also the observation of Harting and Read (1976). Since graphs (17)-(21) represent fillings of up to 90%, equation (125) must be independent of both third and fifth order aberrations.

The deterioration of this relationship for the near focus rays of the 40:1 lens suggests that (125) may be an approximation that is less applicable to strong lenses. We shall investigate this in more detail later in the thesis.

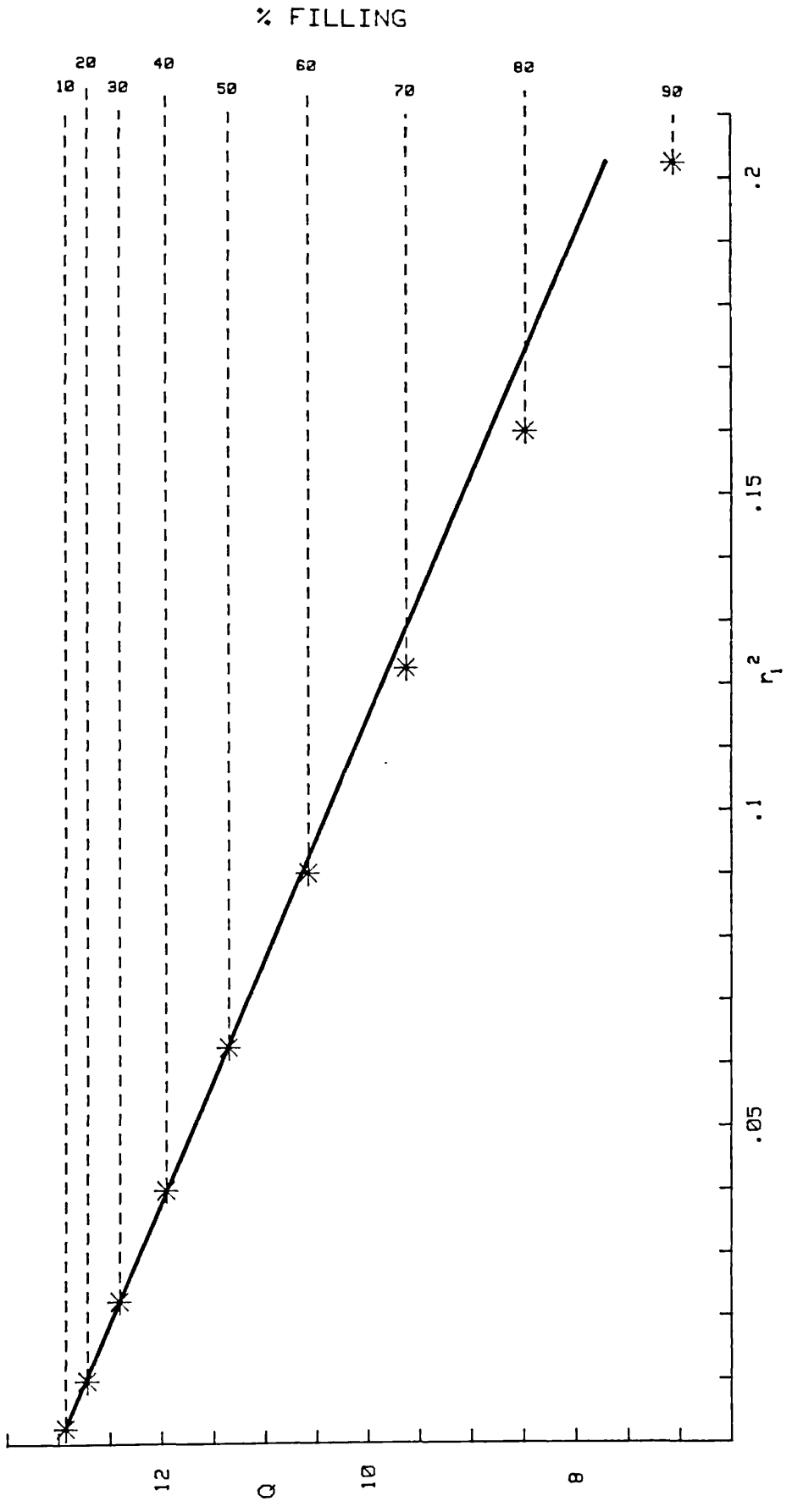

FIGURE 22. Variation of Q with r_1^2 for parallel input rays.
Voltage ratio=2

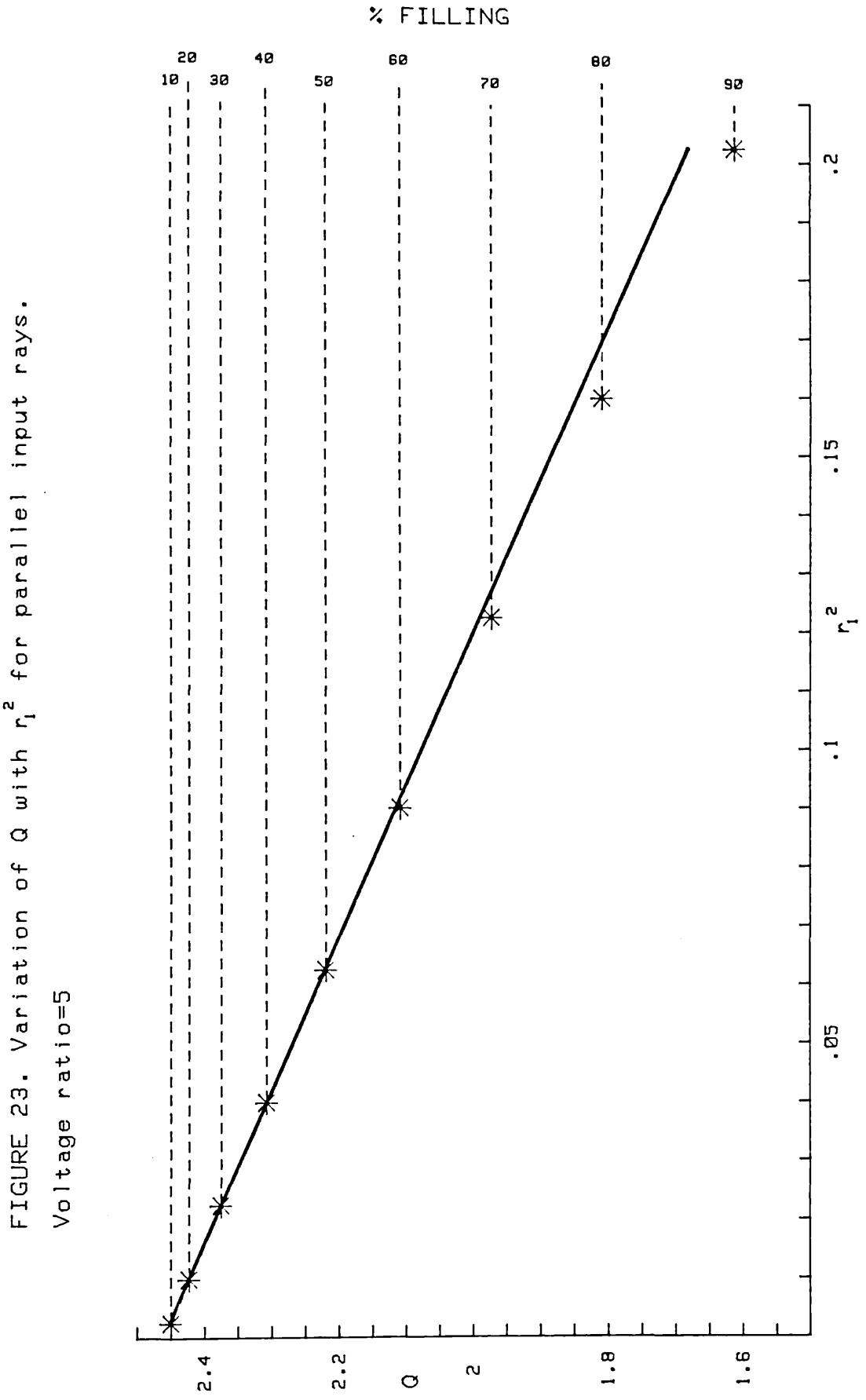

FIGURE 23. Variation of Q with r_1^2 for parallel input rays.

Voltage ratio=5

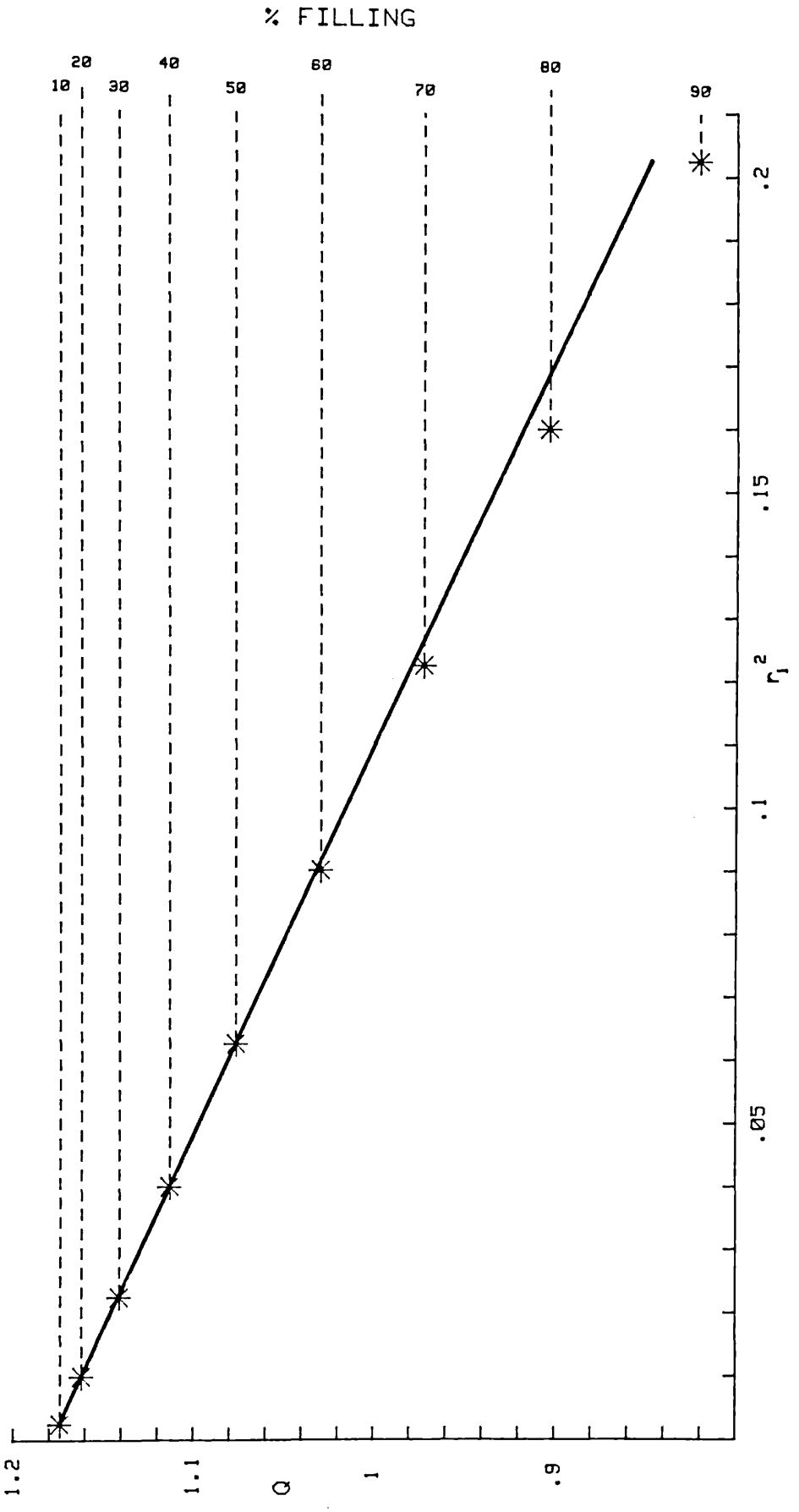

FIGURE 24. Variation of Q with r_1^2 for parallel input rays.
Voltage ratio=10

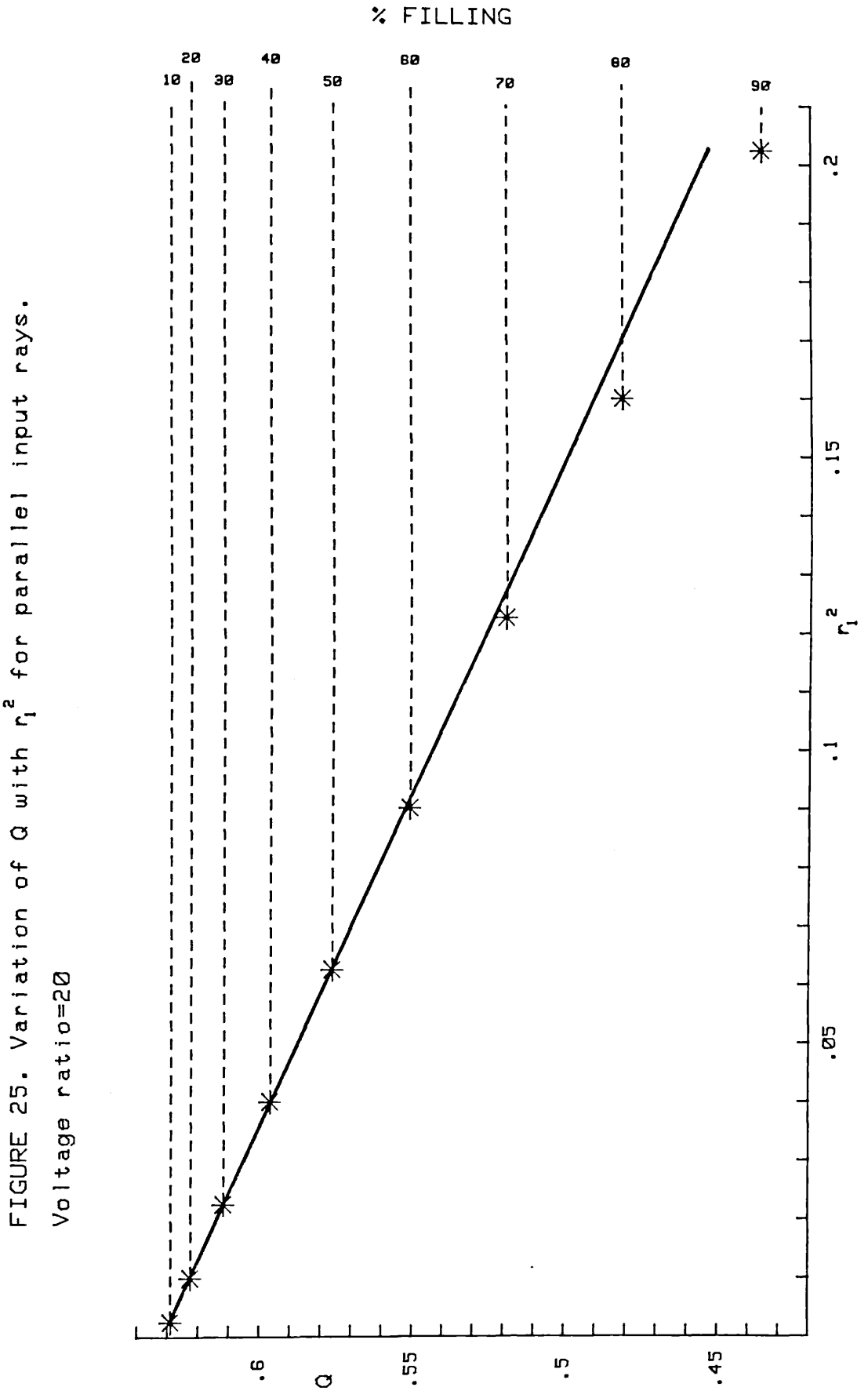

FIGURE 25. Variation of Q with r_1^2 for parallel input rays.

Voltage ratio=20

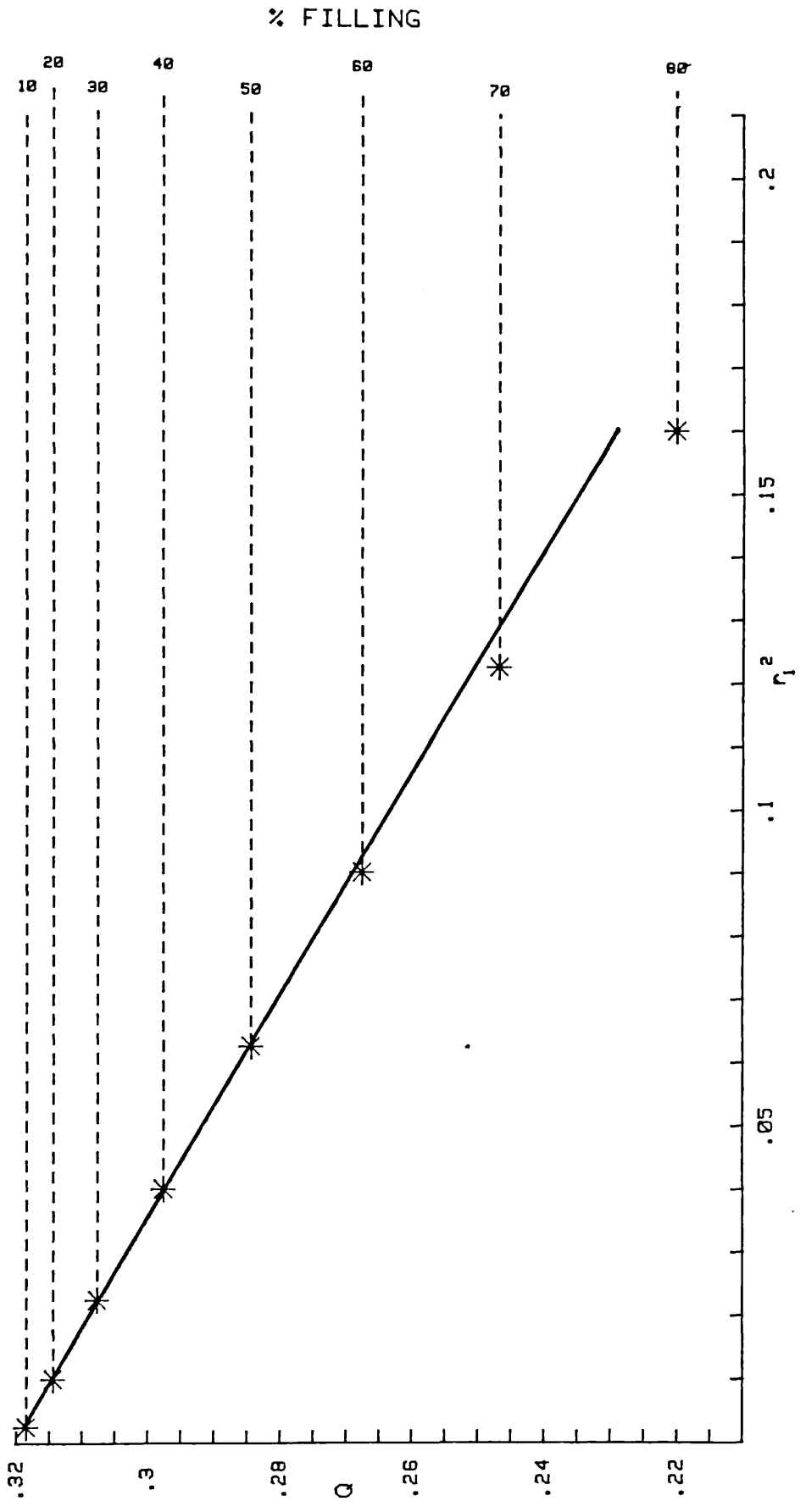

FIGURE 26. Variation of Q with r_1^2 for parallel input rays.
Voltage ratio=40

3.3) RELATIONSHIPS BETWEEN ABERRATION COEFFICIENTS

We shall now show that in the light of the observations that have been made, it is possible to represent all the third and fifth order geometric aberrations using three unique coefficients only.

If we incorporate the partial differentials of equation (125) with respect to r_1 and r_1':-

$$\frac{\partial r_2}{\partial r_1} = f_1 \sigma\left(\frac{1}{f_2} + \frac{\partial r_2'}{\partial r_1}\right) \tag{129}$$

$$\frac{\partial r_2}{\partial r_1'} = f_1 \left(1 + \sigma.\frac{\partial r_2'}{\partial r_1'}\right) \tag{130}$$

into the Lagrange Invariant which was derived in section one (equation (55)), then we can show that:-

$$(1 + r_2'^2)^{3/2} = (1 + r_1'^2)^{3/2}\left(\sigma.\frac{\partial r_2'}{\partial r_1'} - f_2\frac{\partial r_2'}{\partial r_1}\right) \tag{131}$$

If we use the binomial expansion:-

$$(1 + r'^2)^{3/2} = 1 + \frac{3r'^2}{2} + \frac{3r'^4}{8} + \ldots\ldots \tag{132}$$

then we can substitute for r_2' and its derivatives by using equations (112), (114) and (116). A rather lengthy calculation will show:-

$$\sigma m_{15} = 3m_{16} + 3/2 \tag{133}$$

$$\sigma m_{14} = m_{15} \tag{134}$$

$$3\sigma m_{13} = m_{14} - 3/2 \tag{135}$$

$$\sigma q_{15} = 5q_{16} - 3m_{16} + 3/8 \tag{136}$$

$$2\sigma q_{14} = 4q_{15} - 3m_{15} \tag{137}$$

$$3\sigma q_{13} = 3q_{14} - 3m_{14} - 9/4 \tag{138}$$

$$4\sigma q_{12} = 2q_{13} - 3m_{13} \tag{139}$$

$$5\sigma q_{11} = q_{12} + 15/8 \tag{140}$$

Hence, given equations (122) and (123) we can express all the third and fifth order geometric aberrations in terms of just three coefficients: m_{16} , q_{16} and σ.

To some extent we can check the validity of equations (133) - (140) by extending a method used by Verster (1963) which utilised the isotropic properties of an electrostatic field. An extremely lengthy fifth order calculation enables three of the third order and five of the fifth order coefficients to be expressed in terms of the others:-

$$m_{25} = 3m_{16} + 3/2 \tag{141}$$

$$m_{24} = m_{15} \tag{142}$$

$$3m_{23} = m_{14} - 3/2 \tag{143}$$

$$q_{25} = 5q_{16} - 9m_{16}^2 - 3m_{15}m_{26} + 3m_{16}/2 + 3/8 \quad (144)$$

$$2q_{24} = 4q_{15} + 6m_{16}m_{16} - 6m_{14}m_{26} - 3m_{15} \quad (145)$$

$$3q_{23} = 3q_{14} + 3m_{15}^2 - 9m_{13}m_{26} - 6m_{16}m_{14} - 9m_{16}/2 - 15m_{14}/2 - 9/4 \quad (146)$$

$$4q_{22} = 2q_{13} - 18m_{13}m_{16} + 2m_{15}m_{14} - 12m_{13} - 3m_{15} \quad (147)$$

$$5q_{21} = q_{12} + m_{14}^2 - 3m_{14}/2 - 3m_{15}m_{13} + 15/8 \quad (148)$$

Inspection will show that our relationships are compatible with these results.

3.4) CALCULATING THE ABERRATION COEFFICIENTS

It is a relatively straight forward matter to use the data from the trajectories to determine the value of σ for a given voltage ratio. We have from equation (127) that for parallel incidence:-

$$Q = F_2 - f_1\sigma\left(1 + \frac{r_1}{f_2 r_2'}\right) \quad (149)$$

Using a Least Squares fit on the output parameters of trajectories of up to 60% filling the value of σ was determined for a range of voltage ratios. These are shown in Table 4.

The determination of the m_{16} and q_{16} coefficients was, however,

found to be more involved. For parallel incidence the variation of r_2' with r_1 is given by:-

$$r_2' = -r_1/f_2 + m_{16}r_1^3/f_2^3 + q_{16}r_1^5/f_2^5 \qquad (150)$$

Problems arise when fitting data to this fifth order relationship due to the presence of higher order variations. If we are to derive the correct values for m_{16} and q_{16}, then it is necessary to consider as wide a spread in incident rays as possible. However, if the spread is too large then 7th and higher order effects will detract from the accuracy of the coefficients. It was found to be too haphazard to try and resolve this problem by attempting to determine the optimum maximum filling factor that should be considered. Consequently, the m_{16} and q_{16} coefficients were calculated by fitting a higher order polynomial to r_2'. In fact for the weaker lenses it was necessary to consider 11th order variations before q_{16} became stationary.

The derived values of m_{16} and q_{16} are shown in Tables (5) and (6), along with the values of all the other third and fifth order coefficients which have been calculated from these using equations (122),(123) and (133)-(140).

TABLE 4. THE COEFFICIENT σ AS A FUNCTION OF VOLTAGE RATIO.

(2 Cylinder Lens. g/D = 0.1)

V_2/V_1	2	5	10	20	40
σ	1.187	1.47	1.75	2.17	2.96
$(V_2/V_1)^{1/4}$	1.189	1.50	1.78	2.11	2.51

By considering the standard deviations in the Least Squares analysis we were able to estimate the accuracy of the quoted values. We believe m_{16} and q_{16} to be accurate to within 1% and 5% respectively. The other coefficients are derived from these two and σ. They are therefore less accurate. Inspection of equations (122), (123) and (133)-(140) will show that the largest errors should occur in m_{19} and q_{11} . We estimate these errors to range from 1% and 5% respectively for the 2:1 lens, to 10% and 20% respectively for the 40:1 lens. Kuyatt quotes accuracies of 10% for (most of) his third order coefficients and describes his fifth order coefficients as accurate to about a factor of 2.

It can be seen that the present results are generally in good agreement with the results of Kuyatt and Read.

TABLE 5. ABERRATION COEFFICIENTS IN THE EXPANSION OF r_2'

(Two cylinder lens. g/D = 0.1)

$V_2/V_1 = 2$

	$-m_{13}$	$-m_{14}$	$-m_{15}$	$-m_{16}$	$-q_{11}$	$-q_{12}$	$-q_{13}$	$-q_{14}$	$-q_{15}$	$-q_{16}$
Present	283	1010	1190	473	6.7E4	4.0E5	9.5E5	1.1E6	6.7E5	1.6E5
Kuyatt	285	1029	1240	502	1E5					2E5
Read	278	991	1180	467						

$V_2/V_1 = 5$

	$-m_{13}$	$-m_{14}$	$-m_{15}$	$-m_{16}$	$-q_{11}$	$-q_{12}$	$-q_{13}$	$-q_{14}$	$-q_{15}$	$-q_{16}$
Present	7.21	30.3	44.5	22.3	82	600	1800	2700	2000	600
Kuyatt	7.34	31.6	47.0	23.6	72					430
Read	7.02	30.0	44.3	22.2						

$V_2/V_1 = 10$

	$-m_{13}$	$-m_{14}$	$-m_{15}$	$-m_{16}$	$-q_{11}$	$-q_{12}$	$-q_{13}$	$-q_{14}$	$-q_{15}$	$-q_{16}$
Present	1.50	6.59	11.5	7.20	3.8	35	120	220	210	76
Kuyatt	1.44	6.77	12.0	7.06	6.2					94
Read	1.46	6.70	11.9	7.34						

$V_2/V_1 = 20$

	$-m_{13}$	$-m_{14}$	$-m_{15}$	$-m_{16}$	$-q_{11}$	$-q_{12}$	$-q_{13}$	$-q_{14}$	$-q_{15}$	$-q_{16}$
Present	.530	1.95	4.24	3.56	.10	3.0	14	31	37	18
Kuyatt	.460	2.23	4.27	3.44	.27					25
Read	.470	2.06	4.58	3.54						

$V_2/V_1 = 40$

	$-m_{13}$	$-m_{14}$	$-m_{15}$	$-m_{16}$	$-q_{11}$	$-q_{12}$	$-q_{13}$	$-q_{14}$	$-q_{15}$	$-q_{16}$
Present	.235	.590	1.75	2.22	-.09	.44	2.9	8.5	14	9.7
Kuyatt	.186	.722	2.03	2.29	0					5.9
Read	.200	.670	2.27	2.26						

TABLE 6. ABERRATION COEFFICIENTS IN THE EXPANSION OF r_2

(Two cylinder lens. g/D = 0.1)

$V_2/V_1 = 2$

	$-m_{23}$	$-m_{24}$	$-m_{25}$	$-m_{26}$	$-q_{21}$	$-q_{22}$	$-q_{23}$	$-q_{24}$	$-q_{25}$	$-q_{26}$
Present	336	1190	1420	561	8.0E4	4.8E5	1.1E6	1.3E6	8.0E5	1.9E5
Kuyatt	364	1270	1480	575	4E4					3E5
Read	331	1180	1400	553						

$V_2/V_1 = 5$

	$-m_{23}$	$-m_{24}$	$-m_{25}$	$-m_{26}$	$-q_{21}$	$-q_{22}$	$-q_{23}$	$-q_{24}$	$-q_{25}$	$-q_{26}$
Present	10.6	44.5	65.4	32.8	120	890	2600	3900	2900	880
Kuyatt	11.0	47	69	34.7	106					643
Read	10.5	44.3	65.1	32.6						

$V_2/V_1 = 10$

	$-m_{23}$	$-m_{24}$	$-m_{25}$	$-m_{26}$	$-q_{21}$	$-q_{22}$	$-q_{23}$	$-q_{24}$	$-q_{25}$	$-q_{26}$
Present	2.69	11.5	20.1	12.6	6.6	61	220	390	360	130
Kuyatt	2.71	11.4	19.6	12.2	13.5					174
Read	2.74	11.9	20.5	12.8						

$V_2/V_1 = 20$

	$-m_{23}$	$-m_{24}$	$-m_{25}$	$-m_{26}$	$-q_{21}$	$-q_{22}$	$-q_{23}$	$-q_{24}$	$-q_{25}$	$-q_{26}$
Present	1.15	4.24	9.19	7.73	.21	6.4	30	67	79	39
Kuyatt	1.16	5.29	8.05	7.27	.79					66
Read	1.19	4.58	9.12	7.55						

$V_2/V_1 = 40$

	$-m_{23}$	$-m_{24}$	$-m_{25}$	$-m_{26}$	$-q_{21}$	$-q_{22}$	$-q_{23}$	$-q_{24}$	$-q_{25}$	$-q_{26}$
Present	.697	1.75	5.17	6.58	.29	1.3	8.7	25	41	29
Kuyatt	.65	2.19	3.03	6.52	.34					34
Read	.730	2.27	5.27	6.56						

3.5) RAY REVERSAL

If a ray travelling from, say, left to right has its input and output parameters related by equation (125) then it can be seen that σ is a dimensionless quantity. If we denote the parameters of a second ray, travelling in the opposite direction by $\tilde{}$, then it follows that:-

$$\tilde{r}_2 / \tilde{f}_1 = \tilde{r}_1' + \tilde{\sigma}\tilde{r}_1 / \tilde{f}_2 + \tilde{\sigma}\tilde{r}_2' \qquad (151)$$

If these raypaths are coincident then, using (26) and (29):-

$$r_2 / f_1 = r_1' + \tilde{\sigma}^{-1} r_1 / f_2 + \tilde{\sigma}^{-1} r_2' \qquad (152)$$

Comparison of (152) and (125) shows that:-

$$\sigma . \tilde{\sigma} = 1 \qquad (153)$$

Inspection will show that given (122) and (123), this result is consistent with the relationships that we have shown to exist between the aberration coefficients of forward and reverse rays (equations (30)-(33)).
All the relationships derived in this thesis have been tested and found to be self consistent with respect to ray reversal.

SECTION FOUR

FURTHER TREATMENT OF RESULTS

In this section we shall investigate the basis of our results and their limitations. We shall then show how, for a wide range of lenses, they lead to very simple expressions for many of the properties associated with geometric aberration.

4.1) RANGE OF APPLICATION

Earlier on we observed some deterioration in the relationships that we are examining in the case of a 40:1 voltage ratio lens. It would appear, therefore, that these relationships are approximations only, and may not be applicable to the aberrations of stronger lenses. We shall now investigate these limitations and derive a criterion that may be used to assess whether or not the results that have been obtained can be applied to a particular lens. We shall do this by considering the particular problem of spherical aberration.

If we denote the aberration of a ray from a point axial object by its radial displacement, Δr, at the Gaussian image plane (see Figure 31), then we can define the third order spherical aberration coefficient, Cs(M), in terms of Δr, r_i' and M (the linear magnification):-

$$\Delta r = M.Cs(M)r_1'^3 \tag{154}$$

Where it can be shown that:-

$$Cs(M) = Cs_0 + Cs_1 M^{-1} + Cs_2 M^{-2} + Cs_3 M^{-3} + Cs_4 M^{-4} \tag{155}$$

It can also be shown that the following relationships exist between the Cs and the m_{ij} coefficients (Verster, 1963):-

$$Cs_0 = -m_{13} f_2 \tag{156}$$

$$Cs_1 = (4m_{23} + 1.5)f_1 \tag{157}$$

$$Cs_2 = -2m_{24} f_1^2 / f_2 \tag{158}$$

$$Cs_3 = (4m_{16} + 1.5)f_1^3 / f_2^2 \tag{159}$$

$$Cs_4 = -m_{26} f_1^4 / f_2^3 \tag{160}$$

If our results are applicable, then it follows from (122) and (133)-(135):-

$$Cs_0 = -(m_{16} + 0.5)f_2 / \sigma^3 + 0.5 f_2 / \sigma \tag{161}$$

$$Cs_1 = 4(m_{16} + 0.5)f_1 / \sigma^2 - 0.5 f_1 \tag{162}$$

$$Cs_2 = -6(m_{16} + 0.5)f_1^2 / (\sigma f_2) \tag{163}$$

$$Cs_3 = 4(m_{16} + 0.5)f_1^3 / f_2^2 + 0.5 f_1^3 / f_2^2 \tag{164}$$

$$Cs_4 = -(m_{16} + 0.5)\sigma f_1^4/f_2^3 + 0.5\sigma f_1^4/f_2^3 \qquad (165)$$

These inelegant relationships enable us to establish a very simple test of our results. If we define:-

$$Y = Cs_0(\sigma f_1/f_2)^4 + Cs_1(\sigma f_1/f_2)^3 + Cs_2(\sigma f_1/f_2)^2 + Cs_3(\sigma f_1/f_2) + Cs_4 \qquad (166)$$

then inspection will show that Y=0 if our results are valid. Therefore:-

$$Cs_0 + Cs_1(f_2/\sigma f_1) + Cs_2(f_2/\sigma f_1)^2 + Cs_3(f_2/\sigma f_1)^3 + Cs_4(f_2/\sigma f_1)^4 = 0 \qquad (167)$$

must also be true. Comparison with (155) shows that when $M=(f_2/\sigma f_1)^{-1}$ then the limiting system (for which our results are precise) will be free from spherical aberration. The value of the object distance, P, can be derived from (15):-

$$P = F_1 - f_2/\sigma \qquad (168)$$

where, because the linear magnification is positive, $P < F_1$. Since all rays from this object point are unaberrated, they must all pass through the same (virtual) Q:-

$$Q = F_2 - \sigma f_1 \qquad (169)$$

As this is true for all rays P and Q must be interchangeable, and since σ is single valued we must have that:-

$$P = -Q \tag{170}$$

Hence, from (15):-

$$(P-F_1)(-P-F_2) = f_1 f_2 \tag{171}$$

Which means that if P is real and singular:-

$$4f_1 f_2 = (F_1 + F_2)^2 \tag{172}$$

and:-

$$P = (F_1 - F_2)/2 \tag{173}$$

$$\sigma = 2f_2/(F_1+F_2) = (F_1+F_2)/2f_1 \tag{174}$$

$$= (f_2/f_1)^{1/2} = (V_2/V_1)^{1/4} \tag{175}$$

We have in these relationships two results of particular importance. Firstly, equation (172) relates the focal lengths of the systems for which our observations are precise. This is explored in Table 7 where the focal lengths of the simple two tube lens are given along with the percentage error that there

would need to be in each in order that (172) be correct. It is clear from these results that our observations are based on a weak lens model, even though they have been seen to predict accurately the aberrations of lenses with voltage ratios of twenty to one. Secondly, equation (175) enables us to derive the value of the coefficient σ from the overall voltage ratio. This will prove particularly useful in examining the application of our results to more complex lens geometries. In Table 4 we show how the value of σ (which was derived earlier for the two tube lens) compares to $(V_2/V_1)^{1/4}$. It can be seen that, with the exception of the 40:1 lens, there is strong agreement.

TABLE 7. FOCAL LENGTHS OF THE TWO CYLINDER LENS
(g/D = 0.1)

V_2/V_1	f_1	f_2	F_1	F_2	%Error
2	1.10E+1	1.56E+1	1.32E+1	1.30E+1	7.5E-3
5	1.77E+0	3.95E+0	2.78E+0	2.48E+0	2.6E-1
10	8.00E-1	2.54E+0	1.62E+0	1.19E+0	7.2E-1
20	4.60E-1	2.05E+0	1.21E+0	6.40E-1	2.4E+0
40	3.00E-1	1.90E+0	1.03E+0	3.20E-1	5.5E+0

4.2) OTHER LENS GEOMETRIES

The results that we have obtained so far have been derived from the model of the simple two tube lens shown in Figure (7). We shall now investigate their validity for the lenses of more complex geometries that are shown in Figures (1)-(3). For this purpose we shall use the accurate third order spherical aberration coefficients that have been derived by Harting and Read (1976).

Using (175) to derive the value of σ, we have calculated the value of Y given by equation (166), where, if our relationships are valid, we would expect Y to be zero. Tables (8)-(14) show the results for the various lenses. The error that is quoted is the percentage error that there would need to be in each of the Cs coefficients in order that Y should be zero. This error should be compared with the 1% error that Harting and Read quote for their results.

We can summarise the results of the Tables as follows:-

i) The relationships between the coefficients are applicable to weaker lenses and, hence, to systems in which the aberrations are large.

ii) For two element lenses the range of application is limited to voltage ratios of less than 40:1.

iii) The range of application for three element lenses cannot

be so simply defined. It is clear that the criterion lies not in the overall voltage ratio but in the focussing strength of the lens. We have found that, as an approximate rule of thumb, our results are appropriate for lenses in which the value of F_2 is greater than 1/2.

iv) None of the geometries investigated showed any deviation from the comments that we have made. The basic rule seems to be that the larger the aberration coefficients then the more applicable are our results.

TABLE 8. SPHERICAL ABERRATION COEFFICIENTS FOR THE TWO CYLINDER, EQUI-DIAMETER LENS

G/D= .1

V2/V1	CS0	CS1	CS2	CS3	CS4	Y	%ERROR
2.0	4.34E+3	-1.46E+4	1.84E+4	-1.03E+4	2.16E+3	-1.68E+0	4.8E-3
5.0	2.77E+1	-7.17E+1	7.03E+1	-3.10E+1	5.19E+0	-5.13E-3	6.0E-3
10.0	3.70E+0	-7.54E+0	5.99E+0	-2.21E+0	3.20E-1	6.07E-4	1.1E-2
20.0	9.58E-1	-1.49E+0	9.45E-1	-2.93E-1	3.92E-2	2.30E-3	3.8E-1
40.0	3.72E-1	-4.15E-1	2.15E-1	-5.62E-2	7.74E-3	2.59E-3	2.6E+0

G/D= .5

V2/V1	CS0	CS1	CS2	CS3	CS4	Y	%ERROR
2.0	4.62E+3	-1.55E+4	1.96E+4	-1.10E+4	2.31E+3	1.30E+1	3.5E-2
5.0	3.01E+1	-7.90E+1	7.87E+1	-3.53E+1	6.02E+0	2.66E-3	2.8E-3
10.0	4.03E+0	-8.47E+0	6.97E+0	-2.66E+0	4.00E-1	5.07E-3	8.4E-2
20.0	1.04E+0	-1.68E+0	1.13E+0	-3.71E-1	5.16E-2	3.20E-3	4.5E-1
40.0	3.94E-1	-4.73E-1	2.63E-1	-7.34E-2	1.02E-2	2.70E-3	2.2E+0

G/D= 1

V2/V1	CS0	CS1	CS2	CS3	CS4	Y	%ERROR
2.0	6.22E+3	-2.10E+4	2.66E+4	-1.50E+4	3.17E+3	-1.10E+1	2.2E-2
5.0	4.22E+1	-1.14E+2	1.18E+2	-5.48E+1	9.67E+0	1.40E-1	9.9E-2
10.0	5.55E+0	-1.24E+1	1.09E+1	-4.43E+0	6.98E-1	3.64E-3	3.8E-2
20.0	1.36E+0	-2.44E+0	1.80E+0	-6.31E-1	9.08E-2	4.91E-3	4.3E-1
40.0	4.90E-1	-6.72E-1	4.12E-1	-1.24E-1	1.72E-2	3.03E-3	1.6E+0

TABLE 9. SPHERICAL ABERRATION COEFFICIENTS FOR THE TWO CYLINDER, ASYMMETRIC LENS

D2 = 2*D1

V2/V1	CS0	CS1	CS2	CS3	CS4	Y	%ERROR
2.0	6.75E+3	-2.28E+4	2.88E+4	-1.62E+4	3.43E+3	-9.80E+0	1.8E-2
5.0	4.06E+1	-1.08E+2	1.09E+2	-4.91E+1	8.40E+0	1.31E-1	1.0E-1
10.0	5.08E+0	-1.09E+1	9.05E+0	-3.46E+0	5.15E-1	8.35E-4	1.0E-2
20.0	1.23E+0	-2.06E+0	1.39E+0	-4.50E-1	6.07E-2	2.40E-3	2.7E-1
40.0	4.50E-1	-5.59E-1	3.07E-1	-8.42E-2	1.12E-2	2.36E-3	1.6E+0

D2 = 1.5*D1

V2/V1	CS0	CS1	CS2	CS3	CS4	Y	%ERROR
2.0	5.51E+3	-1.85E+4	2.34E+4	-1.32E+4	2.77E+3	-2.86E+1	6.4E-2
5.0	3.41E+1	-8.97E+1	8.94E+1	-4.00E+1	6.80E+0	2.47E-2	2.3E-2
10.0	4.40E+0	-9.25E+0	7.55E+0	-2.85E+0	4.20E-1	-6.15E-5	9.4E-4
20.0	1.10E+0	-1.78E+0	1.18E+0	-3.75E-1	5.05E-2	3.81E-3	5.1E-1
40.0	4.13E-1	-4.92E-1	2.64E-1	-7.11E-2	9.57E-3	2.43E-3	2.0E+0

D2 = D1/1.5

V2/V1	CS0	CS1	CS2	CS3	CS4	Y	%ERROR
2.0	5.51E+3	-1.84E+4	2.31E+4	-1.29E+4	2.70E+3	8.97E-1	2.0E-3
5.0	3.57E+1	-9.06E+1	8.72E+1	-3.77E+1	6.21E+0	3.97E-2	3.8E-2
10.0	4.88E+0	-9.61E+0	7.39E+0	-2.64E+0	3.76E-1	7.41E-3	1.1E-1
20.0	1.35E+0	-1.87E+0	1.18E+0	-3.45E-1	4.70E-2	1.74E-2	2.3E+0
40.0	7.92E-1	-3.73E-1	3.06E-1	-6.22E-2	9.98E-3	2.99E-2	2.3E+1

D2 = D1/2

V2/V1	CS0	CS1	CS2	CS3	CS4	Y	%ERROR
2.0	6.81E+3	-2.27E+4	2.84E+4	-1.58E+4	3.29E+3	-6.83E+0	1.2E-2
5.0	4.45E+1	-1.11E+2	1.05E+2	-4.48E+1	7.24E+0	-5.88E-2	4.6E-2
10.0	6.14E+0	-1.18E+1	8.74E+0	-3.02E+0	4.15E-1	-3.80E-3	5.0E-2
20.0	1.66E+0	-2.33E+0	1.35E+0	-3.84E-1	4.95E-2	6.41E-3	7.4E-1
40.0	6.86E-1	-6.45E-1	3.02E-1	-7.17E-2	1.02E-2	6.03E-3	4.1E+0

TABLE 10. SPHERICAL ABERRATION COEFFICIENTS FOR THE THREE CYLINDER LENS. A/D=0.5 G/D=0.1

V3/V1= 2

V2/V1	CS0	CS1	CS2	CS3	CS4	Y	%ERROR
-0.8	2.37E+0	-5.98E+0	7.78E+0	-5.20E+0	1.81E+0	5.67E-1	3.4E+0
-0.6	5.69E+0	-1.80E+1	2.37E+1	-1.51E+1	4.03E+0	2.33E-1	4.9E-1
-0.4	1.48E+1	-5.00E+1	6.62E+1	-4.08E+1	9.86E+0	3.17E-2	2.4E-2
-0.2	3.88E+1	-1.34E+2	1.77E+2	-1.06E+2	2.45E+1	2.46E-1	7.2E-2
0.0	1.01E+2	-3.51E+2	4.61E+2	-2.72E+2	6.09E+1	-5.34E-2	6.1E-3
2.0	4.39E+3	-1.47E+4	1.85E+4	-1.04E+4	2.18E+3	-2.95E+1	8.4E-2
4.0	1.53E+2	-4.93E+2	6.02E+2	-3.30E+2	6.82E+1	-2.57E-1	2.2E-2
6.0	2.33E+1	-7.23E+1	8.71E+1	-4.83E+1	1.04E+1	3.38E-2	2.0E-2
8.0	7.79E+0	-2.27E+1	2.71E+1	-1.56E+1	3.61E+0	5.21E-2	9.7E-2
10.0	3.83E+0	-1.01E+1	1.21E+1	-7.35E+0	1.89E+0	1.74E-1	7.1E-1

V3/V1= 5

V2/V1	CS0	CS1	CS2	CS3	CS4	Y	%ERROR
-1.2	1.43E+0	-3.46E+0	3.93E+0	-2.29E+0	6.39E-1	1.16E-1	2.2E+0
-0.8	3.24E+0	-8.84E+0	9.87E+0	-5.32E+0	1.18E+0	4.05E-2	3.2E-1
-0.4	6.83E+0	-1.90E+1	2.06E+1	-1.04E+1	2.07E+0	1.13E-2	4.4E-2
0.0	1.26E+1	-3.45E+1	3.64E+1	-1.75E+1	3.24E+0	1.77E-2	4.0E-2
2.0	3.08E+1	-7.92E+1	7.78E+1	-3.46E+1	5.89E+0	1.84E-2	1.9E-2
4.0	3.48E+1	-9.20E+1	9.22E+1	-4.15E+1	7.08E+0	5.95E-3	5.3E-3
6.0	2.05E+1	-5.19E+1	5.00E+1	-2.17E+1	3.60E+0	2.72E-2	4.5E-2
8.0	1.09E+1	-2.65E+1	2.49E+1	-1.06E+1	1.76E+0	6.16E-2	2.0E-1
10.0	6.27E+0	-1.47E+1	1.36E+1	-5.85E+0	9.88E-1	1.56E-2	9.4E-2

V3/V1= 10

V2/V1	CS0	CS1	CS2	CS3	CS4	Y	%ERROR
-1.6	8.80E-1	-1.89E+0	1.83E+0	-9.05E-1	2.08E-1	2.96E-2	1.7E+0
-1.3	1.17E+0	-2.59E+0	2.45E+0	-1.16E+0	2.36E-1	1.48E-2	6.6E-1
-0.8	1.78E+0	-3.96E+0	3.60E+0	-1.57E+0	2.81E-1	1.03E-2	3.2E-1
-0.4	2.32E+0	-5.11E+0	4.48E+0	-1.86E+0	3.08E-1	2.04E-3	5.2E-2
0.0	2.86E+0	-6.15E+0	5.21E+0	-2.06E+0	3.23E-1	4.48E-3	9.9E-2
2.0	3.97E+0	-7.86E+0	6.12E+0	-2.24E+0	3.31E-1	5.94E-3	1.1E-1
4.0	4.30E+0	-9.16E+0	7.76E+0	-3.09E+0	4.86E-1	3.38E-3	5.0E-2
6.0	4.74E+0	-1.03E+1	8.70E+0	-3.40E+0	5.17E-1	-1.40E-3	1.8E-2
8.0	4.41E+0	-9.31E+0	7.63E+0	-2.88E+0	4.25E-1	3.69E-3	5.6E-2
10.0	3.71E+0	-7.58E+0	6.02E+0	-2.22E+0	3.22E-1	3.57E-4	6.8E-3

V3/V1= 20

V2/V1	CS0	CS1	CS2	CS3	CS4	Y	%ERROR
-2.0	5.20E-1	-8.89E-1	6.81E-1	-2.67E-1	4.78E-2	5.81E-3	1.3E+0
-1.0	7.21E-1	-1.21E+0	8.56E-1	-2.99E-1	4.46E-2	2.72E-3	5.0E-1
0.0	8.84E-1	-1.42E+0	9.36E-1	-2.99E-1	4.05E-2	2.46E-3	4.2E-1
2.0	1.01E+0	-1.51E+0	9.35E-1	-2.89E-1	4.00E-2	3.24E-3	5.4E-1
4.0	1.02E+0	-1.55E+0	1.02E+0	-3.46E-1	5.23E-2	3.87E-3	5.8E-1
6.0	1.06E+0	-1.73E+0	1.22E+0	-4.30E-1	6.48E-2	4.34E-3	5.5E-1
8.0	1.13E+0	-1.91E+0	1.37E+0	-4.79E-1	6.98E-2	4.17E-3	4.8E-1
10.0	1.17E+0	-2.01E+0	1.42E+0	-4.83E-1	6.81E-2	3.19E-3	3.6E-1

TABLE 11. SPHERICAL ABERRATION COEFFICIENTS FOR THE THREE CYLINDER EINZEL LENS. A/D=0.5 G/D=0.1

V2/V1	CS0	CS1	CS2	CS3	CS4	Y	%ERROR
-0.5	5.37E+0	-1.68E+1	2.38E+1	-1.68E+1	5.37E+0	9.40E-1	1.3E+0
0.0	2.42E+2	-9.54E+2	1.43E+3	-9.54E+2	2.42E+2	6.00E+0	1.5E-1
0.5	4.47E+4	-1.79E+5	2.68E+5	-1.79E+5	4.47E+4	-6.00E+2	8.3E-2
1.5	2.03E+5	-8.10E+5	1.22E+6	-8.10E+5	2.03E+5	6.00E+3	1.8E-1
2.0	5.68E+3	-2.27E+4	3.40E+4	-2.27E+4	5.68E+3	-4.00E+1	4.4E-2
3.0	2.36E+2	-9.33E+2	1.39E+3	-9.33E+2	2.36E+2	-4.00E+0	1.0E-1
4.0	4.71E+1	-1.81E+2	2.67E+2	-1.81E+2	4.71E+1	-8.00E-1	1.1E-1
5.0	1.72E+1	-6.31E+1	9.19E+1	-6.31E+1	1.72E+1	1.00E-1	3.9E-2
6.0	8.65E+0	-2.97E+1	4.24E+1	-2.97E+1	8.65E+0	2.99E-1	2.5E-1
7.0	5.29E+0	-1.67E+1	2.33E+1	-1.67E+1	5.29E+0	4.79E-1	7.1E-1
8.0	3.69E+0	-1.05E+1	1.43E+1	-1.05E+1	3.69E+0	6.80E-1	1.5E+0
9.0	2.83E+0	-7.17E+0	9.46E+0	-7.17E+0	2.83E+0	7.80E-1	2.6E+0
10.0	2.33E+0	-5.14E+0	6.62E+0	-5.14E+0	2.33E+0	9.99E-1	4.6E+0

TABLE 12. SPHERICAL ABERRATION COEFFICIENTS FOR THE TWO APERTURE LENS. T/D=0.05 D1=D2=D

A/D= .5

V2/V1	CS0	CS1	CS2	CS3	CS4	Y	%ERROR
2.0	5.96E+3	-2.00E+4	2.52E+4	-1.41E+4	2.96E+3	1.03E+1	2.1E-2
5.0	3.95E+1	-1.02E+2	1.00E+2	-4.41E+1	7.34E+0	-3.52E-2	2.9E-2
10.0	5.51E+0	-1.13E+1	8.93E+0	-3.23E+0	4.53E-1	2.09E-3	2.7E-2
20.0	1.51E+0	-2.37E+0	1.48E+0	-4.34E-1	5.19E-2	2.51E-3	2.7E-1
40.0	6.39E-1	-7.22E-1	3.54E-1	-8.26E-2	8.59E-3	2.29E-3	1.4E+0

A/D= 1

V2/V1	CS0	CS1	CS2	CS3	CS4	Y	%ERROR
2.0	6.08E+3	-2.05E+4	2.58E+4	-1.45E+4	3.05E+3	-4.90E+1	1.0E-1
5.0	4.12E+1	-1.09E+2	1.10E+2	-4.95E+1	8.48E+0	2.12E-1	1.6E-1
10.0	5.69E+0	-1.22E+1	1.02E+1	-3.91E+0	5.84E-1	1.02E-2	1.1E-1
20.0	1.51E+0	-2.54E+0	1.73E+0	-5.60E-1	7.35E-2	2.45E-3	2.3E-1
40.0	6.08E-1	-7.62E-1	4.22E-1	-1.12E-1	1.30E-2	2.48E-3	1.3E+0

TABLE 13. SPHERICAL ABERRATION COEFFICIENTS FOR THE THREE APERTURE LENS. A/D=0.5

V3/V1= 2

V2/V1	CS0	CS1	CS2	CS3	CS4	Y	%ERROR
-1.0	3.72E+0	-1.08E+1	1.41E+1	-9.24E+0	2.75E+0	3.88E-1	1.3E+0
-0.8	8.60E+0	-2.81E+1	3.72E+1	-2.34E+1	5.98E+0	1.99E-1	2.7E-1
-0.6	2.04E+1	-6.95E+1	9.22E+1	-5.64E+1	1.35E+1	1.43E-1	8.0E-2
-0.4	4.82E+1	-1.67E+2	2.21E+2	-1.32E+2	3.04E+1	4.73E-1	1.1E-1
0.0	2.60E+2	-9.01E+2	1.18E+3	-6.87E+2	1.51E+2	1.95E+0	8.7E-2
2.0	5.63E+3	-1.89E+4	2.38E+4	-1.33E+4	2.80E+3	2.22E+1	4.9E-2
4.0	3.08E+2	-1.00E+3	1.23E+3	-6.71E+2	1.38E+2	2.89E+0	1.2E-1
6.0	4.91E+1	-1.55E+2	1.87E+2	-1.02E+2	2.13E+1	1.43E-1	4.0E-2
8.0	1.62E+1	-4.92E+1	5.87E+1	-3.25E+1	7.03E+0	5.35E-2	4.7E-2
10.0	7.75E+0	-2.23E+1	2.64E+1	-1.50E+1	3.41E+0	7.95E-2	1.5E-1

V3/V1= 5

V2/V1	CS0	CS1	CS2	CS3	CS4	Y	%ERROR
-1.0	5.31E+0	-1.47E+1	1.64E+1	-8.54E+0	1.78E+0	6.89E-2	3.3E-1
-0.8	7.29E+0	-2.03E+1	2.23E+1	-1.13E+1	2.27E+0	7.29E-2	2.6E-1
-0.6	9.76E+0	-2.72E+1	2.94E+1	-1.46E+1	2.83E+0	3.17E-2	8.8E-2
-0.4	1.27E+1	-3.51E+1	3.75E+1	-1.83E+1	3.43E+0	5.21E-3	1.1E-2
-0.2	1.60E+1	-4.39E+1	4.62E+1	-2.21E+1	4.06E+0	1.29E-2	2.3E-2
0.0	1.96E+1	-5.32E+1	5.52E+1	-2.60E+1	4.66E+0	-3.15E-2	4.7E-2
2.0	3.69E+1	-9.54E+1	9.39E+1	-4.17E+1	7.06E+0	1.56E-2	1.3E-2
4.0	4.32E+1	-1.14E+2	1.14E+2	-5.08E+1	8.61E+0	1.66E-1	1.2E-1
6.0	3.07E+1	-7.81E+1	7.52E+1	-3.26E+1	5.35E+0	-3.78E-2	4.1E-2
8.0	1.85E+1	-4.54E+1	4.25E+1	-1.80E+1	2.92E+0	1.14E-2	2.2E-2
10.0	1.14E+1	-2.72E+1	2.50E+1	-1.05E+1	1.70E+0	3.86E-3	1.2E-2

V3/V1= 10

V2/V1	CS0	CS1	CS2	CS3	CS4	Y	%ERROR
-1.6	1.70E+0	-3.82E+0	3.55E+0	-1.60E+0	3.00E-1	1.35E-2	4.2E-1
-0.8	2.75E+0	-6.08E+0	5.34E+0	-2.21E+0	3.63E-1	2.68E-3	5.7E-2
0.0	3.73E+0	-7.95E+0	6.63E+0	-2.57E+0	3.89E-1	-3.59E-4	6.2E-3
2.0	4.74E+0	-9.59E+0	7.60E+0	-2.81E+0	4.13E-1	4.78E-3	7.2E-2
4.0	5.24E+0	-1.11E+1	9.20E+0	-3.56E+0	5.40E-1	-2.52E-3	3.1E-2
6.0	5.86E+0	-1.26E+1	1.05E+1	-4.01E+0	5.96E-1	6.77E-3	7.5E-2
8.0	5.87E+0	-1.24E+1	1.01E+1	-3.74E+0	5.38E-1	1.06E-2	1.2E-1
10.0	5.36E+0	-1.10E+1	8.70E+0	-3.15E+0	4.43E-1	2.69E-3	3.6E-2

V3/V1= 20

V2/V1	CS0	CS1	CS2	CS3	CS4	Y	%ERROR
-2.0	7.72E-1	-1.33E+0	9.60E-1	-3.44E-1	5.27E-2	2.66E-3	4.3E-1
-1.0	9.46E-1	-1.57E+0	1.08E+0	-3.59E-1	5.02E-2	3.22E-3	4.7E-1
0.0	1.08E+0	-1.73E+0	1.14E+0	-3.61E-1	4.82E-2	3.48E-3	4.8E-1
2.0	1.20E+0	-1.86E+0	1.18E+0	-3.71E-1	5.02E-2	1.94E-3	2.6E-1
4.0	1.26E+0	-1.97E+0	1.30E+0	-4.24E-1	5.93E-2	4.18E-3	5.0E-1
6.0	1.33E+0	-2.17E+0	1.48E+0	-4.94E-1	6.89E-2	3.29E-3	3.5E-1
8.0	1.42E+0	-2.38E+0	1.65E+0	-5.47E-1	7.43E-2	3.93E-3	3.8E-1
10.0	1.51E+0	-2.55E+0	1.75E+0	-5.68E-1	-7.50E-2	-1.46E-1	1.5E+1

TABLE 14. SPHERICAL ABERRATION COEFFICIENTS FOR THE THREE APERTURE EINZEL LENS. A/D=0.5

V2/V1	CS0	CS1	CS2	CS3	CS4	Y	%ERROR
-0.6	1.10E+1	-3.86E+1	5.56E+1	-3.86E+1	1.10E+1	8.00E-1	5.1E-1
-0.4	4.21E+1	-1.61E+2	2.38E+2	-1.61E+2	4.21E+1	3.99E-1	1.2E-1
-0.2	1.74E+2	-6.86E+2	1.02E+3	-6.86E+2	1.74E+2	-4.00E+0	2.9E-1
0.0	8.11E+2	-3.23E+3	4.83E+3	-3.23E+3	8.11E+2	-8.00E+0	1.2E-1
0.5	1.31E+5	-5.25E+5	7.87E+5	-5.25E+5	1.31E+5	-1.00E+3	1.9E-1
1.5	5.19E+5	-2.08E+6	3.11E+6	-2.08E+6	5.19E+5	-1.20E+4	2.8E-1
2.0	1.40E+4	-5.59E+4	8.39E+4	-5.59E+4	1.40E+4	1.00E+2	1.7E-1
3.0	5.51E+2	-2.19E+3	3.28E+3	-2.19E+3	5.51E+2	2.00E+0	9.1E-2
4.0	1.05E+2	-4.11E+2	6.12E+2	-4.11E+2	1.05E+2	0.00E+0	0.0E+0
5.0	3.68E+1	-1.41E+2	2.08E+2	-1.41E+2	3.68E+1	-8.00E-1	1.4E-1
6.0	1.77E+1	-6.53E+1	9.53E+1	-6.53E+1	1.77E+1	1.99E-1	1.5E-1
7.0	1.03E+1	-3.64E+1	5.25E+1	-3.64E+1	1.03E+1	5.99E-1	4.1E-1
8.0	6.80E+0	-2.29E+1	3.25E+1	-2.29E+1	6.80E+0	6.00E-1	6.5E-1
9.0	4.91E+0	-1.56E+1	2.18E+1	-1.56E+1	4.91E+0	8.39E-1	1.3E+0
10.0	3.80E+0	-1.13E+1	1.56E+1	-1.13E+1	3.80E+0	1.20E+0	1.3E+0

4.3) FURTHER SIMPLIFICATION OF ABERRATION COEFFICIENTS

We have shown that our relationships are erroneous in the case of very strong lenses. It follows, therefore, that for the lenses to which they can be applied the aberration coefficients will be appreciable.

If we assume that $q_{16} >> m_{16} >> 0$ then we can simplify equations (133)-(140):-

$$m_{16} = \sigma m_{15}/3 = \sigma^2 m_{14}/3 = \sigma^3 m_{13} \tag{176}$$

$$q_{16} = \sigma q_{15}/5 = \sigma^2 q_{14}/10 = \sigma^3 q_{13}/10 = \sigma^4 q_{12}/5 = \sigma^5 q_{11} \tag{177}$$

Incorporating these and (122) and (123) into equations (114)-(117):-

$$M_1(k) = m_{16}(\sigma+k)^3 \tag{178}$$

$$M_2(k) = \sigma m_{16}(\sigma+k)^3 \tag{179}$$

$$Q_1(k) = q_{16}(\sigma+k)^5 \tag{180}$$

$$Q_2(k) = \sigma q_{16}(\sigma+k)^5 \tag{181}$$

Hence, from (110), (112) and (113) we have that:-

$$r_2' = -r_1/f_2 + m_{16}(r_1'/\sigma + r_1/f_2)^3 + q_{16}(r_1'/\sigma + r_1/f_2)^5 \tag{182}$$

$$r_2/f_1 = r_1' + \sigma m_{16}(r_1'/\sigma + r_1/f_2)^3 + \sigma q_{16}(r_1'/\sigma + r_1/f_2)^5 \tag{183}$$

Furthermore, it can be shown that the converse expressions are given by:-

$$r_1' = r_2/f_1 + \sigma m_{16}(r_2' - r_2/(\sigma f_1))^3 + \sigma q_{16}(r_2 - r_2/(\sigma f_1))^5 \quad (184)$$

$$r_1 / f_2 = -r_2' + m_{16}(-r_2' + r_2/(\sigma f_1))^3 + q_{16}(-r_2' + r_2/(\sigma f_1))^5 \quad (185)$$

These greatly simplified relationships incorporate all the third and fifth order meridional aberrations and enable the output parameters of a ray to be calculated from a knowledge of only two aberration coefficients and the lens constant σ. We have tested the validity of these expressions by comparing the values of r_2 and r_2' predicted by equations (182) and (183) to those actually produced by ray tracing through the computer model. These results are shown in Tables (15)-(18). In order to give a fair test of the practical use of equations (182) and (183) we have taken the focal lengths as being those values derived from the Picht equation (see Cook and Heddle, 1976). Moreover we have taken the value of σ to be the 4th root of the overall voltage ratio (equation (175)). The values of m_{16} and q_{16} are taken from our results for parallel trajectories (Table 5).

In the case of zero magnification, r_2, which is derived from Q via equation (104), is very sensitive to small errors in the focal lengths. In spite of this, the accuracy of expressions (182) and (183) can be seen to be very good for a

wide range of voltage ratios and linear magnifications.

TABLE 15. COMPARISON OF THE OUTPUT PARAMETERS OF RAYS THROUGH THE COMPUTER MODEL TO THOSE CALCULATED FROM EQUATIONS (182) AND (183).

(TWO CYLINDER LENS. G/D=0.1 D1=D2=D V2/V1=2)

P=14 MAGNIFICATION =-12.3

		COMPUTER MODEL		CALCULATED	
R1'	%FILLING	R2'	R2	R2'	R2
4.00E-3	11	-2.51E-4	4.35E-2	-2.50E-4	4.36E-2
8.00E-3	22	-6.35E-4	8.54E-2	-6.35E-4	8.54E-2
1.20E-2	34	-1.32E-3	1.23E-1	-1.30E-3	1.23E-1
1.60E-2	45	-2.49E-3	1.54E-1	-2.41E-3	1.55E-1
2.00E-2	56	-4.52E-3	1.75E-1	-4.18E-3	1.79E-1

P=19 MAGNIFICATION =-1.8

		COMPUTER MODEL		CALCULATED	
R1'	%FILLING	R2'	R2	R2'	R2
4.00E-3	15	-1.57E-3	4.31E-2	-1.57E-3	4.31E-2
8.00E-3	30	-3.50E-3	8.17E-2	-3.48E-3	8.18E-2
1.20E-2	46	-6.24E-3	1.09E-1	-6.14E-3	1.10E-1
1.40E-2	53	-8.14E-3	1.16E-1	-7.90E-3	1.19E-1
1.60E-2	61	-1.06E-2	1.16E-1	-1.00E-2	1.23E-1

P=INFINITY MAGNIFICATION=0

		COMPUTER MODEL		CALCULATED	
R1	%FILLING	R2'	R2	R2'	R2
6.00E-2	12	-3.89E-3	-3.44E-4	-3.89E-3	-3.58E-4
1.20E-1	24	-7.95E-3	-2.89E-3	-7.95E-3	-2.91E-3
1.80E-1	36	-1.23E-2	-1.03E-2	-1.23E-2	-1.00E-2
2.40E-1	48	-1.74E-2	-2.62E-2	-1.73E-2	-2.46E-2
3.00E-1	60	-2.37E-2	-5.69E-2	-2.31E-2	-5.02E-2

TABLE 16. COMPARISON OF THE OUTPUT PARAMETERS OF RAYS THROUGH THE COMPUTER MODEL TO THOSE CALCULATED FROM EQUATIONS (182) AND (183).

(TWO CYLINDER LENS. G/D=0.1 D1=D2=D V2/V1=5)

P=2.8 MAGNIFICATION =-50.1

		COMPUTER MODEL		CALCULATED	
R1'	%FILLING	R2'	R2	R2'	R2
2.00E-2	11	-2.32E-4	3.49E-2	-2.34E-4	3.49E-2
4.00E-2	22	-8.21E-4	6.90E-2	-8.10E-4	6.90E-2
6.00E-2	34	-2.17E-3	1.01E-1	-2.10E-3	1.01E-1
8.01E-2	45	-4.79E-3	1.29E-1	-4.57E-3	1.30E-1
1.00E-1	56	-9.33E-3	1.53E-1	-8.77E-3	1.55E-1

P=4.2 MAGNIFICATION =-1.2

		COMPUTER MODEL		CALCULATED	
R1'	%FILLING	R2'	R2	R2'	R2
2.00E-2	17	-7.50E-3	3.45E-2	-7.51E-3	3.45E-2
4.00E-2	34	-1.63E-2	6.58E-2	-1.62E-2	6.58E-2
5.00E-2	42	-2.16E-2	7.89E-2	-2.16E-2	7.91E-2
6.00E-2	50	-2.80E-2	8.95E-2	-2.78E-2	8.99E-2
7.01E-2	59	-3.58E-2	9.65E-2	-3.53E-2	9.75E-2

P=INFINITY MAGNIFICATION=0

		COMPUTER MODEL		CALCULATED	
R1	%FILLING	R2'	R2	R2'	R2
6.00E-2	12	-1.53E-2	-2.27E-4	-1.53E-2	-2.10E-4
1.20E-1	24	-3.12E-2	-1.68E-3	-3.12E-2	-1.71E-3
1.80E-1	36	-4.81E-2	-5.96E-3	-4.81E-2	-5.96E-3
2.40E-1	48	-6.69E-2	-1.48E-2	-6.67E-2	-1.47E-2
3.00E-1	60	-8.85E-2	-3.12E-2	-8.79E-2	-3.02E-2

TABLE 17. COMPARISON OF THE OUTPUT PARAMETERS OF RAYS THROUGH THE COMPUTER MODEL TO THOSE CALCULATED FROM EQUATIONS (182) AND (183).

(TWO CYLINDER LENS. G/D=0.1 D1=D2=D V2/V1=10)

P=1.7 MAGNIFICATION =-9.3

		COMPUTER MODEL		CALCULATED	
R1'	%FILLING	R2'	R2	R2'	R2
3.00E-2	10	-1.08E-3	2.38E-2	-1.05E-3	2.39E-2
6.00E-2	20	-2.44E-3	4.74E-2	-2.35E-3	4.75E-2
9.02E-2	31	-4.36E-3	7.02E-2	-4.18E-3	7.04E-2
1.20E-1	41	-7.24E-3	9.17E-2	-6.87E-3	9.23E-2
1.51E-1	51	-1.14E-2	1.11E-1	-1.07E-2	1.12E-1

P=2.4 MAGNIFICATION =-1

		COMPUTER MODEL		CALCULATED	
R1'	%FILLING	R2'	R2	R2'	R2
3.00E-2	14	-9.48E-3	2.37E-2	-9.44E-3	2.37E-2
7.01E-2	34	-2.36E-2	5.34E-2	-2.34E-2	5.35E-2
9.02E-2	43	-3.19E-2	6.66E-2	-3.17E-2	6.67E-2
1.10E-1	53	-4.16E-2	7.79E-2	-4.13E-2	7.81E-2
1.20E-1	58	-4.70E-2	8.28E-2	-4.68E-2	8.30E-2

P=INFINITY MAGNIFICATION=0

		COMPUTER MODEL		CALCULATED	
R1	%FILLING	R2'	R2	R2'	R2
6.00E-2	12	-2.38E-2	-1.57E-4	-2.38E-2	-1.37E-4
1.20E-1	24	-4.83E-2	-1.16E-3	-4.82E-2	-1.12E-3
1.80E-1	36	-7.40E-2	-3.93E-3	-7.39E-2	-3.89E-3
2.40E-1	48	-1.01E-1	-9.65E-3	-1.01E-1	-9.58E-3
3.00E-1	60	-1.32E-1	-1.99E-2	-1.32E-1	-1.96E-2

TABLE 18. COMPARISON OF THE OUTPUT PARAMETERS OF RAYS THROUGH THE COMPUTER MODEL TO THOSE CALCULATED FROM EQUATIONS (182) AND (183).

(TWO CYLINDER LENS. G/D=0.1 D1=D2=D V2/V1=20)

P=1.25 MAGNIFICATION =-8.9

		COMPUTER MODEL		CALCULATED	
R1'	%FILLING	R2'	R2	R2'	R2
5.00E-2	13	-1.34E-3	2.28E-2	-1.31E-3	2.26E-2
1.00E-1	25	-3.11E-3	4.53E-2	-2.96E-3	4.51E-2
1.51E-1	38	-5.73E-3	6.71E-2	-5.35E-3	6.71E-2
2.02E-1	51	-9.68E-3	8.78E-2	-8.93E-3	8.83E-2
2.55E-1	64	-1.55E-2	1.06E-1	-1.43E-2	1.08E-1

P=1.65 MAGNIFICATION =-1

		COMPUTER MODEL		CALCULATED	
R1'	%FILLING	R2'	R2	R2'	R2
5.00E-2	17	-1.12E-2	2.26E-2	-1.12E-2	2.25E-2
1.00E-1	33	-2.35E-2	4.43E-2	-2.34E-2	4.43E-2
1.51E-1	50	-3.78E-2	6.43E-2	-3.78E-2	6.44E-2
1.76E-1	58	-4.62E-2	7.32E-2	-4.63E-2	7.34E-2
2.02E-1	67	-5.55E-2	8.12E-2	-5.59E-2	8.15E-2

P=INFINITY MAGNIFICATION=0

		COMPUTER MODEL		CALCULATED	
R1	%FILLING	R2'	R2	R2'	R2
6.00E-2	12	-2.96E-2	-9.99E-5	-2.96E-2	-8.82E-5
1.20E-1	24	-5.98E-2	-7.33E-4	-5.97E-2	-7.15E-4
1.80E-1	36	-9.11E-2	-2.55E-3	-9.11E-2	-2.46E-3
2.40E-1	48	-1.24E-1	-6.25E-3	-1.24E-1	-6.01E-3
3.00E-1	60	-1.60E-1	-1.28E-2	-1.60E-1	-1.21E-2

4.4) SPHERICAL ABERRATION

Spherical aberration (or the aperture defect) is probably the most important of all the geometric aberrations. It, for example, is responsible for limiting both the screen spot size in a cathode ray tube and, along with diffraction effects, the resolving power of an electron microscope (Zworykin et al, 1945). The reason for its importance lies largely in it being the only geometric defect that is present even for axial objects. Indeed, it can be shown theoretically that it is impossible to eliminate it entirely from any axially symmetric electrostatic or magnetic lens (see, for example, Scherzer, 1936). However, spherical aberration is also of particular interest because it is often taken as a guideline to the overall aberration of a system. This was investigated by Brunt and Read (1975) who found that the spherical aberration of an axial object could be used to indicate an upper limit to the total aberration of a finite size object at that plane. The fact that, in general, a lens with small spherical aberration will produce a good image of non-axial objects also follows from the results that we have obtained.

4.4.1) Relationship to Total Aberration

We have seen (Figure 4) how the ideal image of an off-axis object is formed by Gaussian rays. Let us now examine how the third order aberrations of a lens affect this idealised

situation. This is shown schematically in Figure 27. The aberrations have resulted in the radial displacement of a ray at the Gaussian image plane changing from r_g to r_{ab}. We can therefore define the total aberration as:-

$$\Delta r = r_{ab} - r_g \tag{186}$$

From the diagram we also have:-

$$r_{ab} = r_2 + (Q_o - F_2)r_2' \tag{187}$$

Where we have used Q_o to represent the Gaussian image distance.

This can be expressed in terms of the ray parameters in object space by the use of equations (182) and (183):-

$$r_{ab} = f_1 r_1' + \sigma f_1 m_{16}\left(\frac{r_1'}{\sigma} + \frac{r_1}{f_2}\right)^3 + (Q_o - F_2)\left[-\frac{r_1}{f_2} + m_{16}\left(\frac{r_1'}{\sigma} + \frac{r_1}{f_2}\right)^3\right] \tag{188}$$

$$= f_1 r_1' - (Q_o - F_2)\left(\frac{r_1}{f_2}\right) + m_{16}\left(\frac{r_1'}{\sigma} + \frac{r_1}{f_2}\right)^3 \cdot (Q_o - F_2 + f_1\sigma) \tag{189}$$

The last term of (189) represents the total third order aberration of the ray:-

$$\Delta r = m_{16}\left(\frac{r_1'}{\sigma} + \frac{r_1}{f_2}\right)^3 \cdot (Q_o - F_2 + \sigma f_1) \tag{190}$$

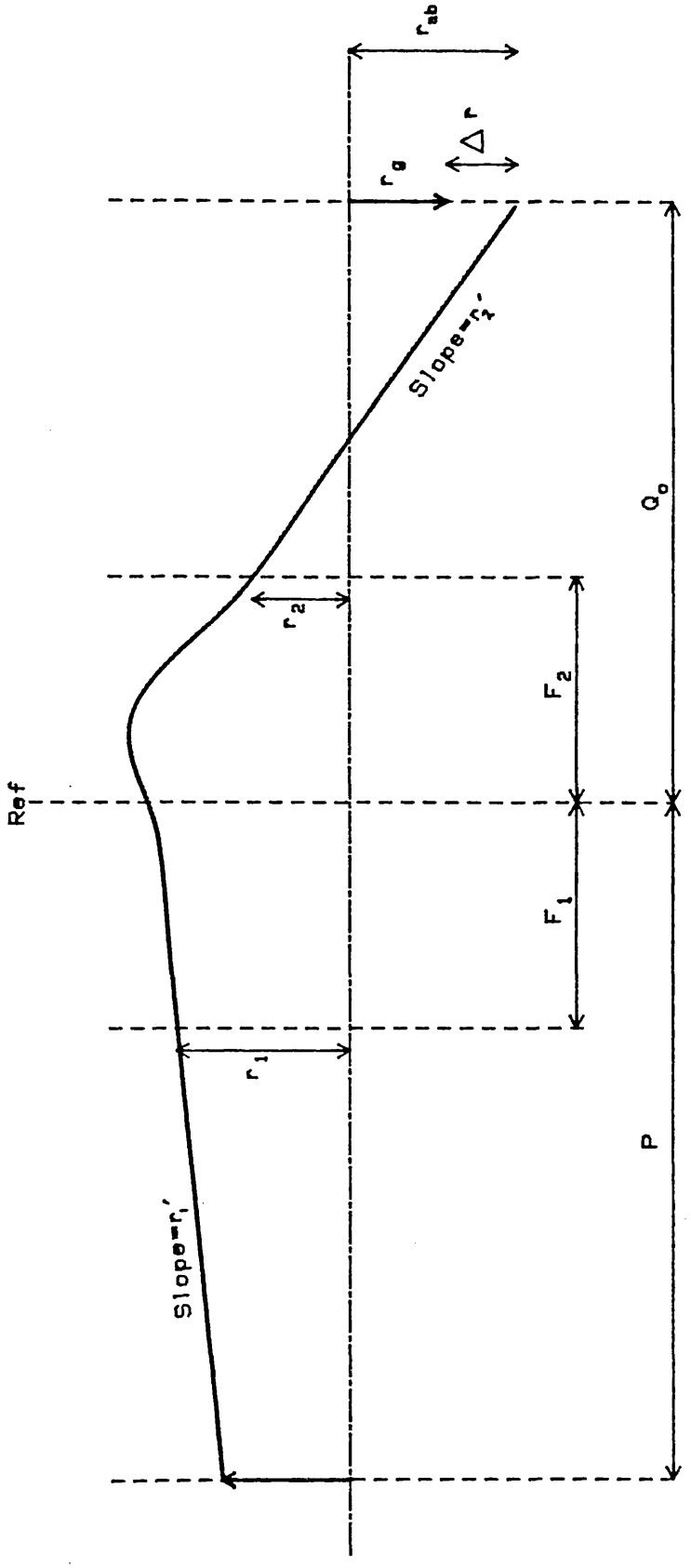

FIGURE 27. Schematic representation of the aberration of an off-axis object. The Gaussian image radius is r_g, whilst an aberrated ray crosses the image plane at radius r_{ab}.

For a given object plane, therefore, the aberration of a ray is given by the following proportionality:-

$$\Delta r \propto (r_1'/\sigma + r_1/f_2)^3 \qquad (191)$$

If we use equation (175) to eliminate σ:-

$$\Delta r \propto (r_1 + r_1'/\sqrt{f_1 f_2})^3 \qquad (192)$$

The importance of this dependence becomes clear if one realises that $(r_1 + r_1'/\sqrt{f_1 f_2})$ is the radial displacement of the ray at a plane which is $\sqrt{f_1 f_2}$ lens diameters to the right of the first principal focus. To a good approximation (see section 4.1) this plane is coincident with the reference plane of the lens. It follows that rays from a particular object plane will be aberrated according to the filling as measured at the reference plane and independent of the axial displacement of the point of origin of the ray. For a given filling factor, the spherical aberration of a point axial object gives an upper limit to the total aberration of an object of finite size situated at the same plane. This conclusion can also be drawn from the investigation of Brunt and Read, as long as we remember that these results are not applicable to extremely strong lenses.

4.4.2) Magnitude of the aberration

In Section 4.1 we showed how the spherical aberration of a lens may be represented by five coefficients and, in turn, how each of these must be related to the single m_{16} aberration coefficient (equations 161-165). For the lenses that we are considering $m_{16} >> 0$ and these equations can be simplified greatly:-

$$Cs_0 = -m_{16} f_2 / \sigma^3 \qquad (193)$$

$$Cs_1 = 4 m_{16} f_2 / \sigma^4 = -4 Cs_0 / \sigma \qquad (194)$$

$$Cs_2 = -6 m_{16} f_2 / \sigma^5 = 6 Cs_0 / \sigma^2 \qquad (195)$$

$$Cs_3 = 4 m_{16} f_2 / \sigma^6 = -4 Cs_0 / \sigma^3 \qquad (196)$$

$$Cs_4 = -m_{16} f_2 / \sigma^7 = Cs_0 / \sigma^4 \qquad (197)$$

It follows that, just as with the m_{ij} coefficients, the third order spherical aberration of a lens can be represented by a single coefficient. Although this result is important because of the practical significance of spherical aberration, it is not surprising since spherical aberration is just one of the geometric aberrations which are explicitly described by the m_{ij} coefficients.

The size of the spherically aberrated disc at the Gaussian image plane becomes:-

$$\Delta r = M.Cs_0(1 - 1/\sigma M)^4 r_1'^3 \qquad (198)$$

and it follows from equation (154) that the third order spherical aberration coefficient is given by:-

$$M.Cs(M) = M.Cs_0(1 - 1/\sigma M)^4 \qquad (199)$$

This expression is plotted in Figure 28 for the two cylinder lens at various accelerating potentials. Also plotted are the functions M.Cs(M) as derived from Harting and Read's coefficients. It can be seen that, particularly in the case of the weaker lenses, the agreement is excellent.
When a lens is being operated with zero magnification (object at infinity) equation (199) is inappropriate and the aberration will be given by:-

$$\Delta r(M=0) = \sigma f_1 m_{16}\left(\frac{r_1}{f_2}\right)^3 = -Cs_4\left(\frac{r_1}{f_1}\right)^3 = -\frac{Cs_0}{\sigma^4}\left(\frac{r_1}{f_1}\right)^3 \qquad (200)$$

4.4.3) Retarding Lenses

The spherical aberration of a retarding lens (whose parameters we shall denote by $\sim$) can be deduced from equation (199):-

$$\tilde{Cs}(M) = \tilde{Cs}_0(1 - 1/\tilde{\sigma}\tilde{M})^4 \qquad (201)$$

Where $\tilde{Cs}(M)$ is the aberration coefficient of the retarding

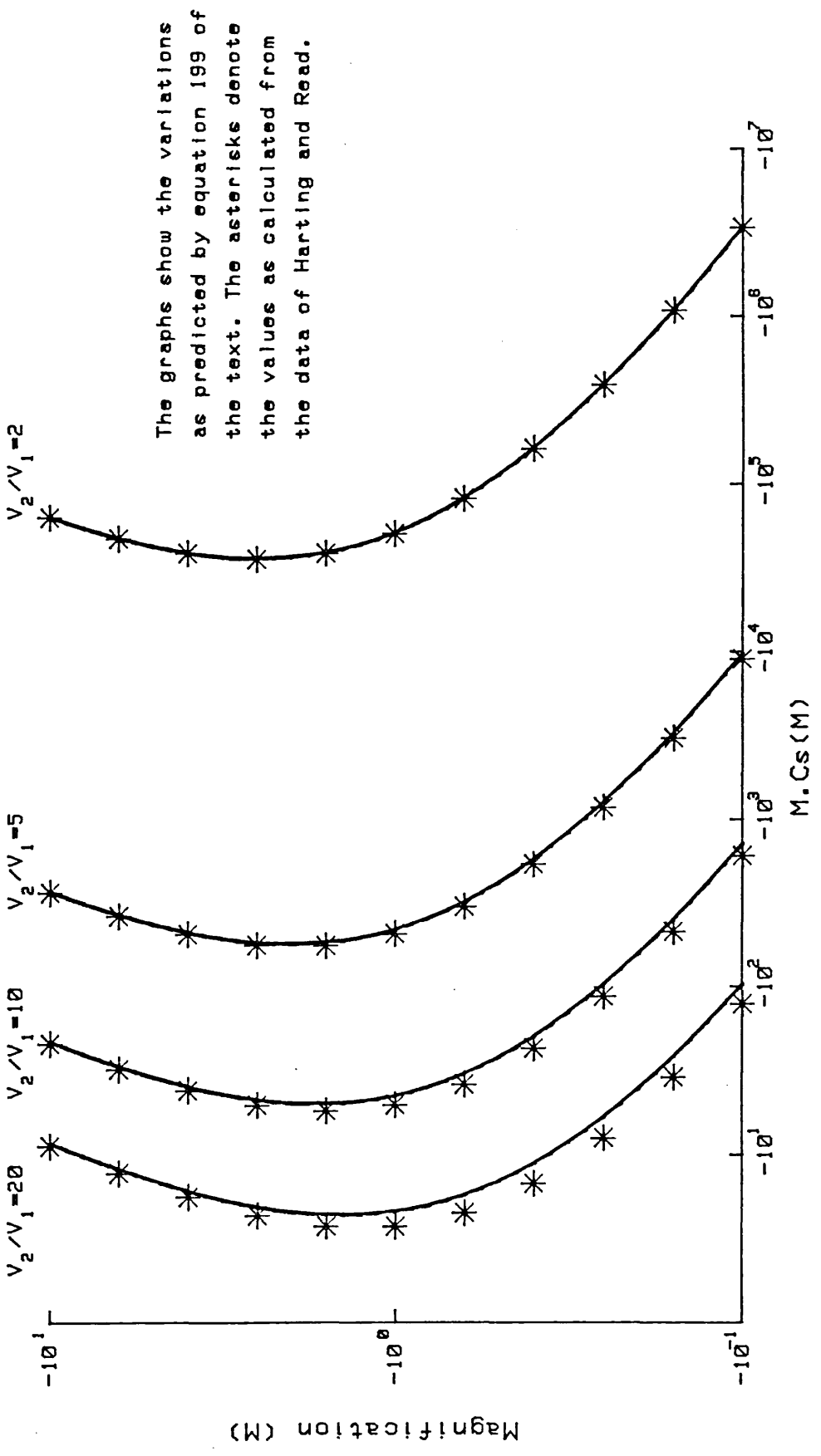

FIGURE 28. Variation of spherical aberration with linear magnification.
Two cylinder lens, g/D=0.1

lens operating with a magnification of M, $\tilde{M}$ being equal to 1/M and $\tilde{Cs}_o$ being derived from equation (193):-

$$\tilde{Cs}_o = -\tilde{m}_{16}\,\tilde{f}_2/\tilde{\sigma}^3 \qquad (202)$$

which can be rewritten using the results that we derived earlier:-

$$\tilde{Cs}_o = -m_{16}\,f_2/\sigma = Cs_o\,(V_2/V_1)^{1/2} \qquad (203)$$

Hence:-

$$\tilde{Cs}(M) = Cs(M).M^4\,(V_2/V_1)^{3/2} \qquad (204)$$

So the spherical aberation coefficient of a retarding lens can be derived from that of the corresponding accelerating lens operating at the same magnification. V_2/V_1 is the overall voltage ratio of the accelerating lens. Since this is greater than unity it follows that, for a given magnification, a lens will always be more aberrated when used to decelerate rather than accelerate. This is in agreement with the experimental results of Klemperer and Wright (1939, see also Klemperer, 1971, Figures 6.5 and 6.11). They used a pepperpot method to measure the longitudinal aberration of parallel rays entering a two cylinder lens. It is interesting to note, however, that although they found the lens to be more aberrated when used to retard rather than accelerate, their aberration coefficient

was actually greater in the accelerating case. This is because it was defined in terms of the ray slope in image space, r_2' (cf equation 154). It is therefore not only a function of the aberration and the magnification but also, in accordance with the Helmholtz-Lagrange relationship, dependent upon the relative potentials of object and image space.

4.5) DISC OF LEAST CONFUSION

It can be seen from Figure 8 that the image of a point axial object will have minimum cross section at a plane some way before the Gaussian image plane. This is the disc of least confusion and we shall now derive its size and position using the results of the previous work. For algebraic simplicity we shall consider the incoming rays to be parallel to the optic axis and we shall neglect fifth and higher order aberrations. Once again referring to Figure 8, the position and size of the disc of least confusion is defined by the intersection of the outermost ray of the object beam and one other. This is shown schematically in Figure 29. If the coordinates of the point in image space where the outermost (below axis) ray of the beam intercepts any other ray are given by (F_2-z,d) then:-

$$r_2' = (r_2+d)/z \qquad (205)$$

$$R_2' = (R_2-d)/z \qquad (206)$$

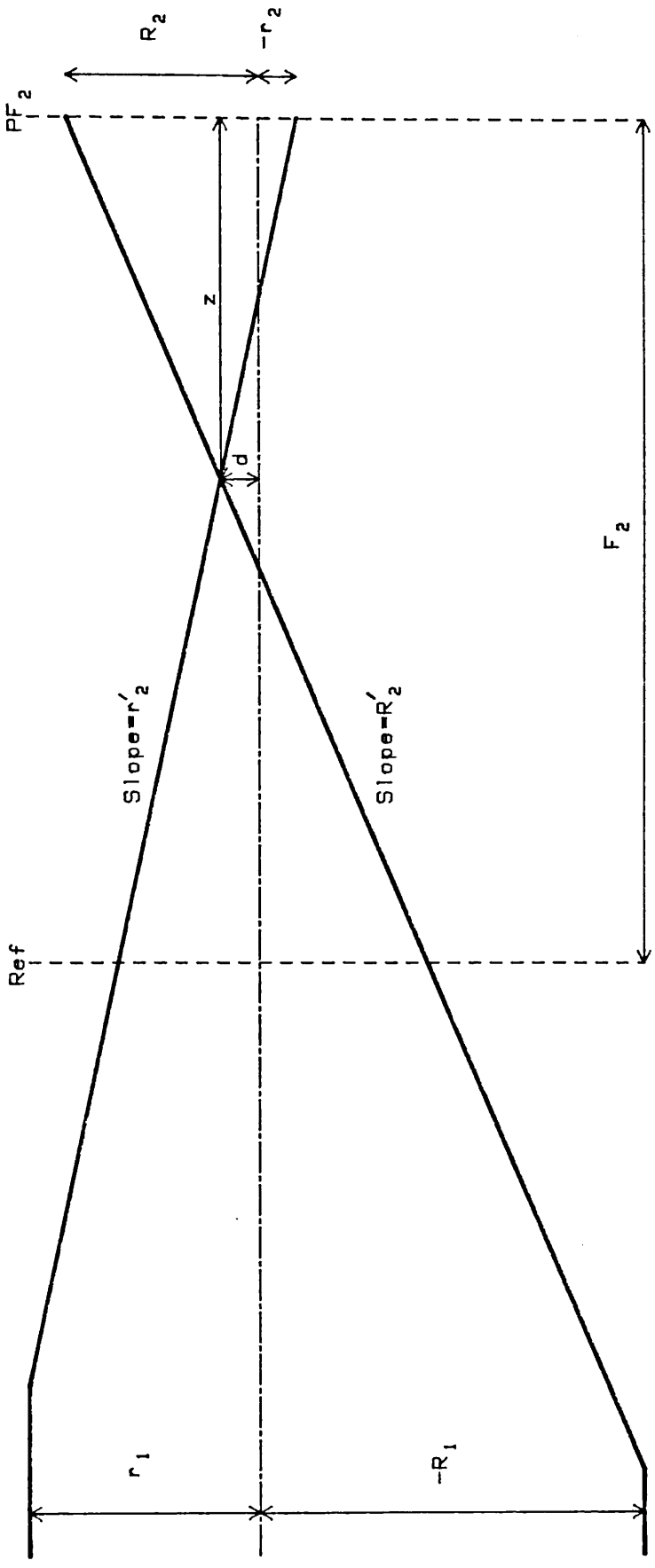

FIGURE 29. Schematic representation of the rays that locate the disc of least confusion. The object beam is parallel to the optic axis and has overall radius R_1.

Therefore:-

$$d = (R_2 r_2' - r_2 R_2')/(r_2' + R_2') \tag{207}$$

When the magnitude of d is a maximum for this bundle of rays, this intersection will define the size and position of the disc of least confusion (D and Z). Setting the differential of (207) with respect to r_1 equal to zero and using (182) and (183), it can be shown that to the third order of R_1:-

$$D = \frac{f_1 \sigma m_{16}}{4}\left(\frac{R_1}{f_2}\right)^3 \tag{208}$$

$$Z = -\frac{3 f_1 \sigma m_{16}}{4}\left(\frac{R_1}{f_2}\right)^3 \tag{209}$$

The sign of Z denotes that the disc of least confusion is to the left of the Gaussian image plane. The overall radius of the image at the Gaussian plane can be derived from equation (183) by letting $r_1'=0$:-

$$\Delta r = f_1 \sigma m_{16}\left(\frac{R_1}{f_2}\right)^3 \tag{210}$$

It can be seen that the image size at the minimum beam waist is 1/4 that at the Gaussian image plane. This is in agreement with the observations of other authors.

4.6) CURVATURE OF THE PRINCIPAL SURFACES

The principal surfaces H_1 and H_2 are defined by the loci of the intercepts of the incoming and outgoing rays for parallel incidence and emergence respectively. (See Figure 30). The results that we have obtained allow us to derive simple expressions for $H_1(r)$ and $H_2(r)$.

Using the notation defined in Figure 30, it can be seen that:-

$$F_2 + H_2(r) = (r_2 - r)/r_2' \tag{211}$$

By substituting for r_2 and r_2' from equations (182) and (183) we can show that, to the third order of r:-

$$F_2 + H_2(r) = f_2 + m_{16}(f_2 - f_1\sigma)(r/f_2)^2 \tag{212}$$

$$= f_2 + f_1 m_{16}\sigma(\sigma-1)(r/f_2)^2 \tag{213}$$

In a similar fashion it can be shown that:-

$$F_1 - H_1(r) = f_1 - (m_{25}/\sigma)(f_2 - f_1\sigma)(r/f_2)^2 \tag{214}$$

$$= f_1 - (m_{16}f_1/\sigma^2)(\sigma-1)(r/f_2)^2 \tag{215}$$

Since for accelerating voltages $\sigma > 1$, it follows that both principal surfaces curve towards the high voltage side of the

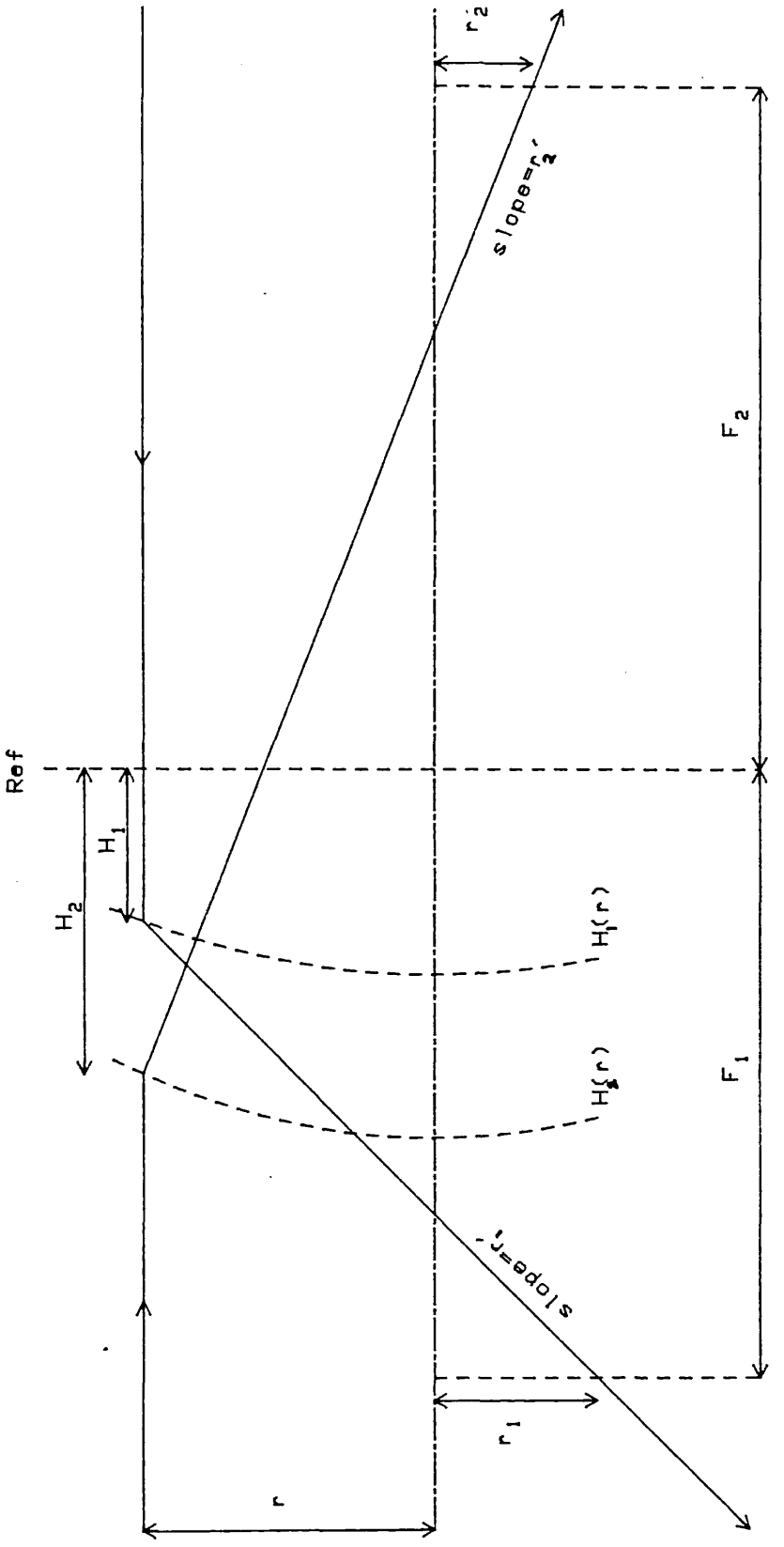

FIGURE 30. The principal surface, H(r) is defined by the intersection of the asymptotes in object and image space of a ray that enters the lens parallel to the axis. There are two surfaces corresponding to object space being to the right or the left of the reference plane.

lens. This is in agreement with the findings of Kuyatt (1972).

4.7) APPLICATION TO LENS DESIGN

We shall now consider how the results that we have obtained can be used to assist in the choice of lens geometry and operating conditions for a particular problem. We shall try to show how, subject to various design constraints, the aberrations of the image can be minimised. Since our aim is to ascertain the optimum lens without necessarily quantifying the magnitude of the aberrations, we shall consider the object in each case to be axial and of negligible cross section.

4.7.1) Optimum Magnification

There are circumstances under which a designer is given little freedom to minimise a system's aberrations by using alternative electrode geometries. For example, the need for uncomplicated power supplies and associated control electronics might mean that a lens must be limited to two electrodes and, as we shall see later on, there is little difference between the aberrations of comparable double element lenses. He is therefore left with the problem of how best to use a particular geometry. We have already seen in Figure 28 that the aberrations of a lens are magnification dependent and that there is a minimum corresponding to an optimum object position. We shall now derive this.

We have from equation (198):-

$$\Delta r = M.Cs_o(1 - 1/\sigma M)^4 r_i'^3 \tag{216}$$

When Δr is a minimum:-

$$\frac{\partial(\Delta r)}{\partial M} = 0 \tag{217}$$

$$= Cs_o\left((1-1/\sigma M)^4 + (4/\sigma M)(1-1/\sigma M)^3\right) r_i'^3 \tag{218}$$

This is satisfied by:-

$$M = -3/\sigma \tag{219}$$

The object position corresponding to this magnification can be derived from equation (15). The minimum value of Δr is given by:-

$$\Delta r\ (M=-3/\sigma) = -9.481(Cs_o/\sigma)r_i'^3 = 2.370Cs_i r_i'^3 \tag{220}$$

In deriving (220) we have assumed that were it not for spherical aberration the image would be infinitesimally small. When the object cannot be assumed to be point axial, (219) may not represent the optimum magnification for minimum image cross section, although it is still indicative of the requirements for minimum image aberration.

4.7.2) Best Lens for Finite Magnification

Consider the design problem that is illustrated in Figure (31). A lens is sought such that the spherical aberration, Δr, at the image is a minimum. The object-image separation (L), the linear magnification (M), the maximum half angle of the object rays (r_1') and the potentials in object and image space are fixed.

The value of Δr is given by equation (198):-

$$\Delta r = M.Cs_o(1 - 1/6M)^4 r_1'^3 \qquad (221)$$

Since the only constraint on our choice of lenses is the overall voltage ratio, we can optimise not only the lens geometry but also its scale size. Before we can analyse this we need to discuss the units of the lens parameters that we are using.

Most tables for focal lengths and aberration coefficients give the values of these parameters in terms of some principal length. For systems of cylindrical symmetry this is commonly the diameter of the narrowest cylinder or aperture, and we shall refer to it as D, the scale size. So if for example the value of F_1 for a particular lens is quoted as 2 then this means that $F_1 = 2*D$.

If, in minimising Δr, we are to allow ourselves the freedom to

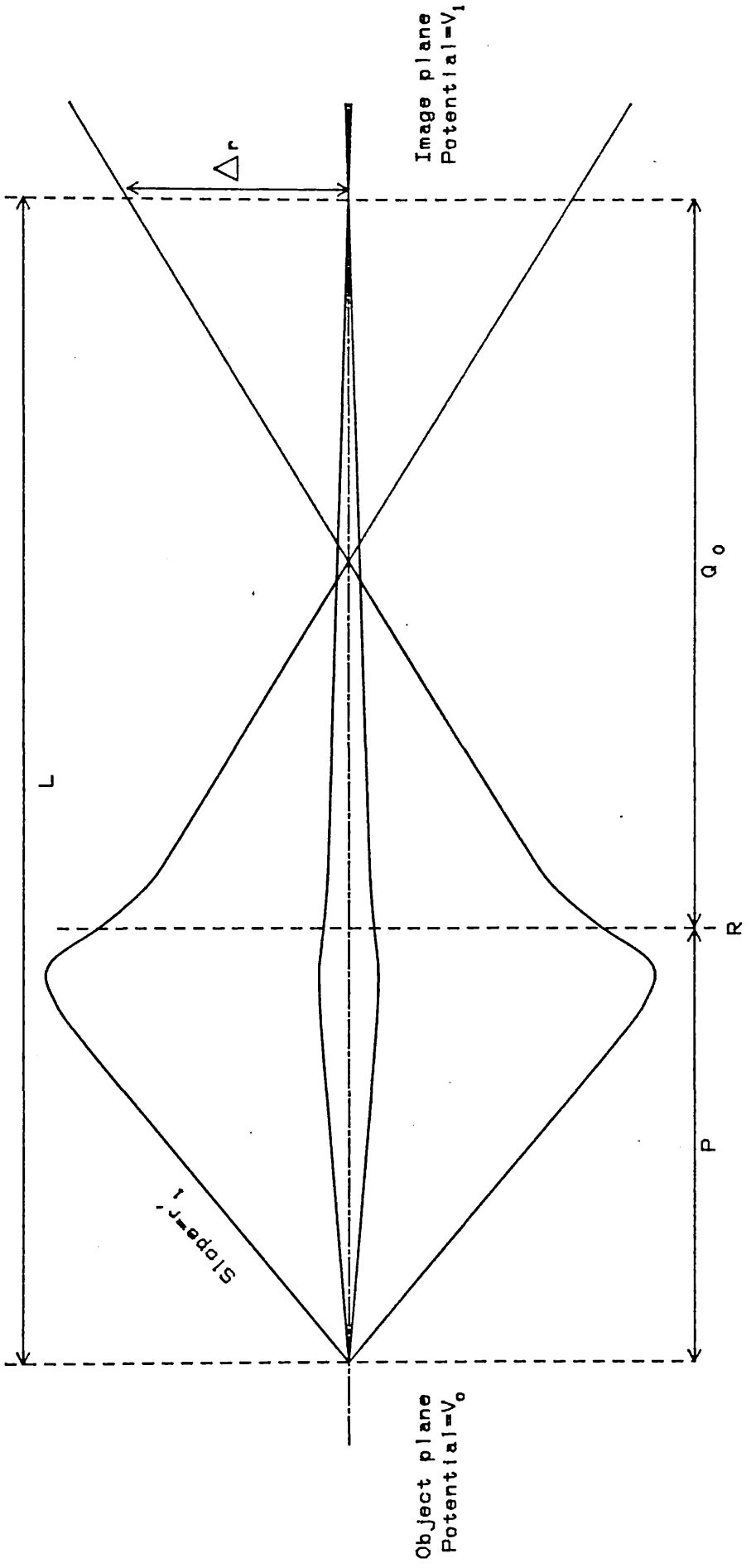

FIGURE 31. Spherical aberration of an image of a point axial object.
L is the overall seperation of the object and image planes.

select the best scale size of the lens and we assume that all the Cs coefficients and the focal lengths are given in terms of D, then we can rewrite equation (221):-

$$\Delta r = M.Cs_o.D.(1 - 1/\sigma M)^4 r_1'^3 \qquad (222)$$

If the only constraint on D is the object-image separation:-

$$L/D = (P + Q)/D = F_1 + F_2 - f_1/M - f_2 M \qquad (223)$$

Hence:-

$$D = L.(F_1 + F_2 - f_1/M - f_2 M)^{-1} \qquad (224)$$

If we substitute for D in equation (222):-

$$\Delta r = \frac{LCs_o M(1 - 1/\sigma M)^4 r_1'^3}{F_1 + F_2 - f_1/M - f_2 M} \qquad (225)$$

Although this expression could be used for comparing lenses, any figure of merit derived from it in its present form would be dependent on the magnification of the system. It would be unhelpful in assessing the general quality of a lens. However, if the lens is not too strong, a figure of merit can be derived which is independent of magnification. If we incorporate the relationship that we derived earlier (172)

between the focal lengths of a weaker lens then (225) becomes:-

$$\Delta r = \frac{LCs_o M(1 - 1/\sigma M)^4 r_1'^3}{2\sqrt{f_1 f_2} - f_1/M - f_2 M} \qquad (226)$$

And if we define:-

$$a = -1/(\sigma M) \qquad (227)$$

Then:-

$$\Delta r = \frac{-LCs_o(1 + a)^4 r_1'^3}{\sigma a(2\sqrt{f_1 f_2} + a\sigma f_1 + f_2/a\sigma)} \qquad (228)$$

Recalling that $\sigma = (f_2/f_1)^{1/2}$:-

$$\Delta r = -L(Cs_o/f_2)(1+a)^2 r_1'^3 \qquad (229)$$

Hence:-

$$\Delta r = -gL(1 - 1/\sigma M)^2 r_1'^3 \qquad (230)$$

Where the figure of merit for the system is given by:-

$$g = Cs_o/f_2 \qquad (231)$$

since all the other terms in equation (230) are determined by the specifications for the system.
We have in (231) a figure of merit for this design problem which is independent of the system magnification. It should be noted, however, that in its derivation we have assumed that the magnification is not zero.

4.7.3) Best Lens for Zero Magnification

The results that we have just derived are inappropriate for a system that needs to focus a parallel beam into a minimum cross section (Figure 32).
The Gaussian image distance will be given by F_2 for that lens:-

$$L = F_2 . D \tag{232}$$

and the radius of the image can be derived from equation (190) by realising that $r_1' = 0$ and $Q_0 = F_2$:-

$$\Delta r = m_{16} \left(\frac{r_1}{f_2 D} \right)^3 . (f_1 D \sigma) \tag{233}$$

$$= \frac{f_1 m_{16} \sigma}{D} \left(\frac{r_1}{f_2} \right)^3 \tag{234}$$

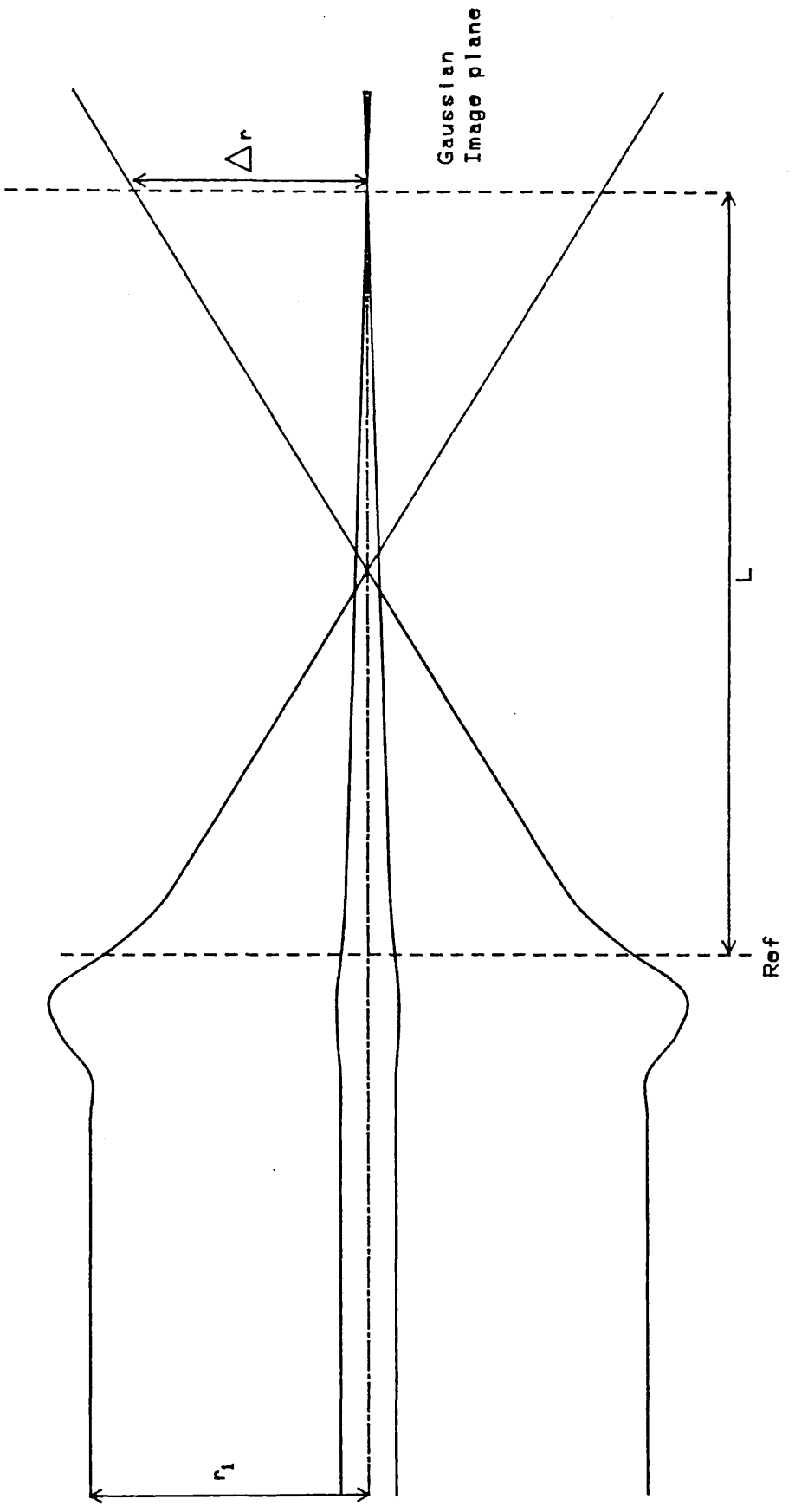

FIGURE 32. Figure of merit for a lens with zero magnification.
Δr needs to be minimised whilst keeping r_1,L and the potentials of object and image space fixed.

If we substitute for D from (232) and express m_{16} in terms of the Cs coefficients (equations (193)-(197)):-

$$\Delta r = -g_0 r_1^3 / L^2 \qquad (235)$$

where:-

$$g_o = Cs_o F_2^2 / (f_2^2 f_1) \qquad (236)$$

$$= Cs_4 F_2^2 / f_1^3 \qquad (237)$$

The latter of these two expressions can also be derived by a method independent of our relationships.

4.7.4) Figures of Merit for Retarding Lenses

Most tables of lens parameters do not give data on retarding lenses. However, since the focal lengths and spherical aberration coefficients of a decelerating lens can be derived from those for the accelerating lens (equations 26 and 198), it is possible to inter-relate the figures of merit for the system in each mode.

The figure of merit for a lens of finite magnification is given by equation (231). If, as before, we denote the parameters of the retarding lens by $\sim$, then it follows that:-

$$\tilde{g} = \tilde{Cs}_0 / \tilde{f}_2 \tag{238}$$

$$= (V_2/V_1)^{3/2} Cs_4 / f_1 \tag{239}$$

Hence, using equations (175) and (197):-

$$\tilde{g} = (Cs_0/\sigma^4 f_1).(V_2/V_1)^{3/2} \tag{240}$$

$$= (Cs_0/f_2).(V_2/V_1) \tag{241}$$

$$= g.(V_2/V_1) \tag{242}$$

The value of $\tilde{g}$ can therefore be deduced easily from that of g.

For a system with zero magnification we have from equation (237):-

$$\tilde{g}_0 = \tilde{Cs}_4 \tilde{F}_2^2 / \tilde{f}_1^3 \tag{243}$$

$$= (V_2/V_1)^{3/2}.Cs_0 F_1^2 / f_2^3 \tag{244}$$

$$= Cs_0 F_1^2 / f_1^3 \tag{245}$$

This expression enables the figure of merit for a retarding lens of zero magnification to be evaluated.

4.7.5) Choice of Lens Geometry

We have evaluated the figure of merit, g, for a number of two element lenses of the cylinder and aperture type. The results are shown in Table 19. They have been derived from the values of Cs_o and f_2 given by Harting and Read. It is clear that, as far as aberrations are concerned, there is little to choose between these two element lenses. In the case of cylinder lenses, those with equidiameters are marginally better over the voltage range considered. Of the two aperture lenses considered, the one with greater electrode separation is slightly less aberrated.

The figures of merit of the two triple element lenses are plotted in Figures 33 and 34. For a particular overall voltage ratio, g is dependent on the potential of the intermediate electrode. There are two maxima in this curve corresponding to $V_2 = V_1$ and $V_2 = V_3$. At these potentials the number of electrodes is effectively reduced to two and the overall voltage ratio is V_3/V_1. It is clear therefore that a lens with three elements will always be less aberrated than a comparable one with two. This effect is particularly true when the overall voltage ratio is low.

Table 19. The Figure of Merit (g) for Two Element Lenses. (*)

Voltage Ratio	2	5	10	20
Cylinder, $D_2=D_1$ (**)	278	7.02	1.45	.468
Cylinder, $D_2=1.5D_1$	299	7.61	1.56	.496
Cylinder, $D_2=2D_1$	326	8.26	1.68	.525
Cylinder, $D_2=D_1/1.5$	282	6.95	1.44	.482
Cylinder, $D_2=D_1/2$	296	7.17	1.47	.476
Aperture, A/D=0.5	314	8.12	1.72	.571
Aperture, A/D=1.0	270	7.31	1.58	.526

* Geometries are defined in Figures 1-3
** Cylinder gap=0.1D

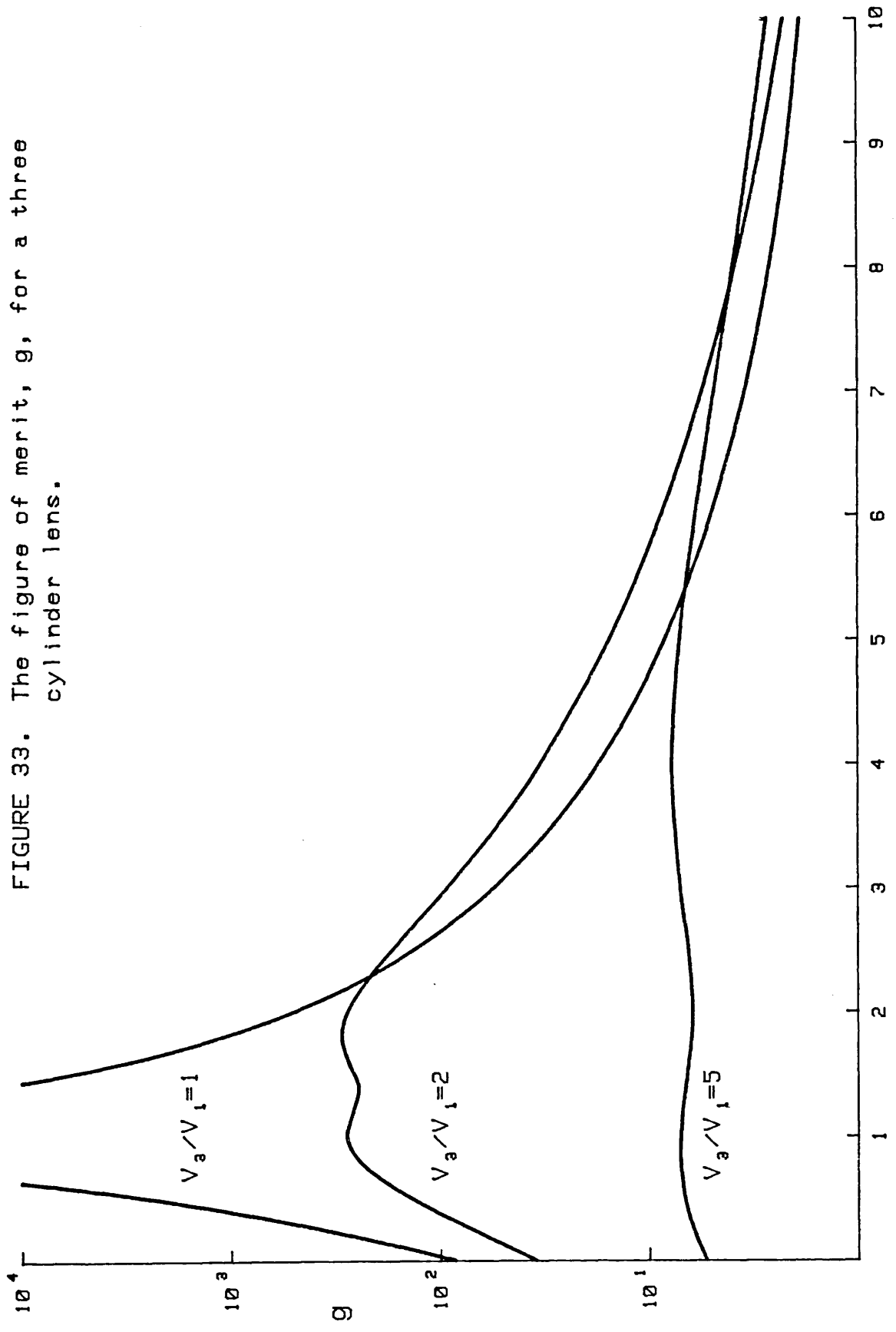

FIGURE 33. The figure of merit, g, for a three cylinder lens.

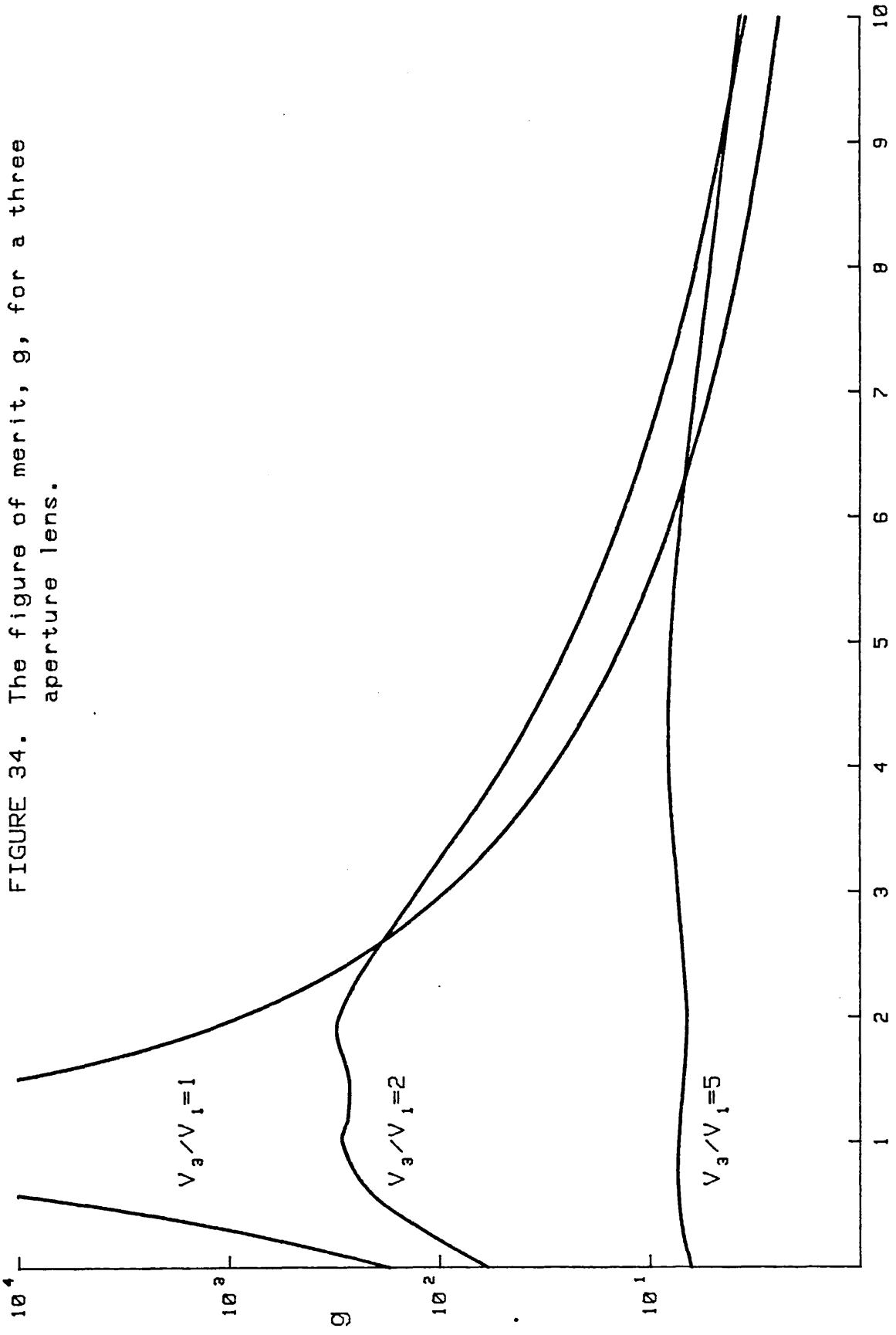

FIGURE 34. The figure of merit, g, for a three aperture lens.

4.8) Current Density Profiles

A designer's concern with the aberrations of a lens lies generally with the effect that they have upon the current density profile at the image plane. Whilst for high current systems the principal aberration will be due to space charge interactions (see 1.2), geometric effects will impose some limitation on the image definition of all lenses. It is useful, therefore, to be able to relate the aberration coefficients that have been discussed to the distribution of current density at the image plane. Since we can describe the third order aberrations in terms of one coefficient only, the process is rather straight forward. We shall demonstrate by considering the system shown in Figure 35, where the incident beam is parallel to the optic axis and of uniform current density, J_1. Its overall radius is R_1.
The current passing through a ring of radius r_1 at the object plane will be given by:-

$$dI = J_1 2\pi r_1 dr_1 \qquad (246)$$

It follows that the current density distribution across the image plane ($z=F_2$) is given by:-

$$J(r) = dI/(2\pi r dr) \qquad (247)$$

$$= J_1 (r_1/r)(dr_1/dr) \qquad (248)$$

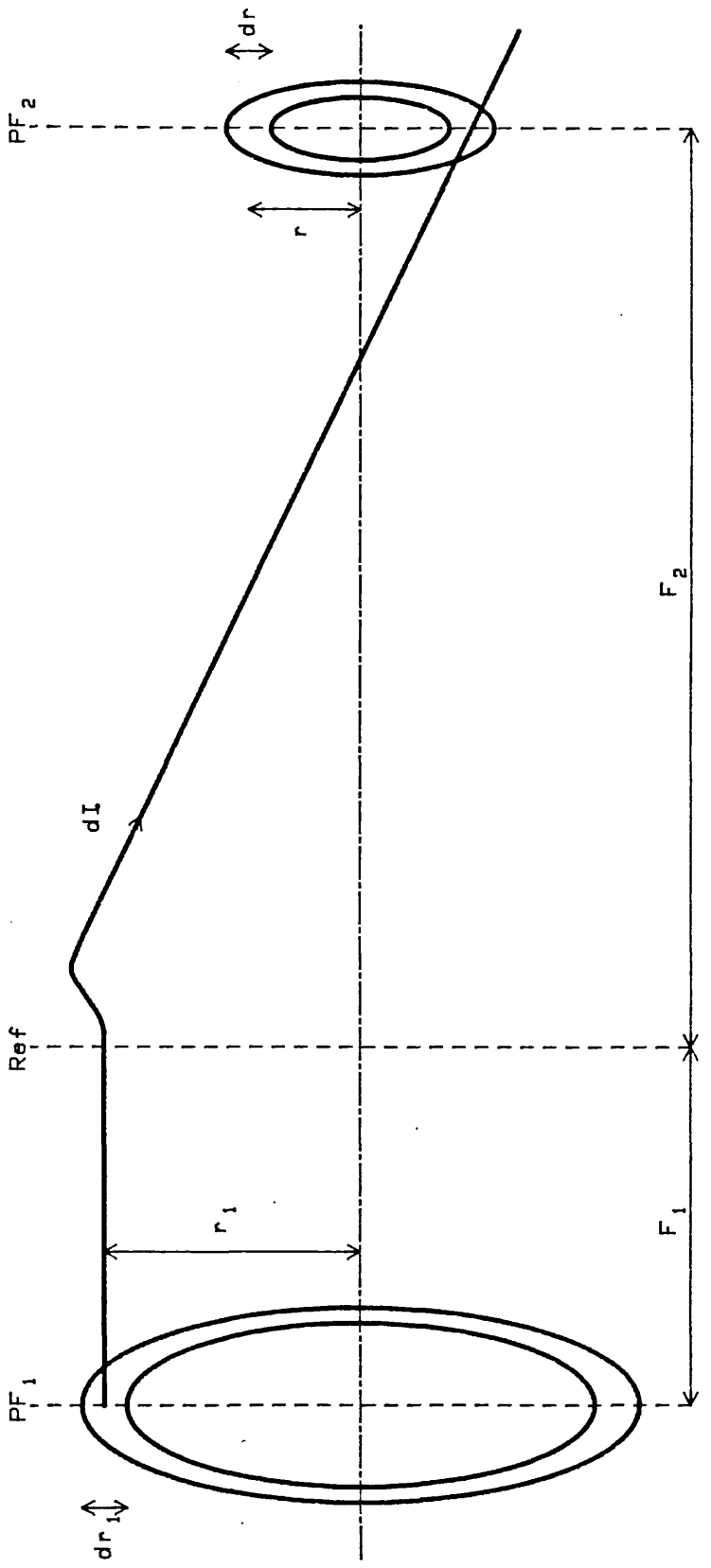

FIGURE 35. Derivation of current density distribution by considering the current passing through annular sections of the object and image plane respectively.

Where r is given by equation (183):-

$$r = f_1 \sigma m_{16} (r_1 / f_2)^3 \qquad (249)$$

Hence:-

$$J(r) = \frac{J_1 f_2^2}{3 (f_1 \sigma m_{16} r^2)^{2/3}} \qquad (250)$$

Which can be expressed in terms of Cs_o by using equations (175) and (193):-

$$J(r) = \frac{J_1}{3} \left(\frac{f_1 f_2^2}{Cs_o r^2} \right)^{2/3} \qquad (251)$$

Since the overall radius of the image is given by:-

$$R = f_1 \sigma m_{16} (R_1 / f_2)^3 \qquad (252)$$

$$= Cs_o \frac{f_2}{f_1} \left(\frac{R_1}{f_2} \right)^3 \qquad (253)$$

We can check equation (251) by calculating the total image current:-

$$I = \int_0^R J(r) . 2\pi r dr = J_1 \pi R_1^2 \qquad (254)$$

Which, as expected, is the current input into the lens.

The predicted current density distributions for a two cylinder lens ($D_1=D_2=D$) are shown in Figure 36 for a number of voltage ratios. We have taken the input beam to have diameter D/2. It can be seen that, as is the case for an unaberrated lens, the current density on axis is infinite. However the profile has a skirt which becomes more pronounced as the lens becomes weaker. It should be emphasised that space charge effects have not been taken into account. If they were we would expect the current density on axis to be finite and the profile to be generally broader.

It is possible to derive a figure of merit for the above system, where a parallel beam of uniform current density is to form an image at a distance L from the lens centre. The design criterion is that there is to be a maximum current (I_{im}) incident on a disc of radius r_{im} situated at the image plane. This current is given by:-

$$I_{im} = \int_0^{r_{im}} 2\pi r . J(r) . dr \qquad (255)$$

$$= J_1 \pi \left(\frac{f_1 f_2^2}{C s_o} \right)^{2/3} . \; r_{im}^{2/3} \qquad (256)$$

Allowing ourselves the freedom to scale the diameter of the lens:-

$$I_{im} = J_1 \pi \left(\frac{f_1 f_2^2}{C s_o} \right)^{2/3} D^{4/3} \; r_{im}^{2/3} \qquad (257)$$

FIGURE 36. Image current density profiles of a two cylinder lens at different voltage ratios.

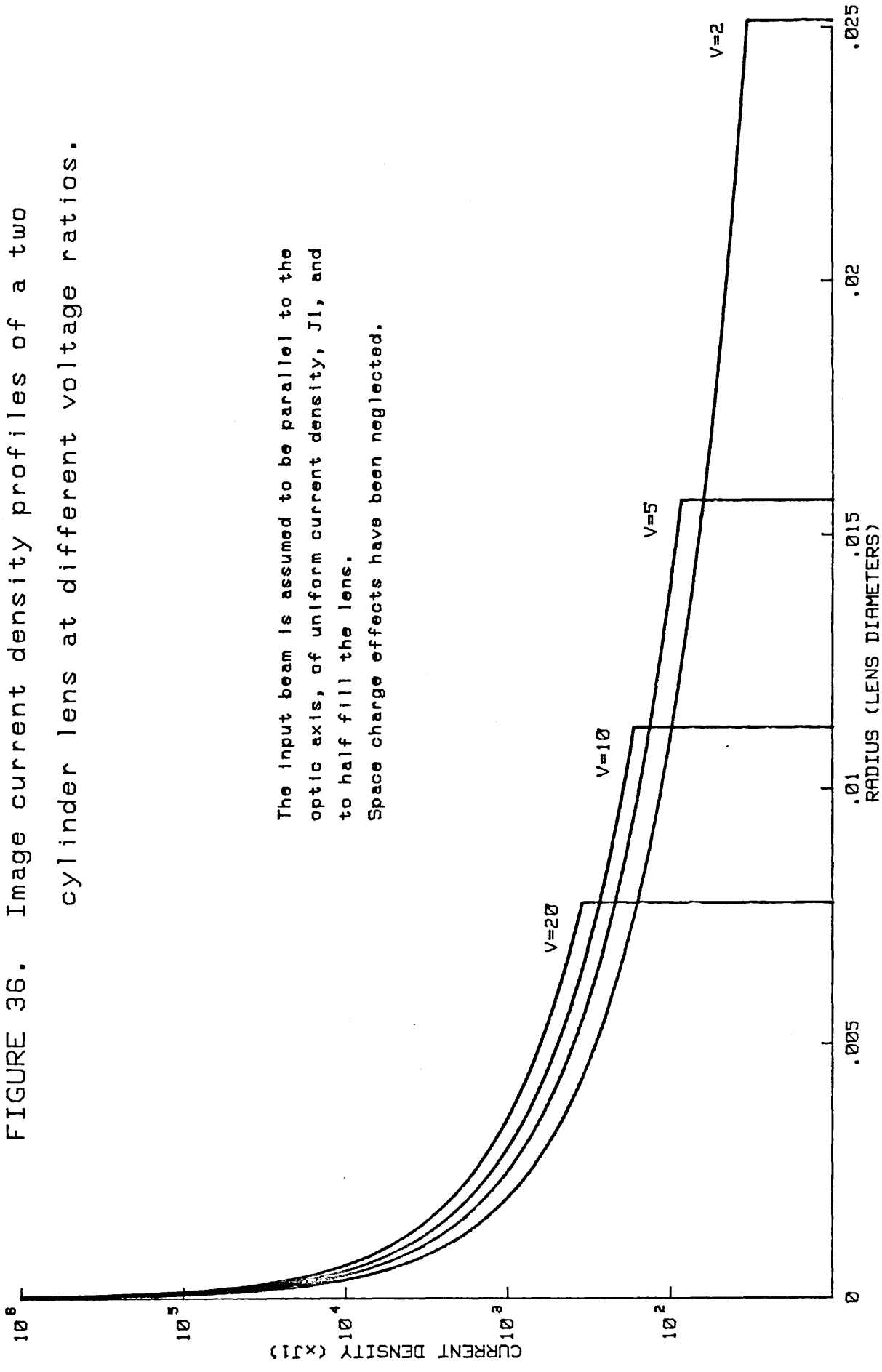

Where:-

$$D = L/F_2 \tag{258}$$

hence:-

$$I_{im} = J_1 \pi L^{4/3} r^{2/3} / g' \tag{259}$$

Where the figure of merit is given by:-

$$g' = \left(\frac{C s_o F_2^2}{f_1 f_2^2} \right)^{2/3} \tag{260}$$

It can be seen that g' strongly resembles g_o (equation 236) which is the figure of merit corresponding to minimum overall image size for this system.

CONCLUSION

5.1) SUMMARY

We have developed a computer model that has enabled us to make a detailed study of the geometric aberrations of a two cylinder lens. We have shown that all the third order aberrations of this lens (at all magnifications) can be described by a single coefficient. This coefficient depends on the lens geometry and voltage ratio alone. Fifth order effects have also been examined and we have shown these to be fully described by an additional coefficient. The only constraint on this description is the voltage ratio. For example at 40:1 the lens is very strong and our results become erroneous. In practice this should be a minor limitation, not only because lenses of this strength are rarely used but also because their aberration coefficients are considerably smaller.
The basis of this simplified treatment of aberrations lies in equation (125):-

$$r_2/f_1 = r_1' + \sigma r_1/f_2 + \sigma r_2' \qquad \text{where} \quad \sigma = (V_2/V_1)^{1/4} \tag{261}$$

which accurately relates a ray's radial position and slope in image and object space, irrespective of the degree of aberration. We suggest that this should be used for describing aberrated rays in the same way that the Helmholtz-Lagrange

relationship applies to paraxial rays:-

$$r_2/f_1 = -f_2 r_2' r_1'/r_1 \qquad (262)$$

Treating the rays in this fashion, we have developed equations (182)-(185) which can be used to calculate the slope and position of any ray in image space, in terms of its slope and position in object space and one aberration coefficient (or two for fifth order effects). From these results we have been able to calculate the position and curvature of a lens' focal planes. Moreover we have shown the size and position of the aberrated image to be readily calculable, both at the Gaussian image plane and at the disc of least confusion.

The particular problem of spherical aberration has also been examined and we have derived an expression (198) which descibes the aberration at all magnifications using only one coefficient (third order). We have also shown that this expression can be used to give an upper limit to the aberration of an object of finite size.

The application of our results to more complex lens geometries has been investigated and we have found them to be equally accurate so long as neither principal focus is within half a lens diameter of the reference plane (ie $F_1 > 1/2$, $F_2 > 1/2$). Although no details are given in the main text (see Appendix) we have also considered lenses of planar rather than cylindrical symmetry and found that our results are still applicable, within the same constraints on lens strength.

We have given details to show how our results can be used to assist in the design of a lens. The criterion we have used is that the lens is to have minimum aberration and we have shown that, in general, the figure of merit is given by (equation 231):-

$$g = Cs_o / f_2 \qquad (263)$$

and the suitability of a lens is independent of the required magnification. (If the system is to have zero magnification a slightly modified version of this expression (236) should be applied.)

Finally, we have demonstrated that image current density profiles can be calculated readily from a knowledge of a single aberration coefficient. This analysis, however, neglects space charge interactions.

5.2) FUTURE WORK

We can see three areas in which this work might be developed in the future:-

1) The lenses that we have considered have been electrostatic and, for the most part, of cylindrical symmetry. A treatment that simplifies the eight third order aberration coefficients of a magnetic lens would be very useful. So indeed would an investigation of the lenses used in certain high current

applications (for example ion implanters) where the electrodes are of planar symmetry with rectangular apertures. This could require three dimensional analysis.

2) The work that we have done on current density profiles has been in the absence of space charge. It would be extremely useful if a simple method could be devised that enabled both the current density and emittance of an output beam to be described where space charge effects have not been neglected. In order to achieve this the computer model would need to be extended to solve Poisson's equation. However, this would almost certainly require an iterative solution and a great deal of optimisation would be necessary if the run time was not to be excessive.

3) Little work has been done on the aberrations of lenses where the object is immersed in the field. This is particularly pertinent to electron guns and other emission systems. Such an investigation could be mounted using the computer although the model in its present form would be inappropriate. This type of study would be especially useful if space charge interactions were not neglected.

APPENDIX

LENSES OF PLANAR SYMMETRY

We have examined briefly the relevance of our work to planar lens geometries (those with a plane of reflection rather than an axis of rotational symmetry). The results indicate that the aberration coefficients of these types of lenses can be rationalised in the same way that those of cylindrically symmetric lenses can be.

The two geometries that we have considerd are shown in Figure 37. We shall refer to the five aberration coefficients pertaining to a point axial object by C_i. Analogous to equation (154) the width of the aberrated image at the Gaussian plane is given by:-

$$\Delta x = M.C(M)\alpha_1^3 \qquad (264)$$

Where:-

$$C(M) = C_0 + C_1M^{-1} + C_2M^{-2} + C_3M^{-3} + C_4M^{-4} \qquad (265)$$

and α_1 is the maximum half angle of the object rays with respect to the plane of symmetry.

The values of these coefficients for the two lens geometries are shown in Table 20 (from Harting and Read). Also shown are the values of Y, which equation (166) predicts to be zero if

the aberration coefficients are related in the same way as in cylindrically symmetric lenses (equations 161-165). The percentage error that is quoted is that which would need to be present in each of the C_i coefficients in order that Y be zero. This should be compared to the 1% error that Harting and Read give for their results.

For the rectangular tube lens the the relationship between the coefficients becomes too erroneous for $V_2/V_1=8$. For the two slit lens the upper limit on the voltage ratio is 12:1. For both geometries these upper limits correspond to the voltage ratio at which F_2 becomes less than H/2.

These results indicate that the relationships that we have derived for cylindrically symmetric lenses may also be applied to planar lenses, within the same constraint on focal strength.

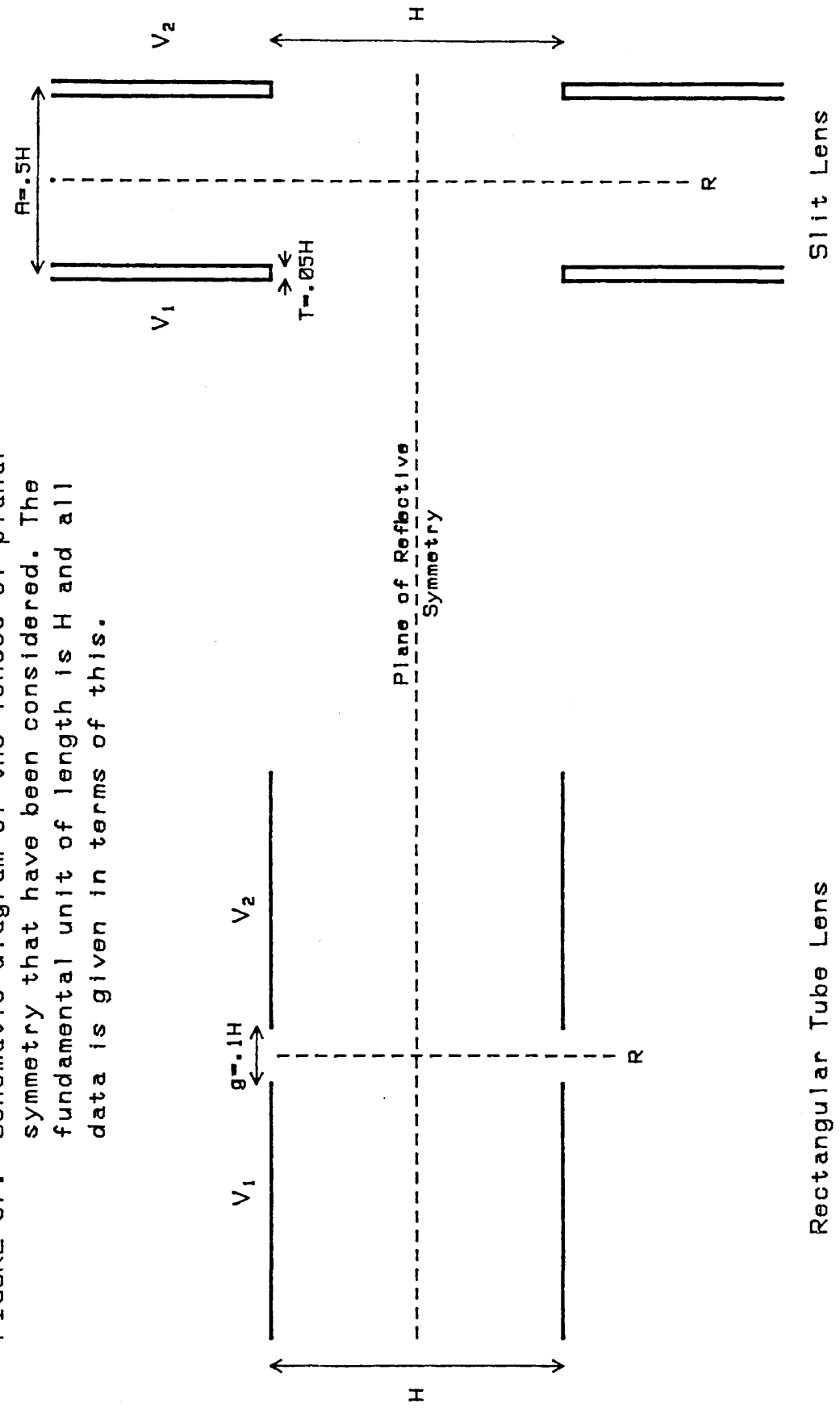

FIGURE 37. Schematic diagram of the lenses of planar symmetry that have been considered. The fundamental unit of length is H and all data is given in terms of this.

TABLE 20. SPHERICAL ABERRATION COEFFICIENTS FOR LENSES OF PLANAR SYMMETRY

TWO RECTANGULAR TUBE LENS. G/H=0.1

V2/V1	C0	C1	C2	C3	C4	Y	%ERROR
2.0	7.85E+2	-2.23E+3	2.37E+3	-1.12E+3	2.00E+2	5.73E-1	1.2E-2
4.0	1.79E+1	-3.56E+1	2.73E+1	-9.50E+0	1.27E+0	9.09E-2	2.3E-1
6.0	5.09E+0	-8.04E+0	5.11E+0	-1.54E+0	1.85E-1	3.82E-2	6.1E-1
8.0	2.61E+0	-3.44E+0	1.92E+0	-5.30E-1	6.17E-2	2.84E-2	1.3E+0
10.0	1.72E+0	-1.93E+0	9.83E-1	-2.55E-1	2.99E-2	2.61E-2	2.6E+0
12.0	1.29E+0	-1.25E+0	5.95E-1	-1.48E-1	1.78E-2	2.36E-2	4.1E+0
14.0	1.05E+0	-8.84E-1	4.01E-1	-9.56E-2	1.21E-2	2.27E-2	6.2E+0
16.0	9.03E-1	-6.61E-1	2.91E-1	-6.65E-2	8.95E-3	2.22E-2	8.7E+0
18.0	8.03E-1	-5.13E-1	2.23E-1	-4.86E-2	7.05E-3	2.19E-2	1.1E+1

TWO SLIT LENS. A/H=0.5

V2/V1	C0	C1	C2	C3	C4	Y	%ERROR
2.0	1.65E+3	-4.70E+3	5.02E+3	-2.39E+3	4.26E+2	-3.70E+0	3.8E-2
4.0	4.01E+1	-8.00E+1	6.06E+1	-2.06E+1	2.66E+0	1.34E-1	1.5E-1
6.0	1.21E+1	-1.93E+1	1.18E+1	-3.31E+0	3.59E-1	4.37E-2	3.0E-1
8.0	6.54E+0	-8.79E+0	4.58E+0	-1.12E+0	1.09E-1	3.19E-2	6.3E-1
10.0	4.48E+0	-5.26E+0	2.40E+0	-5.28E-1	4.37E-2	1.83E-2	7.3E-1
12.0	3.47E+0	-3.64E+0	1.48E+0	-2.98E-1	2.52E-2	1.69E-2	1.1E+0
14.0	2.88E+0	-2.75E+0	1.01E+0	-1.88E-1	1.53E-2	1.37E-2	1.4E+0
16.0	2.51E+0	-2.21E+0	7.31E-1	-1.29E-1	1.01E-2	8.97E-3	1.2E+0
18.0	2.25E+0	-1.85E+0	5.57E-1	-9.26E-2	7.16E-3	6.79E-3	1.3E+0

REFERENCES

Berger C and Baril M 1982 J.Appl.Phys. 53(6) 3950-3956

Bonjour P 1979 Rev.Phys.App. 14 533-540

Born M and Wolf E 1959 Principles of Optics 3rd edn (London: Pergamon)

British Association Mathematical Tables Vol 6 1958 (Cambridge: Royal Society)

Brunt J N H and Read F H 1975 J.Phys.E. 8 1015-1020

Buckingham R A 1962 Numerical Methods (London: Pitman)

Busch H 1926 Ann.Phys.Lpz. 81 974

Carre B A and Wreathall W M 1964 Radio Electron. Engr. 27 446

Cook R D and Heddle D W 1976 J.Phys.E. 9 279-282

Dahl P 1973 Electron and Ion Optics (London:AP)

Davisson C J and Calbick C J 1931 Phys.Rev. 38 585

El Kareh and El Kareh 1970 Electron Beams, Lenses and Optics (London:ap)

Grivet P 1972 Electron Optics 2nd edn (Oxford:Pergamon)

Harting E and Read F H 1976 Electrostatic Lenses (Amsterdam: Elsevier)

Klemperer O and Barnet M E 1971 Electron Optics 3rd edn (Cambridge: Cambridge UP)

Klemperer O and Wright W D 1939 Proc.Phys.Soc 51 296

Kuyatt C E, Natali S and Di Chio D 1972 Rev.Sci.Instrum. 43 84-87

Natali S, Di Chio D and Kuyatt C E 1972 J.Res.N.B.S. 76A 27-35

Picht J 1939 Theorie der Elektronoptik (Berlin)

Read F H, Adams A and Soto-Montiel J R 1971 J.Phys.E. 4 625-632

Read F H 1978 Inst.Phys.Conf 38 249-256

Renau A 1979 M.Sc. Thesis (Manchester)

Renau A, Read F H and Brunt J N 1982 J.Phys.E. 15 347-354

Stephenson G 1973 Mathematical Methods (London: Longman)

Sturrock P A 1955 Static and Dynamic Electron Optics (Cambridge: Cambridge UP)

Verster J L 1963 Philips.Res.Rep 18 465-605

Zworykin V K, Morton G A, Ramberg E G, Hillier J and Vance A W 1945 Electron Optics and The Electron Microscope (New York:Wiley)

Scherzer O 1936 Z.Physik 101 593-603

ACKNOWLEDGEMENTS

I would like to express my gratitude to Professor D.W.O. Heddle for his help and advice throughout the course of this work. I would like also to thank the Science Research Council for the financial assistance which enabled me to begin this research. In particular I am grateful to my wife, Caroline, for the patience and encouragement which enabled me to finish.